THE REGENERATION OF A WEAK ACID CATION EXCHANGER WITH AN AQUEOUS SOLUTION OF SULPHUR DIOXIDE

by
Raul Raiter B.Sc. (Eng)

Johannesburg
September, 1980

THE REGENERATION OF A WEAK ACID CATION EXCHANGER WITH AN AQUEOUS SOLUTION OF SULPHUR DIOXIDE

A dissertation submitted to the Faculty of Engineering, University of the Witwatersrand, in fulfilment of the requirements for the degree of Master of Science in Engineering

by
Raul Raiter, B.Sc. (Eng.)

Johannesburg
September, 1980

DECLARATION

I hereby wish to declare that:

(a) The work described herein was carried out by me in the Chemical Engineering Department, University of the Witwatersrand, and

(b) it has not been submitted for a degree at any other University.

R. Raiter

.....

RAUL RAITER

ACKNOWLEDGEMENTS

I wish to express my gratitude and appreciation to Professor D. Glasser, Professor and Head of the Department of Chemical Engineering, University of the Witwatersrand, for his guidance and assistance provided through the preparation of this work, and for helping me to write this manuscript in an acceptable English.

My thanks also go to Professor O.B. Volckman and Professor A.W. Bryson and to all the members of the Chemical Engineering Department, every one individually, for the valuable discussions we had and for their comments.

I would like to thank the Unive sity of the Witwatersrand and A.E.C.I. Company (Dr.C. Schlesinger) for their financial support and their interest in the idea on which this work is based.

My debt also is to Mr. M.J. Buker and Mr. B.N. Fairbrother of the Glass Blowing Service of this University, who constructed the columns and the new flow meter used in the experiments.

I am grateful to N.I.M. Library Staff, for their assistance in finding valuable information.

To Mrs. J Penmar and Mrs. M. Marler I am thankful for typing this manuscript.

And last, but by no means least, my most sincere thanks go to Dr. S. Evans, whose work inspired me and who introduced me into the ion exchange field.

SYNOPSIS

Ion exchange processes are mainly used in water treatment and recovery processes.

The application of ion exchangers is frequently limited by the high cost of regeneration (particularly with cation exchangers). Furthermore, the regeneration effluents pose a difficult disposal problem reducing the usefulness of these processes.

A new process using an aqueous solution of sulphur dioxide as a regenerant for weak acid cation exchange resins, has been investigated.

Demineralized, tap and hard water were all used to prepare the abovementioned solutions.

Two typical cations - Calcium and Copper were chosen and investigated in some detail.

Fixed and fluidized bed techniques were used in designing a suitable regeneration cycle.

The regeneration efficiency of the sulphur dioxide solution was compared with the commonly used regenerants and good results were obtained even with hard waters.

A Kinetic study of the process was also carried out. The intraparticle diffusion coefficient ($\bar{D}$) obtained, is in good agreement with the values reported in the literature.

During the investigation of the regeneration process, a new type of flowmeter was also built and tested. Its construction was aimed to answer flow measurement problems developed during the investigation.

Treatment of the regeneration effluent was also investigated and it was shown that there is a possibility of recycling all the components.

The industrial application of the regeneration process is described, the use of the process being seen as a link between water and air pollutant treatment.

A scrubbing tower for SO_2 removal from flue gases and an associated ion exchange unit have been designed.

GENERAL LAYOUT

LIST OF CHAPTERS

APPENDICES AND THEIR CONTENTS

APPENDIX A. DETAILS OF THE REGENERATION WITH SO_2 IN WATER CARRIED OUT ON A WEAK CATION EXCHANGER WITH Cu^{++}, or Ca^{++}, Mg^{++} and Na^{+}

APPENDIX B. THE DESIGN AND CONSTRUCTION OF A NEW TYPE OF FLOW METER

LIST OF FIGURES

CHAPTER 2

CHAPTER 3

CHAPTER 4

LIST OF TABLES

CHAPTER 2

CHAPTER 3

CHAPTER 4

Appendix B

Appendix C

CHAPTER 1

WEAK ACID (CARBOXYLIC) CATION EXCHANGE RESINS : LITERATURE SURVEY

INTRODUCTION

For many years, the advancement of ion exchange technology has evolved around the developments made in the area of cation exchangers. For almost a century, all the technology concentrated around the natural and synthetic alumino-silicates. This period, which started in 1850-54 with the discovery of ion exchange by Thomson and Way in England, [1] and which includes the commercial use of ion exchange developed by Gans in Germany (1905)(1) ended in 1935 with the discovery of synthetic ion exchange resins by Adams and Holmes [1]. Their patent was licenced in the United States of America in 1939.

Since 1948, there have been three major developments in the ion exchange field: the development of the styrene and acrylic based ion exchange resins, pioneered by D'Alelio [2, 3] and the work of McBurney [4] on the use of the chloromothylated styrene divinylbenzene copoliner as a base for a wide range of anion, cation and even chelating exchange resins.

In many respects, much of our current thinking in terms of cation exchange technology has been centered around the strongly acidic cation exchangers, and although much technology has developed over the years around weakly acidic cation exchangers, full advantage of these resins has not been taken.

This chapter will review some of the basic functions of the carboxylic cation exchanger, the variety of its applications and will also try to clarify the importance of the carboxylic cation exchange resins.

1. APPLICATIONS

To understand the importance of the regenerating agents for the carboxylic cation exchange resins, one must realize the wide range of applications of this type of resin.

The weak acid cation exchange resins under their commercial trade names (IRC-84, IRC-50, DP-1, ZEROLITE 236, LEWATIT CNP, BIOREX-70, PERMUTIT H-70, MERCK IV, etc) are widely used. Therefore, it is not possible to review

all the applications; however, a few examples of each type of application will be given.

1.1. Water Treatment

The main areas of water treatment in wnich weak cation exchange resins are used, are water softening, desalination and waste water treatment.

Complete desalination schemes in which weak cation resins play a decisive role, have been developed over the last two decades. A wel. known DESAL Process [5] developed by Kunin and described in many articles [6, 7, 8] has been further developed in Italy [9, 10] as the SIRA Process.

The most fascinating development in the water treatment field, based exclusively on weak ion exchangers is the SIROTHERM Process, developed in Australia [11, 12].

Weak cation exchange resins have found applications in the recycling and re-use of industrial effluents. Such a use is described by Stepanova, Z.S., in her article [13] ; by A.J. Gilmore [14], in the Japanese patents [15], [16] and by G. Boari [17].

1.2. Recovery and purification of metals (Extractive metallurgy).

Although the working pH range of the weak cation resins is restricted to a narrower one than the strong cation exchangers, weak cation exchangers have found applications in extractive metallurgy, competing well with the strong cation exchange resins.

At least one patent and many works were published on the loading of uranyl cations (UO_2^{++}) and other cations on weak cation resins [18, 19, 20, 21].. Other applications have already been mentioned [14 - 16].

1.3. Purification of sugars and biological materials

A Japanese patent [22] describes a method of refining beet

sugar after carbonitation using a column which contains a mixture of weak acid and basic cation and anion exchangers. In a similar process [23] a sugar solution was refined using among other types, a weak acid cation resin. A weak cation exchanger has been used also as a beer stabilizator, according to a U.S. Patent [24]. It was also found [25] that a weak acid, cation exchange resin could be used to absorb acid phosphate from skim milk.

Weak cation exchange resins have also been used for adsorbtion of proteins (such as propain) from solutions [26], to recover vanillin from the controlled alkaline oxidation of lignosulphoric acid compounds [27] or to manufacture boric acid [28].

1.4. Medical and Pharmaceutical applications

Weak acid cation exchangers have found various applications in this field, being administered to humans and animals as anthelmentics [29], as gastric acid indicators [30] or as antiperspirant-deodorants [31].

They have been extensively used for purification and isolation purposes [32 - 35]. Lusozyme was isolated from human milk [36], Gastricsm (a new enzyme) was isolated from gastric material of amines [37],and complex mixtures of amines in human urine [38] were separated by using weak acid cation exchange resins. Even human haemoglobin has been chromatographically separated [39].

Weak cation resins were also used for the purification of blood plasma [40], as a nutrient culture [41] and as a disintegration accelerator tablet. [42].

1.5. Analytical chemistry

Various separations from the medical field, performed with weak cation exchangers have been mentioned already [32 - 40]. Honda [43] reported a separation of copper and nickel, similar to the report made by T. Nortia and J. Sohlman [44].

Edge reported the separation of copper from chromated wood preservatives [45]. Grays and Walton [46] separated lead from silver on Biorex-70.

A method of separation of alkali metals from Mg, Ca, Sr, Ba, Mn, Cu, Co, Ni, Zn, Fe, Al, Th, U and rare earths was worked out [47] and used for the determination of alkali metals in silicate ores while Nickel was separated from Uranium [48].

Lately, the use of complexing agents and chelating resins has become a common tool in analytical chemistry and there have been many quantitative micro separations using this tool. These separations are based on the fact that the weak cation resins complexes or in the ligant form, are highly selective towards certain cations. The desorption of these cations is rather difficult and therefore, these special resins are mainly used for analytical purposes.

Having now seen the importance of weak cation exchange resins, a natural question which arises is what are the main differences between a strong and a weak cation exchanger.

2. WEAK ACID CATION EXCHANGERS (PROPERTIES)

Weak acid cation exchangers, or as these are called, carboxylic acid exchangers, can be synthesized by cololymerization reactions. Many organic compounds can be used but the most common are the acrylic and metacrylic acids or their derivatives, which are usually polymerized with divinylbenzene [49] or the hydroxybenzoic acids which are condensed with formaldehyde [50] Another method is the cyanation and hydrolysis of polymeysed vinylbenzene chloride [51].

Carboxylic cation exchangers can be compared with very weak acids, and their dissociation constant, (K_a), ranges between $10^{-4.5}$ to 10^{-7}

Thus, their use is restricted to the range of pH above which the dissociation of RCOOH takes place [52, 53] and which is usually above pH 5 [54]. Therefore, the weak cation exchange resins are effective in neutral and alkaline solutions.

Weak cation exchangers do not exchange with neutral salts by converting them into the corresponding acids. Only the bicarbonate is converted to carbonic acid because it is a weaker acid than the carboxylic acid. [55, 10].

Carboxylic cation exchange resins possess an unusually high affinity for H^+. Accordingly, sorption of some metal ions is found to be poor in H^+ [56 - 63]: The order of ease of replacement for common cations (something like the reverse of affinity) has been found to be [55]:

$$Li^+ > Na^+ > K^+ > Mg^{++} > Ca^{++} > Al^{+++} > Fe^{+++} > H^+.$$

On the other hand, in neutral and alkaline media, it is difficult to keep many cations in solution without using complexing agents. These factors may be partly responsible for the lack of interest shown for a long time in the use of these cation exchangers.

Once it was realized that the increased exchange capacity in alkaline solutions (compared with the strong cation exchangers) could be a value in the sorption and separation of heavy metals, many workers started using the weak cation exchangers in their work.

Summarizing, it can be said that the carboxylic cation exchangers have a high affinity for polyvalent cations. This affinity, is a property of these resins, even at low pH, when the RCOOH does not ionize significantly [61, 21]. Conversely, the strong cation exchange resin indiscriminately adsorbs all the cations, exchanging with neutral salts and converts them into the corresponding acids.

Knowing now the special properties of the weak cation resins and the fact that these can be utilized, the questions arising are : how are these resins regenerated and can their special affinity for H^+ be used to lower the cost of regeneration?

As is well known, ion exchange resins are used in a cyclic way, i.e. being loaded with one or many ions, after which the ions are eluted, the resin being regenerated so that it is ready for reuse.

This cycle is determined by, among other things, the resin capacity and the concentration of ions being absorbed. In any case, the loading cycle is followed by regeneration and this is why it is so important. It can become critical w the loading period is short (short cycle) and when the expenditure on regeneration needs to be kept low.

Weak c tion exchange resin can be almost fully regenerated (~100%) while strong cation exchangers are regenerated usually to a lo r level (70 - 80%). Even more, because of their high affinity towards H^+ cations, the regeneration of weak cation resins can be carried out with only 110% of the required regenerant amount, compared with 200% regenerant amount needed to achieve the abovementioned level of regeneration for the strong cation exchangers [13, 64-65]. This being the case it is understandable why weak cation exchange resins are employed in so many processes. This is especially important for water treatment and desalination schemes [10, 8, 6, 11, 15] where the price of the treated or desalinated water must be kept low.

In practice, the rege eratior of the weak cation exchange resins is done using the regeneration effluent from the strong cation exchanger unit. In this way, the acid needed to regenerate the strong cation resin, (200% of stoicheometric amoung) is used more efficiently. When H_2SO_4 is employed as a regeneration agent for strong cation resin, and the regeneration effluent is to be used for the regeneration of the weak cation unit, the effluent solution must be diluted to avoid the precipitation of Ca SO_4 in the resin bed. When HCl is employed as regenerant agent, dilution is not necessary

As can be seen, the special properties of the weak cation resin are wel exploited in the schemes where strong and weak cation exchangers are employed side by side [12].

On the other hand, there are processes based on weak ion exchangers only [5, 13, 16, 18, 19, 44, 64]. The majority of these processes are in the water treatment and desalination field, in which the running costs must be kept low, so that the price of the water can be as low as possible.

The only way to keep the regeneration cost low, is to employ cheap regenerants and thus, not the conventional strong acids (HCl or H_2SO_4).

3. REGENERATION AND REGENERANTS

The search for new and cheap regenerants started immediately after the discovery of the carboxylic cation exchangers. There are only a few possibilities to be taken into account, and these are the weak acids usually resulting from the dissolution of gases in water

These gases, CO_2, SO_2 and H_2S which are the waste gases of industry can be considered as potential regenerants since they are found in abundance and are cheap.

From the beginning, H_2S has been rules out, since its solubility in water at normal conditions is not high enough.

The remaining two gases have been the subject of much work and many patents which have described their use as regenerants of weak cation resins.

Not long after the discovery of the carboxylic cation exchangers, 15 July, 1950, K.R. Gray filed two patents: one for the "Preparation of sodium salts of carbonic acid by ion exchange" [66] and the other [67],a "Process of recovering chemicals from mel.s obtained in pulping operation". Both patents describe the loading of a carboxylic cation exchanger with sodium salts, and its regeneration (and sodium elution) using CO_2 under pressure of 2-5 atm [66] and SO_2 [67] both dissolved in water.

In his patent [68] dated 13 April 1962, R. Kunin described the treatment of a mixed (cation and anion) bed with an aqueous solution of CO_2 to regenerate a weak cation exchanger. The same regeneration process was reported later in the literature [69].

Another patent filed in 1970 and granted to Larsen in 1972 described the regeneration of a weak cation resin with carbonic acid, formed

by introducing carbon dioxide into water into a pressure of from 100 to 300 psi. [70]. In the same year, a Czechoslovakian patent [71] described the "Regeneration of mixed ion exchanger bed in situ" by using a single feed of water and CO_2 in a counter-current flow.

As can be seen, the above patents deal with the regeneration of carboxylic exchangers, loaded with monovalent cation, using both CO_2 and SO_2.

But the major use of carboxylic cation exchangers in water treatment is to adsorb Ca^{++} and Mg^{++} cations, and therefore, attention has been concentrated on the regeneration of these resins, loaded with Ca^{++} and Mg^{++}. Many of the workers in this field have realized that the regeneration of the weak cation resin loaded with Ca^{++} cations, using aqueous CO_2 can be taken to completion, since the reaction between the regenerant and the cation results in the formation of an unsoluble salt: $Ca\ CO_3$:

$$(RCOO)_2\ Ca + H_2\ CO_3 \rightleftharpoons 2RCOOH + Ca\ CO_3 \downarrow$$

This is probably the reason why SO_2 has been ignored in regenerating weak cation resins loaded with Ca^{++} cations.

In 1975 and 1976, B. Wittmar and H. Southeimer published two papers about the regeneration of weak cation resins, loaded with Ca^{++} cations, using CO_2 [72, 73]. They concluded that the regeneration is possible, and the precipitate of $Ca\ CO_3$ does not clog up the resin.

Weak cation resins have been regenerated using the same feed water which loaded them but this time at an elevated temperature. The new process, developed in Australia (SIROTHERM) had two major advantages: it is based on weak ion exchange resins and does not use any special regenerant, but the feed water at a higher temperature [16, 17, 14]. The latest development in this direction is described in a German Patent [75] granted to H.H. Euman.

During the last decade, new regenerating agents, other than CO_2, SO_2 or temperature have been found.

A Japanese patent [76] described the regeneration of a chilating resin with water, followed by a dilute solution of $Ca\ Cl_2$.

R. Kunin, proposes in his patents [77, 78] a regeneration mixture for weak cation resins, comprising alkali metal chloride, alkali metal carbonate and an alkali metal chilating polycarboxylate.

In parallel with the search for new regenerants, much work has been done to understand the mechanism of loading and regeneration of carboxylic cation exchanger.

We can mention the works of Kunin concerning the behaviour of weak [79] and strong cation and anion [80] resins, his work on DESAL Process [6 - 8], the work of Marinsky [81] and Helffurich [82], the work of Weiss and his team [74] which led to the development of the SIROTHERM Process, and the work of M.B. Hanley [83] and Holl [84, 85] on the Kinetics of neutralization and protonation of weak cation resins. The main conclusions which have emerged from these works are that both the loading and the regeneration of the weak cation resins are particle diffusion controlled, that the regeneration rate is concentration dependent and that the regeneration of these resins can be carried out in low concentration acids (0.1N) [83].

4. DISCUSSION

As previously mentioned, the use of new regenerants which are cheaper than those commonly used, as well as a larger integration of weak resins in ion exchange processes has brought, and will continue to bring a reduction in the overall costs of ion exchange processes.

To summarize weak resins are preferred to strong resins because:

1. They have greater capacities
2. Cheaper regenerants can be used
3. Complete regeneration is nearly stoichiometric
4. Raw water can be used for rinsing.

There is also a steadily increasing environmental need to remove

sulphur dioxide from stack gases. Ion exchange resins were used for this purpose as well.

The works carried out to establish the removal efficiency of SO_2 by microreticular anion exchange resins [86], macroporous anion exchange resins [87, 88, 89] and ordinary anion exchange resins [90 - 94], concluded that there is no damaging (reducing] effect on the resin caused by the SO_2. As in all stack gases situations, it is preferable to find a use for this material rather than to produce an effluent.

In many cases the stack gases are associated with steam rising plants. These plants require that the water be dionized and this process is usually done with ion exchanging resins. These resins are at present regenerated with acids, producing effluents. It is possible that a sulphurous acid solution could be used as the regenerant. This would have the advantage that the effluents from the steam rising plant could be combined so as to produce a smaller total quantity. It is also possible that this latter material could be recycled in a way which will be discussed in later chapters.

In order to use the sulphur dioxide solution as a regenerant, experimental work needs to be done to ascertain its ability to do the regeneration, the efficiency of the process, etc. The work in this thesis will be aimed towards the understanding and solving of problems associated with the use of an aqueous solution of sulphur dioxide as a regenerant for a weak acid cation exchanger.

CHAPTER 2

The regeneration of a weak acid cation exchange resin, loaded with Ca^{++}, Mg^{++}, Na^{+} or $[Cu(NH_3)_4]^{++}$ cations, with an aqueous solution of SO_2

1. THEORETICAL APPROACH

1.1 SO_2 dissolution in water

SO_2 (gas) is more soluble in water than both CO_2 and H_2S (Fig. 2.1) and at ambient temperature (25°C) is solubility is 85 g/l or 1.33 moles/l. This value is an average value obtained from the values given in the literature [95, 96] for SO_2 solubility below and above 25°C. As to be expected, SO_2 solubility decreases with temperature and increases with pressure.

The dissolved SO_2, partially hydrolyses forming a weak acid, H_2SO_3 which dissociates into HSO_3^-, $SO_3^=$ and H^+ ions.

The equilibrium constant can be written in terms of concentrations and activity coefficients.

$$AB \rightleftarrows A^+ + B^-$$

$$\frac{a_{A^+} A_{B^-}}{a_{AB}} = K_a = \frac{f_{A^+} f_{B^-} [A^+][B^-]}{f_{AB}[AB]}$$

where a_{A^+}, $A_{B^-} a_{AB}$ represent the activities of A^+, B and AB, f_{A^+}, f_{AB} represent the activity coefficient of A^+, B^-, AB and the square brackets refer to the molar concentraions of A^+, B^- and AB.

Since in this case we have a fairly dilute solution of a weak electrolyte, all the equilibrium constants can with reasonable accuracy be written in terms of concentrations only.

The SO_2 in solution hydrolyses:

(eq.1) $SO_2 + H_2O \rightleftharpoons SO_2$ hydrolized, (H_2SO_3)

(eq.2) $$K_a = \frac{[SO_2]_h}{[SO_2]_T[H_2O]}$$

where K_a is the hydrolysis constant. The term $[H_2O]$ which is the concentration of water, remains virtually constant and therefore can be incorporated into the K_a constant.

(eq.3) $$K_o = \frac{[SO_2]_h}{[SO_2]_T} = \frac{[SO_2] \text{ hydrolized}}{\text{Total amount of } SO_2 \text{ dissolved}}$$

We next consider the dissociation steps:

(eq.4) $H_2SO_3 \rightleftharpoons HSO_3 + H^+$

(eq.5) $$K_1 = \frac{[HSO_3^-][H^+]}{[H_2SO_3]} \quad K_1 = 1.72 \times 10^{-2} \quad [97]$$

(eq.6) $HSO_3^- \rightleftharpoons SO_3^= + H^+$

(eq.7) $$K_2 = \frac{[SO_3^=][H^+]}{[HSO_3^-]} \quad K_2 = 6.28 \times 10^{-8} \quad [97]$$

The ions in solution must satisfy the electroneutrality condition:

(eq.8) $$Z[M^{Z+}] + [H^+] = [HSO_3^-] + 2[SO_3^=] + [OH^-]$$

where Z represents the valency of the cation M^{2+}

Finally, we can write a mass balance over all the sulphur containing species:

(eq.9) $[SO_2] + [H_2SO_3] + [HSO_3^-] + [SO_3^=] = T_{SO_2}$

where T_{SO_2} is the total mount of SO_2 originally dissolved in water, while $[SO_2^=]$ represents the amount of SO_2 dissolved but not hydralysed.

To these equations the dissociation of the water can be added:

(eq.10) $$H_2O \rightleftharpoons H^+ + OH^-$$

(eq.11) $$K_W^1 = \frac{[H^+][OH^-]}{[H_2O]} = 1.8 \times 10^{-16} \text{ moles/}_1.$$

(eq.12) $$K_W = [H^+][OH^-] = 10^{-14}$$

As the amount of OH^- ions in the solution at low pH's is very small, equations 10, 11, and 12 are not required, and if nothing other than SO_2 was dissolved, we can neglect the appropriate term in eq.8.

Therefore, the equations which describe the relationship between the different ions in an aquous solution of SO_2 are:

$$K_0 = \frac{[H_2SO_3]}{[SO_2]}$$

$$K_1 = \frac{[HSO_3^-][H^+]}{[H_2SO_3]}$$

$$K_2 = \frac{[SO_3^=][H^+]}{[HSO_3^-]}$$

$$Z[M^{z+}] + [H^+] = [HSO_3^-] + 2[SO_3^=] + [OH^-]$$

$$T_{SO_2} = [SO_2] + [H_2SO_3] + [HSO_3] + [SO_3^=]$$

From this set of equations, the concentrations of each ion in solution can be calculated, at any given pH.

Such calculations were done for five different solutions having different pH's. The original solution was prepared by bubbling SO_2 at atmospheric pressure into water until saturation was achieved, It was therefore assumed that 1.33 mole/l of SO_2 had dissolved in water (T_{SO_2} = 1,33 moles/l). Subsequently, this solution was diluted by two, four, four and again four times, the final total amount of SO_2 dissolved being 128 times less than the initial amount. Table 2.1 shows the amounts of the different species present at equilibrium.

The relationship between the hydrolysed species of SO_2 are also calculated, the results fitting quite well with those given in Fig. 2.2. [98]. Fig. 2.2 represents the pseudo mole faction of H_2SO_3, HSO_3^- and $SO_3^=$ ions, as a function of pH. These pseudo mole fractions were calculated by dividing the molar concentraion of each species by the sum of the concentration of these hydrolysed and dissociated species:

(eq.13) $$[H_2SO_3] + [HSO_3^-] + [SO_3^=] = A.$$

The pseudo mole fraction of H_2SO_3 is thus $[H_2SO_3]/A$, of HSO_3^- $[HSO_3^-]/A$ and of $SO_3^=$ is $[SO_3^=]/A$.

The abovementioned set of five equations, together with Fig. 2.2 and Table 2.1 (or Fig. 2.3) enables the calculation of the concentration of any species present in solution, at any given pH, as well as the calculation of the pH resulting from the dissolution of different amounts of SO_2: By knowing the total amount of SO_2 dissolved (T_{SO_2}), the K_0 (Table 2.1 or Fig. 2.3) and the pH of the solution, the pseudo mole fraction of H_2SO_3 can be found (Fig. 2.2) and the total amount of hydrolysed and dissociated sulphur species can be found.

(eq.14) $$A = [HSO_3^-] + [SO_3^=] + [H_2SO_3] = \frac{T_{SO_2}\ K_o}{H_2SO_{3/A}^+ + K_o}$$

Once A is found, the concentration of each species can then be calculated.

Note that the value of K_o (Table 2.1 and Fig. 2.3) should be approximately constant, but there appears to be some variation with concentration, but this is probably within experimental error.

1.2. Sulphite precipitates

Most of the metal salts associated with the sulphite anion ($MeSO_3$) are only slightly soluble in water. Table 2.3 shows the solubility of a few metal sulphites.

For this thesis, the most relevant sulphites are $CaSO_3$, $MgSO_3$, Na_2SO_3 and Cu_2SO_3. From Table 2.2 it can be seen that sodium sulphite is very soluble in water, the Cu_2SO_3 is slightly soluble, $MgSO_3$ has a solubility of 1.25 g/100 ml water, while the solubility of $CaSO_3$ is only 0.0043 g/100 ml water.

This means that Sodium and Magnesium will not create precipitation problems when associated with the $SO_3^=$ ion, while the sulphites of Cu^+ or Ca^{++} precipitate at a certain pH. This pH can be calculated and by knowing it and avoiding it, the precipitation can be prevented.

In our case, the aqueous solution of SO_2, containing a certain total amount of SO_2 dissolved (T_{SO_2}) is passed through an ion exchanger, loaded with Ca^{++} cations. The H^+ ions in solution are loaded on the resin, while Ca^{++} ions are eluted into the solution.

As shown before, the concentration of $SO_3^=$ ions can be calculated by using the values of K_o, T_{SO_2} for each case and the pseudo mole fraction of $[SO_3^=]$ from Fig. 2.2 as a function of pH can be constructed (Fig. 2.4):

Since the H^+ ions are replaced in solution by Ca^{++} ions which are eluted from the resin, the concentration of Ca^{++} increases as the

pH increases. The amount of Ca^{++} ions eluted from the resin can be calculated by calculating the respective amounts of $SO_3^{=}$, HSO_3^{-} and H^{+} from Fig. 2.2 and substituting into the equation

(eq 15) $$2[Ca^{++}] = [HSO_3^{-}] + [SO_3^{=}] + [OH^{-}] - [H^{+}]$$

Therefore, a schematic graph of Ca^{++} ions concentration as a function of pH can be also plotted (Fig. 2.5). Fig. 2.5 shows that less Ca^{++} ions are eluted for smaller initial concentrations of SO_2.

A curve of Ca^{++} concentration needed for precipitation of pH can be constructed by dividing the solubility product of $CaSO_3$ by the concentration of $SO_3^{=}$ as a function of pH, and since the concentration of $SO_3^{=}$ ion in solution depends not only on pH but also on T_{SO_2} (the total amount of SO_2 dissolved initially) a family of curves will result, as shown in Fig. 2.6

Two things can be seen in Fig. 2.6: firstly, that the Ca^{++} concentration needed for precipitation decreases with the increase in pH, (as the concentration of $SO_3^{=}$ increases) and secondly, that the lower the T_{SO_2} the higher is the concentration of Ca^{++} ions needed for precipitation, at any pH.

If the curves from Fig. 2.6 are drawn on Fig. 2.5, the intersection points between the curves plotted for different T_{SO_2} will give the pH at which the precipitation starts, as well as the minimum amount of Ca^{++} ions needed at that pH for the precipitation of $CaSO_3$ (Fig. 2.7).

It can be seen that as the T_{SO_2} decreases, the precipitation starts at increasing levels of pH.

From this analysis of $CaSO_3$ precipitation conditions, it can be concluded that the lower the total amount of SO_2 initially dissolved in water, (T_{SO_2}), the higher is the level of pH at which $CaSO_3$ starts precipitating, and this is due to both lower concentrations of $SO_3^{=}$ and H^{+} existing initially in solution and subsequently, and lower Ca^{++}

ion concentrations eluted from the resin.

Therefore, by choosing a low concentration of SO_2 dissolved in water, the danger of $CaSO_3$ precipitation is pushed to a high level of pH, but on the other hand, the initial pH of the regeneration solution is going to be high, and the elution of Ca^{++} cations is going to be inefficient.

The result of this calculation procedure is that for any initial concentration of total dissolved sulphur dioxide, a pH can be produced above which one should not go at any point in the column. The designer and operator of such a column, can then work to such a figure, to ensure that no precipitation occurs. The designer can specify a certain minimum flowrate which must be used, while the operator can use this exit pH to control the flowrate of regenerant. Obviously, on the other hand, too large a flowrate of regenerant will waste the regenerating capacity of the solution so that this calculated pH will be a useful design and control parameter.

1.3. SO_2 as a reducing agent

It is well known that SO_2 is a powerful reducing agent. Earlier work [86-94] showed that there is apparently no such effect on the resin, although the SO_2 was adsorbed very efficiently on an anion resin.

On the other hand, it is expected that the reducing effect is likely to have an influence on the Copper cations which show a variable valency, as is usual with the heavy metals.

This reducing effect can be enhanced by the presence of NH_4^+ cations [99].

$[Cu(NH_3)_4]^{2+}$ complex for example is fairly unstable having a stability constant equal to 4 [97].

(eq 16) $$K = \frac{[Cu(NH_3)_4^{2+}]}{[NH_3]^4\,[Cu^{2+}]} = 4(1/_{moles})^4 \text{ (Ref.97)}$$

In the reduction process, initiated by the presence of SO_2 in solution, one or more precipitates combining copper, ammonia and sulphite can be formed [99-102]. Table 2.3 indicates the three possible sulphite salts and their colour and composition formed in the process of breaking the ammoniacal complex of copper and reducing the Cu^{++} to Cu^{+}.

During the experiments (described further on) the salt formed appeared to be Chevreul's salt because of its red colour.

2. EXPERIMENTAL PROCEDURE

2.1. Choosing the resin and the cations for loading

There are many weak acid cation exchange resins on the market, under different trade names, but having similar characterists. It was decided to use only one resin in the regeneration experiments. The resin chosen was Zerolite-236 made by Diamond Shamrock - London, which is a gel type ion exchanger. Many articles in the literature describe experiments done using this type of resin [11, 21, 44, 61, 62, 74]. In order to be regenerated in the experiments, the resin had to be first loaded with one or more cations. Only a few cations were considered for loading bearing in mind the eventual applications of the regeneration process. These cations were Ca^{++} and Cu^{++}.

The Ca^{++} cation was chosen as the most representative of the alkaline earth metals with which all desalination and softening processes deal. Its concentration in water is usually higher than any other alkaline-earth metal and is the most dangerous from the point of view of scale formation. In relation to this work, Ca^{++} cations are the ones likely to cause most of the problems, the sulphite salt being more unsoluble than those of Mg^{++}, Na^{+} or K^{+}.

Nevertheless, Mg^{++} and Na^{+} cations were sometimes included among the cations which loaded the resin, and this was done to

give a more general aspect to this work, as Mg^{++} and Na^{+} are found together with Ca^{++} in water.

Cu^{++} was chosen as a representative of the heavy metals group which exhibit a variation in their valence state. Cations of these metals are loaded on the weak cation resins both during hydrometalurgical or waste water treatment processes

2.2. Loading Solutions

Solutions of both Ca^{++} and Cu^{++} cations can be prepared by dissolving different salts containing them in water ($CaCl_2$, $Ca(NO_3)_2$, $CuSO_4$, $CuCl_2$, $Cu(NO_3)_2$). These solutions, have a low pH($\sim$3) which is below the working range of the weak cation resins (above 5). Thus, concentrated solutions of calcium formate or acetate were used to load Ca^{++} ions on the resin. The pH of these solutions were within the working range of the resin. To these concentrated solution, small amounts of NaCl or $MgCl_2$ were sometimes added as detailed later.

To load the Cu^{++} cation, it was decided to use its ammoniacal complex $[Cu(NH_3)_4]^{2+}$ which is soluble in water and gives the solution a pH of $\sim$10-11 the entire complex -$[Cu(NH_3)_4]^{2+}$ being loaded on the resin.

2.3. Loading procedure

The loading of all the cations was carried out in a sintered glass column using a down flow stream.

During the loading with Ca^{++} cations, the resin bed shrunk by 13-16%, while it expanded by 70% during the loading with the amoniacal complex of copper.

2.4. Regeneration solution

The regeneration solution used was a saturated aqueous solution of SO_2, which was prepared by bubbling a stream of SO_2 through water

containing different concentrations of cations

A description of all the materials and instruments used in the experiments is given in Appendix A.

Fig. 2.8 shows schematically the arrangement used to carry out the regeneration.
(1) is the column in which the resin (2) is contained. (3) is a flow meter which enables one to monitor the flow rates during the different steps: loading, rinsing, regeneration.

(4) is a pH meter which monitors the changes in pH. (6) is the effluent outlet and (5), (7), (8) are the loading solution, regeneration solution and rinsing solution inlets, respectively.

From Fig. 2.8 it can be seen that by closing and opening the correct valves, the regeneration or rinsing solutions can be passed in downflow or upflow through the column (1), while the flow rate and the pH are continuously monitored.

2.5. Ways of ensuring the end of the loading and regeneration steps, and checking the composition of the precipitates

The loading and regeneration steps had to be performed accurately, and methods of ensuring this were developed and applied. As well as this.a method for testing the composition of precipitates was devised.

Five methods were used for these purposes:

a) Checking the pH of the effluent
b) Precipitation in the exit stream
c) Colouring the resin
d) A proper regeneration test (P.R.T.)
e) KM_nO_4 test

a) Usually the pH of the feed solution differed from that of the effluent during the regeneration or loading phase, due to the exchange of cations which took place in the resin:

$$2RH + Ca^{++}(\text{high pH}) \rightleftarrows R_2Ca + 2H^{+}\ (\text{low pH})$$

$$R_2Ca + 2H^{+}(\text{low pH}) \rightleftarrows 2RH + Ca^{++}(\text{high pH})$$

Keeping the resin in a fixed bed form, and the flow rate of the loading or regeneration solution at a low level the difference between the inlet and outlet pH values remains constant while the regeneration or loading takes place.

Equalization between input and output pH clearly indicates the end of the regeneration or loading and the end is fairly sharp.

The method can be successfully applied in the case of weak ion exchangers which demand a stoichiometric amount of cations for loading or regeneration.

b) By increasing the pH value of the effluent, the precipitation of a fairly insoluble compound can be favoured. In the case of loading, an increase in pH of the effluent will not have any effect until the loading is finished, then the unused loading cations will be eluted and will precipitate In the case of regeneration, an increase in pH of the effluent will precipitate the fairly insoluble cations (Ca^{++}, Cu^{++}) while the regeneration takes place. As soon as the regeneration is completed, no more cations are eluted from the resin and no more precipitation will take place in the effluent.

c) "Colouring" the resin with an indicator which changes colour with pH. The indicator is permanently absorbed on the resin and in this case, methyl red was used giving the weak cation exchanger a pink colour in an acid medium and leaving it white in a basic medium. The change in the resin form from loaded (with Ca^{++}) to regenerated

(H^+) form was indicated by a change in the resin colour (from white to pink). A change in colour from pink to white was observed during the loading.

d) After the regeneration with the aqueous solution of SO_2 was completed and the resin washed, 50ml of IN (HCl) were passed through the resin: If the first regeneration was incomplete, a certain amount of Ca^{++} or Cu^{++} ions remained in the resin. That amount was eluted by the HCl solution, which "properly" regenerated the resin. Ca^{++} and Cu^{++} ions could be detected in the effluent, by increasing the pH with NH_4OH. Ca^{++} precipitated as $CaSO_3$ and Cu^{++} coloured the solution dark blue as a result of the production of its ammoniacal complex.

e) $KMnO_4$ test.

$CaSO_3$ is a white precipitate and can be confused with $CaSO_4$ or $Ca(OH)_2$. Thus it was necessary to make sure that any precipitate obtained was $CaSO_3$. A small amount of any white precipitate was washed and then put in contac. with a solution of $KMnO_4$ (pH $\sim$ 7). If the solution did not change its red colour but on lowering the pH the precipitate dissolved, reacting with the MnO_4 - ion and as a result the red colour disappeared (red-ox reaction) then the test indicated clearly that the precipitate was $CaSO_3$ and not $CaSO_4$ or $Ca(OH)_2$. This test was performed on all white precipitates.

3. THE EXPERIMENTS

3.1. Qualitative experiments

These experiments were carried out to pinpoint likely problem areas and solve them qualitatively if necessary. One possible problem could be the precipitation of $CaSO_3$ or Chereul's salt amongst the beads of the resin clogging them and stopping further flow of the regeneration solution.

Another possible but more serious problem could be the precipitation of the abovementioned salts inside the beads of the resin, which could cause a permanent decrease in the loading capacity of the resin.

To gain information on the precipitation of $CaSO_3$ and where it is likely to occur, a small amount of resin loaded with Ca^{++} cations was contacted with a solution of $NaSO_3$. A visible precipitate was formed outside the resin. The precipitate was separated from the resin by rinsing the resin a few times with distilled water. Thereafter, both the resin and the precipitate were checked: the resin to see if there was any Ca^{++} left inside the beads in a precipitated form and the precipitate, to make sure that it was $CaSO_3$ ($KMnO_4$ test). The resin was checked by means of eluting the cations with an acid as described before. If no cations were eluted there was no precipitate in the pores.

The conclusions drawn from these experiments were that the precipitation occurs outside the resin, and could clog up the resin in a fixed bed arrangement, and that the precipitate is $CaSO_3$ and its appearance could be prevented by keeping the pH at a sufficiently low level.

A similar regeneration test was performed with a small amount of resin loaded with the ammoniacal complex of copper, this time using a solution of SO_2 in water. During the regeneration a red precipitate appeared outside the resin and this was assumed to be Chevreul's salt. Once separated, the precipitate could not be dissolved in the aqueous solution of SO_2 and it only dissolves when 5N HCl was added to the solution.

Following these tests, a few qualitative regeneration runs were carried out. A downflow regeneration of 25 ml resin loaded with Ca^{++} cations was carried out. It was found that the pH could not

be effectively controlled, since it increases during the regeneration as a result of the H^+ ions being replaced by Ca^{++} ions. Thus, tne pH of the solution front, increases above the level at which $CaSO_3$ starts precipitating clogging up the resin and stopping the solution from flowing through the bed. This precipitate was dissolved by the latter solution which has a lower pH.

Following the experiment it was decided to fluidize the bed for a short period at the beginning of the regeneration, using the regeneration solution. This procedure should avoid any precipitation of $CaSO_3$ by not allowing the pH to increase too much. Two experiments were performed and these showed that no precipitation occurred.

A few experiments in which 25 ml resin loaded with $[Cu(NH_3)_4]^{2+}$ was regenerated with an aqueous solution of SO_2, were also carried out with a short fluidized bed regeneration period at the beginning. These experiments showed that carrying out the regeneration quickly is not the only thing necessary for a good regeneration. Precipitates must also be removed from the column as quickly as possible to avoid them settling on and in the resin.

Thus, it was decided to use a syphon to continuously remove the precipitate from above the resin bed. A few regeneration experiments were carried out to improve this technique, which proved to be the answer to the precipitation problem

3.2. Quantitative regeneration experiments

Five sets of experiments were carried out during which different amounts of resin, loaded with Ca^{++}, or Ca^{++}, Mg^{2+} and Na^+, or $[Cu(NH_3)_4]^{2+}$ cations were regenerated with different aqueous solutions of SO_2.

In the first two sets of experiments, the resin was loaded with

Ca^{++} cations, while in the third set, the resin was loaded with Ca^{2+}, Mg^{++} and Na^{+} cations.

In the last two sets, the resin was loaded with $[Cu(NH_3)_4]^{2+}$ cation.

The amount of resin used in the first and fourth set was 25 ml while 200 ml resin were used in the experiments carried out on the second, third and fifth sets.

The regeneration solution used in the experiments was of three types: Demineralized water, saturated with SO_2 was used in the first and fourth set of experiments,and in a few experiments in the second and fifth set. Hard water saturated with SO_2 was used in the third set and a few experiments in the second and fifth set. In a few experiments of the second and fifth set, very hard water, saturated with SO_2 was used to regenerate the loaded resin.

The use of different types of solutions as regenerants was done to gain information about the effect of the water purity on the regeneration process. The solution was thus changed from demineralized to soft and then to hard water, to simulate what might be required if the new regeneration process were applied in industry.

P.R. Tests were usually performed as the last experiment in the set, to see if any accumulation of the loaded cation occurred during the experiments. The arrangement used for the loading and regeneration of the weak cation resin is given in Fig. 2.8 .

3.2.1. First set of experiments:

Seven experiments were carried out during which the weak cation resin, loaded with Ca^{++} cations was regenerated. The regeneration solution consisted of demineralized water saturated with SO_2.

A small part of the regeneration solution was passed upwards through the resin, after which, the rest of the regeneration solution was passed downwards through the resin. The regeneration was stopped when the pH of the effluent dropped to 1 ± 0.5. After the regeneration, the resin was rinsed with demineralized water. At the end of the regeneration, the resin returned to its original volume, colour and shape. After the first, second and seventh regeneration, "Proper Regeneration Tests" (P.R.T.) were carried out.

The results of the loading and regeneration experiments in this set, are listed in Tables 2.4 and 2.5.

3.2.2. Second set of experiments

Five experiments were carried out in this set, during which the weak cation resin was regenerated with three different solutions.

SO_2 was dissolved in three different types of water: demineralized, soft, and hard.

The regeneration was performed in the same way as in the previous set of experiments. First, a short counter current (upwards flow) period after which a long co current regeneration followed. After the regeneration, the resin was rinsed with demineralized water. P.R. Tests were performed only at the end of the fifth experiment. The results of these experiments are listed in Tables 2.6 and 2.7.

3.2.3. Third set of experiments

200 ml of the resin Zerolite 236 were used in this set of experiments. Four experiments were carried out, three in which the resin was regenerated and one in which the effluent from the previous three experiments was treated.

The regeneration step was performed with both up and dowr flow. During these experiments the regeneration solution was not split in two parts as before but was either passed completely downwards or upwards. After the regeneration the bed was washed with demineralized water.

In each of the experiments the same type of water was used both for loading and regeneration.

These three experiments were carried out to get information about the efficiency of regenerating a weak cation exchanger loaded with Ca^{++}, or Ca^{++}, Mg^{+2} and Na^{+}. The results of these experiments are shown in Tables 2.8 and 2.9.

The question of what is to be done with the regeneration effluent which contains a nigh concentration of cations, and therefore cannot be disposed of as it is, especially in this case, when the regeneration effluent is also unpleasant (SO_2 evolves continuously from the solution) it was given a trial answer: A lime treatment was tested.

The effluent solution from regeneration was contained 2810 mg/l Ca^{++}, 49 mg/l Na^{+} and 44 mg/l Mg^{++}, was treated with a slurry of 2% $Ca(OH)_2$.

After treatment, the clear solution, above the precipitate was analysed:

It contained 90 mg/l Ca^{++}, 6 mg/l Mg^{++} and 40 mg/l Na^{++}.

3.2.4. Fourth and fifth set of experiments

In the case of $[Cu(NH_3)_4]^{2+}$ being eluted from the weak acid cation exchange resin, the situation was more complicated because of the complexity of the reactions involved.

As discussed previously, during the elution, reduction -

oxidation reactions occur between the Cu^{++} ions and the regeneration solution.

Cu^{++} ions are reduced to Cu^{+} by the H_2SO_3 which is a powerful reductant. The resin itself seemed to participate in the reduction -- oxidation, but the methyl-red, which coloured the regeneration solution red, appeared to inhibit the ion exchanger from being active in the reduction-oxidation reaction.

Another problem is the wide range of pH's which exists between the loaded resin (at pH 10) and the regeneration solution at pH 1. Working together, these three factors caused precipitation of either Cu^{++} or Cu^{+} in different insoluble salts. The precipitates can block the flow of the regeneration solution.

The problems were solved using a counter current flow which fluidized the bed of the resin and by colouring the regeneration solution with methyl-red. By using a fluidized bed the regeneration solution arrives at each bead of the resin at approximately the same time, shortening the residence time of the regeneration solution but avoiding the creation of a large pH range over the bed of the resin. On the other hand, part of the regeneration solution passes through the fluidized bed without reacting, and therefore is wasted.

The effluent resulting from the elution of Cu^{++} ions, are supposed to be free of any other cations, in order to recycle them to the ammoniacal leach solution, and no attempt was made to treat these effluents.

The results of the experiments and P.R. Tests are listed in the Tables 2.10, 2.11, 2.12 and 2.13.

3.2.5. Experimental results and calculations

As mentioned before, the results of the experiments carried

out in the five sets as well as the P.R. Tests, are listed in the Tables 2.4 - 2.13.

For each set of experiments, there are two tables, the first, containing the quantities and concentrations of the solutions used for loading, rinsing (washing) and regeneration as well as the concentrations and quantities of the effluent solutions from those steps and P.R.T. The second table contains the actual amounts of different cations (in mg) in different stages, and they were obtained by multiplying the quantities of the respective solutions by their concentrations.

In this way, the results listed as IN, OUT, ELUTED, ELUTED by P.R.T. were obtained.

The results given as LOADED, are the differences between the amounts listed as IN and OUT.

The results given as ACCUMULATED are the differences between the amounts LOADED and those ELUTED (ELUTED plus ELUTED by P.R.T.)

The efficiency of elution (using an aqueous solution of SO_2) was calculated by dividing the amount eluted by that loaded and multiplying by 100.

Two step by step calculation examples are given in Appendix A.

It can be seen from the results listed that while $[Cu(NH_3)_4]^{2+}$ was loaded almost quantitatively, the loading efficiency of the Ca^{++} cations was quite poor. This can be explained by the pH of the solution which was very high and therefore favourable in the case of the ammoniacal complex, but was low and on the border of the working range

of the resin in the case of Ca^{++} solution. A higher pH could not be employed since the Ca^{++} would have precipitates. In both cases concentrated loading solutions were used to save time on the loading step which is not relevant to this work.

Both Ca^{++} and Cu^{++} cations were successfully eluted from the resin as can be seen from the results obtained, and therefore, it can be assumed that the regeneration was effective too. The elution efficiency which is equal to the regeneration efficiency is very high in the case when the solution is saturated with SO_2, and its pH is 1.0.

Fig. 2.9 shows the ideal changes in pH during the regeneration of the weak cation resin with a solution of SO_2 in water (regardless of the direction of the regeneration : upflow or downflow) as a function of volume (V) or time (T). (L) is the loading period, (B.W.) is the back washing, (3) and (R) show the changes in pH during the regeneration and (RI) is the rinsing period after the regeneraion. (1) and (2) are the pH of the regeneration and loading solution respectively.

Fig 2.10 and 2.11 show the pH changes during the regeneration in which a small part of the regeneration solution was passed upwards through the resin, before the main regeneration (downwards) was started. The dip(x) is the result of the change in direction of the regeneration solution.

3.2.6. Regenerant usage

The regenerant usage is defined as the ratio between the regenerant necessary to regenerate the resin (the stoichiometric amount) and the amount of regenerant actually used in the regeneration process.

In our case, in which the regeneration is carried out by

the acid generated in the process of the SO_2 dissolution in water, the regeneration can be theoretically carried out to completion providing enough SO_2 exists in the solution. Therefore, for the calculation of the regenerant usage, the amount of regenerant taken into account should be the entire amount of sulphur dioxide dissolved in the regeneration solution, i.e. 1.33 moles/litre = 2.66 eq/litre.

(eq 16) Regenerant usage = $\frac{\text{Equivalent taken up by the resin}}{\text{2.66 eq/l x number of litres of regeneration solution}}$

It can be seen that a regenerant usage close to unity means a high efficiency in the regenerant use.

Table 2.14 shows the value of the regeneration usage for few of the experiments described previously. These values show that most of the regenerant was wasted during the regeneration, the usage being in the range of 1-3%.

3.2.7. Regeneration and elution efficiency

The regeneration efficiency is defined as the ratio between the equivalents taken up by the resin during loading after the regeneration, to the equivalents taken up by the resin before the regeneration.

The regeneration efficiency can be calculated in this way only when the loading is conducted to exhaustion.

When the loading is not conducted to exhaustion, as in our case, the regeneration efficiency can be calculated from the ratio between the equivalents taken up by the resin to the equivalents eluted during the regeneration. A value of regeneration efficiency close to unity will show that the regeneration was almost completed.

When the regeneration is not efficient enough, part of

the loaded ion remains on the resin, not being eluted by the regenerant and it can accumulate and poison the resin.

The values of the regeneration efficiency for each regeneration carried out in different steps, is included in the tables 2.4 to 2.13.

3.3. The influence of pH on the regeneration efficiency

All the experiments described until now, were carried out with a saturated solution of SO_2 in water. These solutions had a pH = 1.00 and they were made up by bubbling a stream of SO_2 through the respective solution. The regenerations carried out with these solutions had a very high regeneration efficiency even though the water used in preparing the solution was changed from distilled water to very hard water.

Having therefore concluded that the regeneration of a weak cation exchange resin, loaded with Ca^{++} cations can be carried out with a regeneration efficiency which is close to 100% by using a saturated solution of SO_2 in water a set of new experiments was designed to look into the influence of pH on the regeneration efficiency.

The arrangement used was the same as that used for the other experiments (fig. 2.8). Five experiments were carried out with the regeneration solution at different pH. This was done by diluting a portion of the original solution.

The regeneration solution for the first experiment was pH=1,00 The pH for the second, third, fourth and fifth experiments were 1.15, 1.57, 1.95 and 2.35 respectively.

25 ml of the resin Zerolite 236 loaded with Ca^{++} cations, was used in each experiment.

Samples of 50 ml were taken during the first, second and third experiments, 100 ml during the fourth experiment and 250 ml during the fifth experiment. The samples were analyzed for

Ca^{++} cations and pH. The analyses of Ca^{++} were carried out with the Atomic Absorption spectraphotometer described before. The pH could be read to two decimal places.

3.3.1. Experimental results

Five regeneration experiments were carried out, each regeneration being done on the same amount of loaded resin, but with a different concentration of H^+ (different pH's).

Table 2.15 shows the concentration of the samples and their pH, as well as the pH of the regeneration solution used in that specific experiment. Fig. 2.12 shows the Ca^{++} breakthrough curves which were constructed from the same data contained in Table 2.15. The amount of calcium in mg. (Table 2.16) was plotted in Fg. 2.13, which shows besides the breakthrough curves of Ca^{++} (in mg), the fractional attainment to complete elution (100%), as a function of pH of the regeneration solution and of the effluent volume.

The top part of Fig.2.13 shows the change in pH during the regeneration.

During the regeneration, part of the H^+ ions were loaded on the resin. Table 2.17 gives the values of hydrogen ion (H^+) in the regeneration solution, as well as in the different effluent samples. These values were plotted in Fig. 2.14 as a function of the effluent volume, and were used to calculate the amount of H^+ loaded on the resin. The amount of H^+ loaded during each regeneration is given in Table 2.17 and plotted as H^+ loaded curves in Fig. 2.15.

The similarity of Fig. 2.15 with Fig. 2.12 or 2.13 shows that while Ca^{++} was eluted from the resin, the hydrogen ions were loaded instead.

By using the same method as shown previously in the regenerant chapter, the generant usage efficiency was calculated for the five regeneration experiments and the value listed in Table 2.16.

A summarising figure which shows the influence of the pH on the regeneration (elution) efficiency, is given in Fig. 2.16.

The figure represents the number of Bed Volumes (B.V.) of the regeneration solution, necessary to achieve 50% regeneration (elution) of the weak acid cation exchanger loaded with Ca^{++} cations, as a function of pH (of the regeneration solution).

The results from these experiments showed that for the first three cases, the regeneration could be conducted to a very high value and to a fair value in the fourth case, while the efficiency dropped to a low value (53%) in the fifth case.

The regenerant usage, increased in the same cases, with the increase in the pH value.

4. DISCUSSION

The experimental results listed in the Tables 2.4-2.13 show that the amount eluted using this new regeneration method remains stable and close to the amount loaded.

These tests show that no significant accumulation occurred between the third and the seventh experiments in the first set and that this regeneration method has no negative effect on the loading capacity of the resin.

During the 5 experiments carried out in the second set, the regeneration solution was changed from demineralized water to soft water and then to hard water. The change in the type of water used for regeneration

was to check the effect of increasing concentration of Ca^{++} in the regeneration solution on the regeneration. The results listed in Tables 2.6 and 2.7 show that the regeneration of the resin loaded with Ca^{++} ions is not affected by the use of a solution of hard water. The loading capacity of the resin did not drop either, following the regeneration of the ion exchanger with SO_2 in soft or hard water and remained the same during the experiments.

The P.R. test was performed only after the last experiment and showed clearly that no accumulation occurred during the five experiments of regeneration with SO_2 in tap and hard water, and that the elution and regeneration efficiencies are the same.

The third set of experiments included only three regenerations and one experiment of treatment a regeneration effluent.

These experiments are the culmination of this research since except for the SO_2 the solution used for regeneration had the same composition as the loading solution. The loading solution, or in other words the solution which must be treated by ion exchange can be successfully used for the regeneration of the resin. This means that no special solution must be prepared for regeneration.

In these experiments ar upflow regeneration (counter current) was also performed, showing that it too could be employed in the regeneration of the weak cation exchanger with SO_2 in water.

In the fourth experiment, by adding $Ca(OH)_2$ slurry to the solution of the regeneration effluents, the acid (H_2SO_3) was neutralized and all the cations were precipitated as sulphites or (eventually) hydroxides. The result of this separate experiment carried out on the regeneration effluent, shows that the effluents from regeneration and rinsing can be treated successfully and the solution recycled. It can be seen that the regeneration was efficient under all conditions from the most ideal when demineralized water only was used, to the least ideal ones when the loading solution was used for regeneration.

It can also be seen that the only difference between the downwards and

the upwards flow regeneration, is in the resulting amount of effluent. The efficiency of the elution in these two cases is the same while the solution needed for the counter-current elution is about 4 times the quantity of the solution needed for the co-current regeneration.

The above experiments show that an efficient way of controlling the regeneration process was to check the changes in pH of the effluent solution. This enables one to pinpoint the approximate time when the regeneration was completed.

Even when the resin was loaded with the ammoniacal complex of copper, the new regenerant proved to be effluent.

All the experiments performed indicate that for a resin loaded with $[Cu(NH_3)_4]^{2+}$ the regeneration must be carried out quickly. A slow flowrate can result in the formation of precipitates among the beads of the resin, as pointed out previously.The precipitation is probably facilitated when the solution used for regeneration contains a large amount of Ca^{++} ions. In the case of $[Cu(NH_3)_4]^{2+}$ loaded resin, the efficiency of elution is affected by a high amount of Ca^{++} ions in the solution. The results listed in the tables 2.12 & 2.13 show that the efficiency of the regeneration dropped slightly when a solution of SO_2 in hard water was used. Although when heavy metals are loaded on the resin, the effect is present, it is not a large one. The use of this type of solution can be considered, if necessary, if there are no restrictions on the purity of the solutions.

The lower efficiency recorded in the second experiment is due to an error which slowed down the regeneration, causing precipitation in the resin. The precipitate could not be dissolved by the regeneration solution, but appeared in the effluent of the next loading.

P.R. Tests were performed only at the end of the set.

The second and fourth regenerations of the Cu^{++} loaded resin, showed that the precipitate which formed, and remained in the resin, was dissolved and eluted from the resin in the next loading step, therefore this does not affect the loading capacity of the resin.

These experiments showed that when precipitates are produced, and the regeneration must be carried out in a fluidized bed manner, the pH cannot be used to determine the end of the regeneration.

Only after converting to a downward flow after the elimination of the precipitates, is it possible to test for the end of the regeneration.

In any event even though the regeneration of the resin loaded with the ammoniacal complex of copper, proved to be very complicated and difficult to carry out, the elution was accomplished with good results.

The experiments aimed to investigate the influence of pH in the regeneration solution on the regeneration efficiency, showed a drop in the efficiency of regeneration and elution of the resin as a function of the increasing pH of the regeneration solution. This is clear from every figure constructed with the data from these experiments. On the other hand, a decrease in H^+ concentration by 4500 times, decreased the efficiency of regeneration by only 50% and this while the regeneration solution needed increased drastically. The amount of regeneration solution with a relatively high pH (2.35) needed to achieve a 50% regeneration is approximately 15 times higher than that with low pH (1.15).

Summarizing the results of the experiments described in this chapter, it can be concluded that the new regeneration process is effective and efficient. It is easily controlled when no precipitates are produced during the regeneration, and it becomes complicated when precipitates must be eliminated during the process. The new regenerate has no effect on the loading capacity of the resin and it can be carried out with any type of water. The efficiency of SO_2 urilization is low, and this could lead to an effluent problem. This could be minimized by recycling the effluent solution.

Although the regeneration can theoretically be conducted to completion the amount of regeneration solution having a pH higher than 1.6, is much too high for an economical regeneration to be carried out.

5. EXPERIMENTAL ERRORS

The accuracy of all the individual measurements was aimed at being better than 5%. Probably the least accurate was the concentration measurement on the atomic absorbtion spectrophotometer and this was not much better than the above figure. Thus, the volumes of the samples were measured to about 2.5% accuracy not to further degrade the accuracy of the results.

The check that this estimate is reasonable can be seen from the P.R. Tests: After a number of runs these tests enabled the overall mass balance to be checked. These results confirm the estimated accuracy.

During the individual experiments, the temperature was 20° ± 4°C. Since this fluctuation affects the pH measurements, the temperature was monitored and the pH-meter corrected with the temperature compensator.

The flow rates were measured with an accuracy of approximately 10%, but since these measurements were not directly used and the effects are not sensitive to flow rate over a fairly wide range they should not appreciably effect the experimental error.

moles / litre								pseudo mole fraction of the species			
pH	H^+	HSO_3^-	$SO_3^=$	H_2SO_3	SO_2 dissolved (Tso_2)	SO_2 dissolved but unhydrolyzed	$HSO_3^- + SO_3^= + H_2SO_3 = A$	$\frac{HSO_3^-}{A}$	$\frac{SO_3^=}{A}$	$\frac{H_2SO_3}{A}$	K_o
1.00	0.1	0.1	6.28×10^{-8}	0.58	1.33	0.6	0.68	0.15	~0	0.85	0.51
1.15	7×10^{-2}	7×10^{-2}	6.28×10^{-8}	0.28	0.66	0.31	0.35	0.20	~0	0.80	0.53
1.57	2.7×10^{-2}	2.7×10^{-2}	6.28×10^{-8}	0.043	0.17	0.10	0.07	0.39	~0	0.61	0.59
1.95	1.1×10^{-2}	1.1×10^{-2}	6.28×10^{-8}	0.007	0.041	0.023	0.018	0.61	~0	0.39	0.41
2.35	4.5×10^{-3}	4.5×10^{-3}	6.28×10^{-8}	0.0012	0.010	0.0023	0.0057	0.78	~0	0.21	0.57

TABLE 2.1 The concentration of different species resulted when SO_2 was dissolved in water.

TABLE 2.2

(From the "Handbook of Chemistry and Physics")
43rd edition (1961)

Compound.	Solubility in Gms/100 ml of Water Cold	Hot	Other	Thermal Stability
$BaSO_3$	0.02^{20}	0.002^{80}	HCL	decomposes
$CaSO_3.2H_2O$	0.0043	0.0011	S. H_2SO_3	decomposes 650°
$Ca(HSO_3)_2$	Sol.		Sol. acid	-
$FeSO_3.3H_2O$	V.Sl.S		Sol. So_2 sol'n.	decomposes 250°c
$K_2SO_3.2H_2O$	100	<100		decomposes
$KHSO_3$	Sol.	Sol.		decomposes 190°
Na_2SO_3	12.54	28.3	Sl. sol. alcohol	decomposes
$Na_2SO_3.7H_2O$	32.8	196.	Sl. sol. alcohol	decomposes decomposes
$NaHSO_3$	V.S.	V.S.	Sl. sol. alcohol	decomposes decomposes
$MgSO_3.6H_2O$	1.25	0.83		decomposes

TABLE 2.3

INTERMEDIATE COPPER SULPHITE PRODUCTS (SOURCE [99])

PRODUCT	COMPOSITION	COLOUR
Chevreul's Salt	Cu_2SO_3; $CuSO_3$; $2H_2O$	Red
Monocupric Hepta-Cuprous Triammonium Sulphite	$Cu_2(NH_4)_3(SO_3)_6 12H_2O$	White
Cuprous Ammonium Sulphite	$Cu_2SO_3(NH_4)SO_3$	Brown to tan

REGENERATION OF A WEAK CATION EXCHANGER (ZEROLITE 236) LOADED WITH Ca^{++}, USING A SOLUTION OF SO_2 IN DEMIN. WATER

TABLE 2.6

EXP.NO.	Feed Solution		Effluent Sol.		Eff. Washing Sol.		Elution Sol.		P.R.T	
	ml.	ppm Ca	ml	ppm Ca	ml	ppm Ca	ml	ppm Ca	ml	ppmCa
1	4000	2150	4000	1975	250	720	1180	420	960	15
2	4000	2150	4250	1905	Included in the Effluent		860	575	750	15
3	4000	2145	4000	1985	250	470	750	700	-	-
4	4000	2120	4000	1935	270	815	630	825	-	-
5	4000	2120	4000	1935	250	737	1170	480	-	-
6	4000	2120	4000	1945	260	520	1250	450	-	-
7	4000	2120	4000	1930	250	730	1170	495	325	5

REGENERATION OF A WEAK CATION EXCHANGER (ZEROLITE 236) LOADED WITH Ca^{++}, USING A SOLUTION OF SO_2 in DEMIN. WATER.

TABLE 2.5.

EXP NO	IN [mg]Ca	OUT [mg]Ca	LOADED [mg]Ca	ELUTED [mg]Ca	ELUTED BY P.R.T. [mg]Ca	ACCUMULATED [mg]Ca	Efficiency %
1	8600	7900 + 180	510	495	14	-	97
2	8600	8096.	503	494	11	- 2	98
3	8580	7940 + 117	522	525	-	+ 2	100
4	8480	7740 + 220	520	519	-	+ 0.2	100
5	8480	7740 + 185	555	561	-	- 5	101
6	8480	7780 + 135	564	562	-	+ 2	100
7	8480	7720 + 182	577	579	2	- 2	100

Exp. No.	Loading solution ml	Ca mg/l	Loading effluent ml	mg/l Ca	Rinsing after loading ml	mg/l Ca	Regeneration solution ml	mg/l Ca	Regeneration effluent ml	mg/l Ca	Rinsing after regeneration ml	mg/l Ca	P.R.T. ml	mg/l
1.	4000 4000 3150	1430 1430 1430	4000 4000 3150	900 1220 1300	600	700	1150	0	1150	2530	1000	55		
2.	11150	1430	4000 4000 3150	920 1220 1330	600	700	1260	35	1260	2190	1050	41		
3.	11150	1430	4000 4000 3150	910 1230 1300	650	710	1050	35	1050	2660	1160	57		
4.	11150	1430	4000 4000 3150	860 1220 1350	600	750	1100	197	1100	2690	1530	77		
5.	11150	1430	4000 4000 3150	890 1210 1290	650	670	1050	197	1050	2950	1920	49	1000	58

TABLE 2.6. : REGENERATION OF A WEAK CATION EXCHANGER (ZEROLITE 236) LOADED WITH Ca^{++} IONS, USING A SOLUTION OF SO_2 IN WATER

Exp. No.	LOADING IN (Ca) mg	LOADING OUT (Ca) mg	LOADED (Ca) mg	REGENERATION IN (Ca) mg	REGENERATION ELUTED (Ca) mg	ACCUMULATED (Ca) mg	ELUTED IN THE P.R.T. (Ca) mg	Effic. %
1.	15944	3600 4880 4095 420	2949	0	2909 55	-15	-	100.5
2.	15944	3680 4880 4189 420	2775	44	2759 43	16	-	99.4
3.	15944	3640 4920 4095 461	2828	37	2793 66	6	-	99.8
4.	15944	3440 4880 4252 450	2922	217	2959 118	62	-	98.1
5.	15944	3560 4840 4063 435	3045	207	3097 94	61	58	98.2

TABLE 2.7 -REGENERATION OF A WEAK CATION EXCHANGER LOADED WITH Ca^{++} IONS, USING A SOLUTION OF SO_2 IN WATER

IONS	EXP NO	LOADING SOL.		LOADING EFFL.		RINSING		REG. SOL.		REG. EFFL.		RINSING AFTER REG		P.R.T.	
		ml	mg/l	ml	average mg/l	ml	mg/l	ml	mg/l	ml	mg/l	ml	mg/l	ml	mg/l
Na^{+}	1C	16000	37	16000	37	-	-	1760	39	1760	53	1370	17	-	-
Mg^{++}			12		11	-	-		13		54		5	-	-
Ca^{++}			202		113	-	-		460		4010		106	-	-
Na^{+}		42000	39	42000	37	-	-		-		-		-	-	-
Mg^{++}			14		12	-	-		-		-		-	-	-
Ca^{++}			425		280	-	-		-		-		-	-	-
Na^{+}	2C	41320	39	41320	37	600	30	4530	39	4530	45	2220	13		-
Mg^{++}			13		10		4		13		34		3		-
Ca^{++}			465		275		157		465		1850		158		-
Na^{+}	3C	30500	39	30500	38	600	23	5020	39	5020	38	1840	11	1150	0
Mg^{++}			12		10		5		12		28		5		0
Ca^{++}			625		387		287		625		1864		112		22

TABLE 2.8

Regeneration of a weak cation exchanger (zerolite 236) loaded with Ca^{++}, Mg^{++} and Na^{+} using a solution of H_2SO_3.

		LOADING				REGENERATION			
Exp No.	Ions	Feed Solution (mg/1)	In (mg)	Out (mg)	Loaded (mg)	In (mg)	Eluted	Accumulated (mg) and Efficiency	P.R.T.
1C	Na^+	37 39	2188	2135	52	69	116 (48)	4 91.4%	-
	Mg^{++}	12 14	746	665	80	24	102 (79)	2 97.6%	-
	Ca^{++}	202 425	21082	13593	7489	810	7203 (6393)	1096 85.4%	-
2C	Na^+	39	1611	1547	64	177	233 (56)	8 86.7%	-
	Mg^{++}	13	537	439	95	5	162 (103)	-8 108.3%	-
	Ca^{++}	465	19214	11457	7757	2106	8731 (6624)	1132 85.4%	-
3C	Na^+	39	1189	1173	16	195	210 (15)	2 88.2% 1 93. %	0
	Mg^{++}	12	381	308	73	63	149 (89)	-10 113.8% -16	0
	Ca^{++}	625	19062	11975	7087	3137	9522 (6397)	690. 92.5%	25

TABLE 2.9 -REGENERATION OF A WEAK CATION EXCHANGER (ZEROLITE 236)
LOADED WITH Ca^{++}, Mg^{++} AND Na^+ USING A SOLUTION OF H_2SO_3

REGENERATION OF WEAK CATION EXCHANGER (ZEOLITE 236) LOADED WITH Cu^{++}, USING A SOLUTION OF SO_2 IN DEMIN. WATER

TABLE 2.10

EXP NO	Feed Solution		Effluent Solution		Effluent washing Sol.		Elution + Washing Sol.		PRT + Washing Sol.	
	ml	ppm Cu	ml	ppm Cu	ml	ppm Cu	ml	ppm Cu	ml	ppm Cu
1	2000	860	2210	80	incl. in the Effluent		1180	1290	330	77
2	2000	840	2224	63	incl. in the Effluent		1110	1380	560	40
3	3000	840	3000	235	260	204	1650	1070	-	-
4	3000	840	3000	230	260	240	1750	1010	-	-
5	3000	840	3020	233	250	210	1670	1055	-	-
6	3000	840	3000	230	250	250	1030	1715	-	-
7	3000	840	3000	230	250	255	1000	1765	490	5

REGENERATION OF A WEAK CATION EXCHANGER (ZEROLITE 236) LOADED WITH Cu^{++} IONS, USING A SOLUTION OF SO_2 IN DEMIN. WATER

TABLE 2.11.

EXP. NO.	IN [mg] Cu	OUT [mg] Cu	LOADED [mg] Cu	ELUTED [mg] Cu	ELUTED BY P.R.T. [mg] Cu	Efficiency %	ACCUMULATED [mg] Cu
1	1720	176	1543	1522	25	98.6	- 4
2	1680	140	1540	1552	22	99.4	- 14
3	2520	705 + 53	1762	1765	-	100.2	- 3
4	2520	690 + 62	1768	1767	-	100.0	+ 0.1
5	2520	707 + 52	1764	1762	-	99.9	+ 2
6	2520	690 + 62	1767	1766	-	99.9	+ 1
7	2521	690 + 64	1766	1765	2	99.9	- 1

	Loading Solution		Loading effluent		Rinsing after loading		Regeneration solution		Regeneration effluent			Rinsing after regeneration			P.R.T.		
	ml	mg/l Cu	ml	Cu mg/l	ml	mg/l Cu	ml	(Ca)mg/l	ml	(Cu)mg/l	(Ca)mg/l	ml	(Cu)mg/l	(Ca)mg/l	ml	(Cu) mg/l	(Ca) mg/l
1	4000	1310	4000	5	600	56	4000	0	4000	2400	0	1260	30	0	-	-	-
	4000	1310	4000	7													
	2000	1310	2000	54			2650	0	2650	1000	0				-		
2	4000	1330	4000	11	600	80	4000	35	4000	2100	24	1260	245	12	-	-	-
	4000	1330	4000	9													
	3000	1330	3000	51			2900	35	2900	1840	45						
3	11000	1330	4000	63	600	159	4100	35	4100	3110	23	1500	62	35	-	-	-
			4000	23													
			3000	101			970	35	970	1000	35						
4	11000	1340	4000	21	600	157	4000	197	4000	2390	180	1380	151	45	-	-	-
			4000	9													
			3000	99			1800	197	1800	950	220						
5	11000	1350	4000	123	600	179	4000	197	4000	2950	175	1460	123	51	2690	153	15
			4000	23													
			3000	113			1800	197	1800	790	203						

TABLE 2.12. REGENERATION OF A WEAK CATION EXCHANGER (ZEROLITE 236) LOADED WITH Cu^{++} IONS, USING A SOLUTION OF SO_2 IN WATER

Exp.No.	LOADING IN mg Cu	LOADING OUT Cu mg	LOADED Cu mg	REGENERATION IN(Ca) mg Cu	REGENERATION ELUTED (Cu) mg	REGENERATION ELUTED (Ca) mg	ACCUMULATED (Cu) mg	ACCUMULATED (Ca) mg	ELUTED IN THE P.R.T. (Cu) mg	ELUTED IN THE P.R.T. (Ca) mg	EFFICIENCY OF REGENERATION (Cu) %	EFFICIENCY OF REGENERATION (Ca) %
1	13000	20 28 108 33	12810	0	10000 2729 44	0	37	0	-	-	99.7	-
2	14630	44 36 153 48	14349	241	8400 5336 309	96 130 15	304	-0.1	-	-	97.8	100
3	14630	252 92 303 95	13888	177	970 12751 93	94 34 52	74	-3	-	-	99.5	101.9
4	14740	84 36 297 94	14229	1143	9560 2106 2084	720 396 62	479	-35	-	-	96.6	103.1
5	14850	492 92 339 107	13820	1143	11800 1422 184	700 365 76	414	2	413	41	97.7	99.8

Table 2.13

REGENERATION OF A WEAK CATION EXCHANGER (ZEROLITE 236) LOADED WITH Cu^{++} IONS, USING A SOLUTION OF SO_2 IN WATER

Set of experiments	Exp. Number	Data from table	Kind of cations loaded	Regenerant usage
First	2 3 4	2.4, 2.5	Ca^{++}	1% 1.3% 1.1%
Second	2 3	2.6, 2.7	Ca^{++}	4.1% 5.0%
Third	2C	2.8, 2.9	Ca^{++}	4.7%
Fourth	2	2.10, 2.11	$[Cu(NH_3)_4]^{2+}$	1.5%
Fifth	2	2.12, 2.13	$[Cu(NH_3)_4]^{2+}$	3.8%

Table 2.14 Regenerant usage efficiency for some of the experiments carried out in the first five sets.

TABLE 2.15

EFFECT OF pH ON THE REGENERATION :

Ca^{++} CONCENTRATIONS OF SAMPLES AND THEIR pH

Exp.	Vol. of the Samples (ml)	Ca^{++} mg/l	pH	pH(reg. solution)
1	50	86	3.27	1.00
	50	6040	2.3	
	50	3080	1.41	
	50	151	1.12	
	50	10	1.05	
2	50	800	2.84	1.15
	50	6000	2.4	
	50	2300	1.49	
	50	128	1.22	
3	50	220	2.6	1.57
	50	1720	2.68	
	50	1880	2.72	
	50	2120	2.63	
	50	1640	2.17	
	50	880	1.87	
	100	340	1.67	
	50	115	1.58	
4	100	270	3.07	1.95
	100	400	3.53	
	100	372	3.57	
	100	372	3.63	
	100	372	3.63	
	100	372	3.36	
	100	372	[illegible]	
	100	300	2.84	
	100	300	2.56	

contd....

Exp.	Vol of the Samples (ml)	Ca^{++} mg/l	pH	pH(reg solution)
5	250	120	3.47	2.35
	250	135	3.49	
	250	135	3.49	
	250	135	3.5	
	250	135	3.54	
	250	135	3.63	
	250	135	3.57	
	500	105	3.9	

TABLE 2.16

Exp	Ca [mg]	Σ Ca	Fractional Completion	Reg. usage
1	4 302 154 8 0	468	100.0%	3.5%
2	40 300 115 6	461	99.5%	8.6%
3	11 86 94 106 82 44 34 6	463	99.8%	16.0%
4	27 40 37 37 37 37 37 30 30	314	65.0%	22%

..../

Exp	$Ca_{[mg]}$	$\sum Ca$	% Elution	Reg. usage
5	30 30.75 30.75 30.75 30.75 30.75 30.75 26	259	55.3%	28.7%

TABLE 2.16 Calcium elution, Regeneration and Regenerant Usage Efficiency

TABLE 2.17

H^+ Concentration in the reg. solution, effluent and resin

$[H^+]$ in g/ℓ

Reg. Solution (IN)	Effluent (OUT)	resin = IN - OUT
0.1	5.37×10^{-4}	0.1
	5×10^{-3}	0.2
	3.9×10^{-2}	0.2
	7.6×10^{-2}	0.3
	8.9×10^{-2}	0.3
7.0×10^{-2}	1.4×10^{-3}	0.1
	$4. \times 10^{-3}$	0.2
	3.2×10^{-2}	0.3
	6×10^{-2}	0.3
2.7×10^{-2}	2.5×10^{-3}	0.02
	2.1×10^{-3}	0.05
	2×10^{-3}	0.07
	2.3×10^{-3}	0.1
	6.76×10^{-3}	0.12
	1.3×10^{-3}	0.13
	2.1×10^{-2}	0.14
	2.6×10^{-2}	0.14
1.1×10^{-2}	8.5×10^{-4}	0.01
	3×10^{-4}	0.02
	2.7×10^{-4}	0.03
	2.3×10^{-4}	0.04
	2.3×10^{-4}	0.05
	4.4×10^{-4}	0.06
	8.9×10^{-4}	0.07
	1.4×10^{-3}	0.08
	2.7×10^{-3}	0.09

Reg. Solution (IN)	Effluent (OUT)	resin = IN - OUT
4.5×10^{-3}	3.4×10^{-4}	4.2×10^{-3}
	3.2×10^{-4}	8.7×10^{-3}
	3.2×10^{-4}	1.3×10^{-2}
	3.2×10^{-4}	1.7×10^{-2}
	2.9×10^{-4}	0.02
	2.3×10^{-4}	0.02
	2.7×10^{-4}	0.03
	1.31×10^{-4}	0.03

Table 2.17

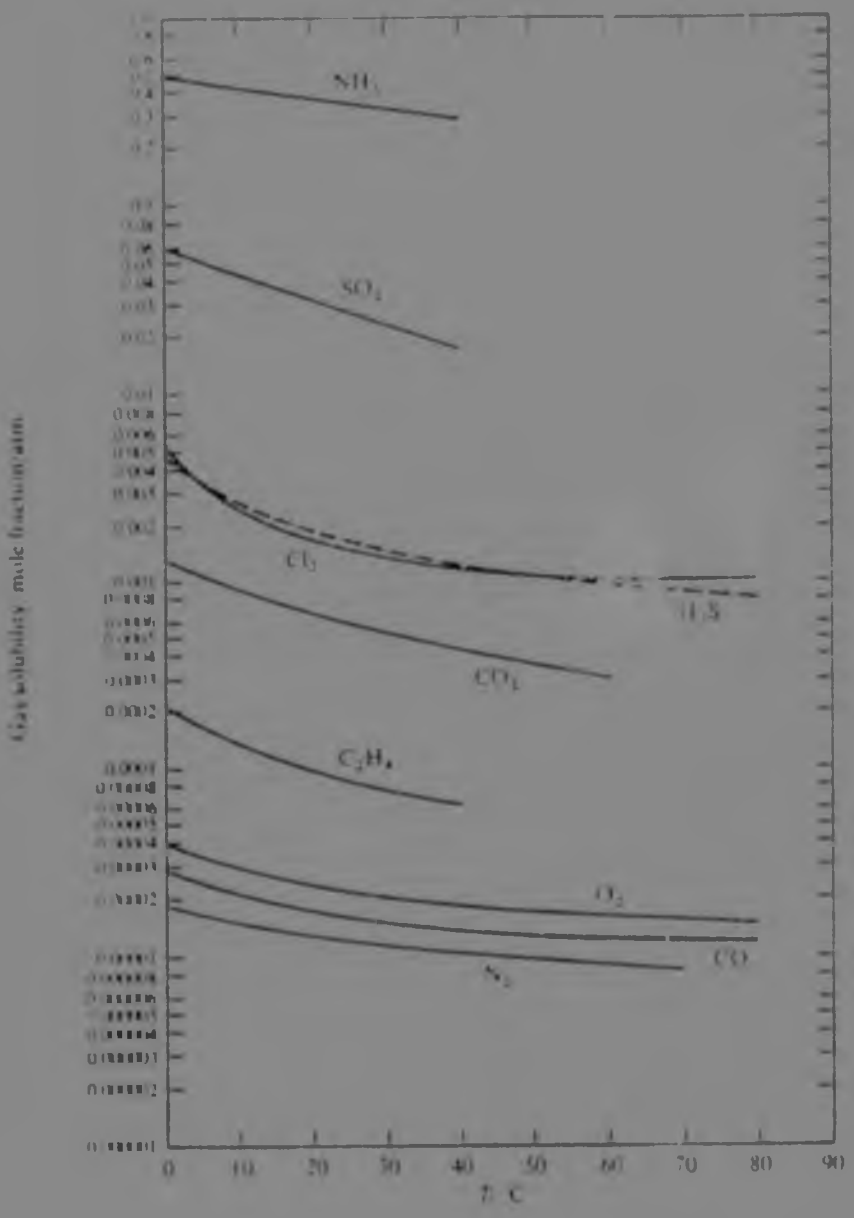

Fig. 2.1. Solubilities of various gases in water at pressures of 5 atm or less (Schmidt & List, 1962). Source [95]

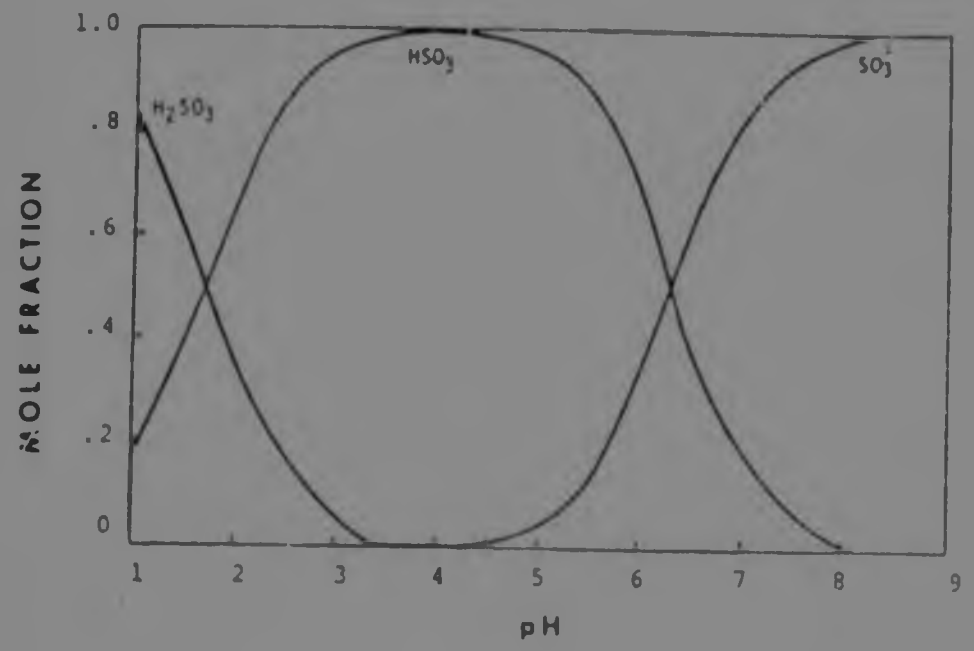

Fig. 2.2. Effect of pH on distnbution of SO_2 species in aqueous medium.

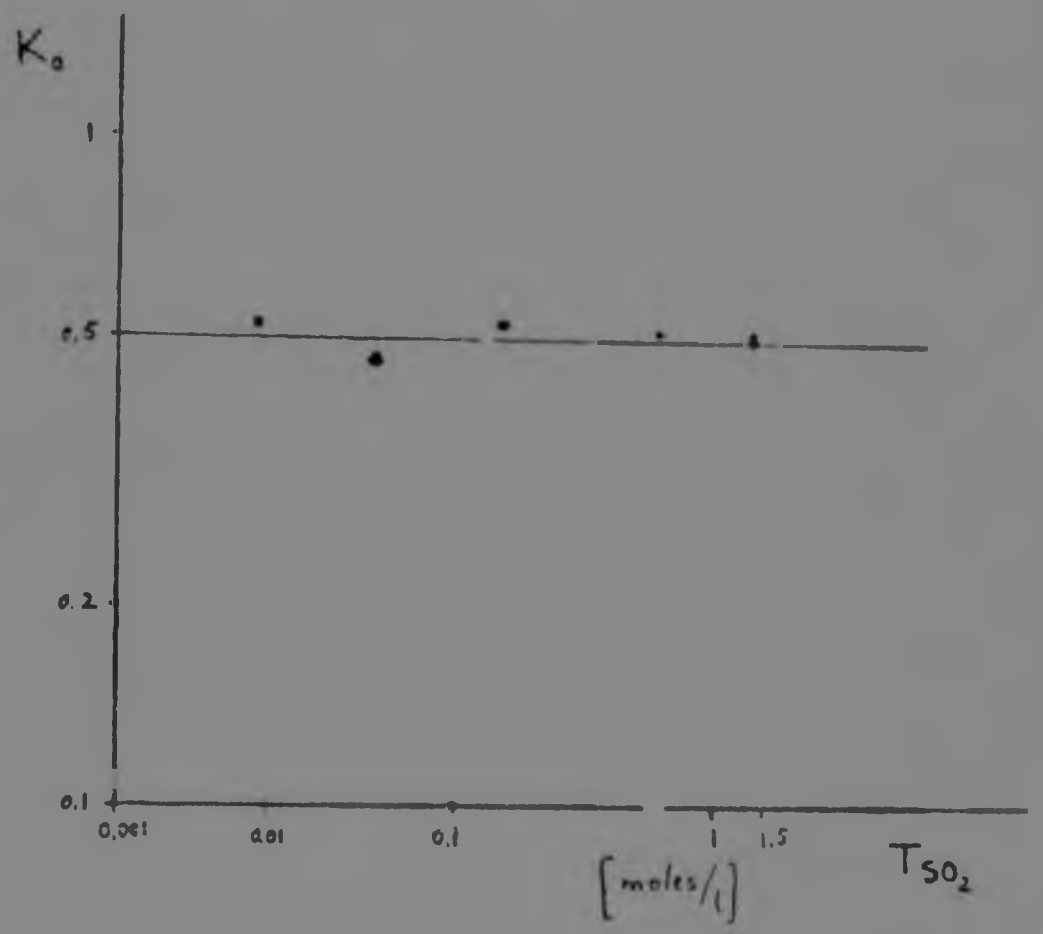

Figure 2.3. K_o as a function of T_{SO_2}

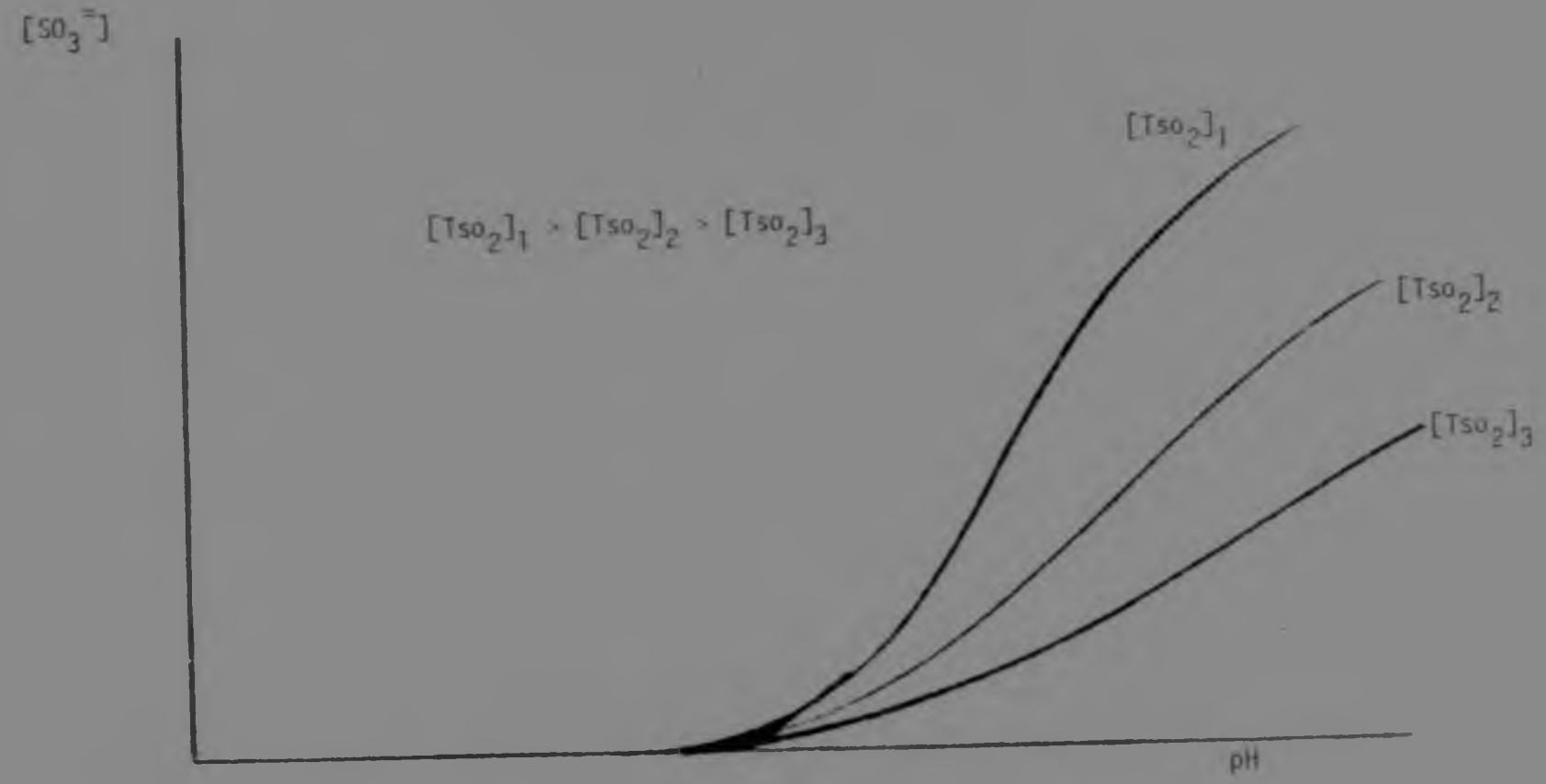

Figure 2.4. Concentraion of $SO_3^{=}$ ions as a function of pH

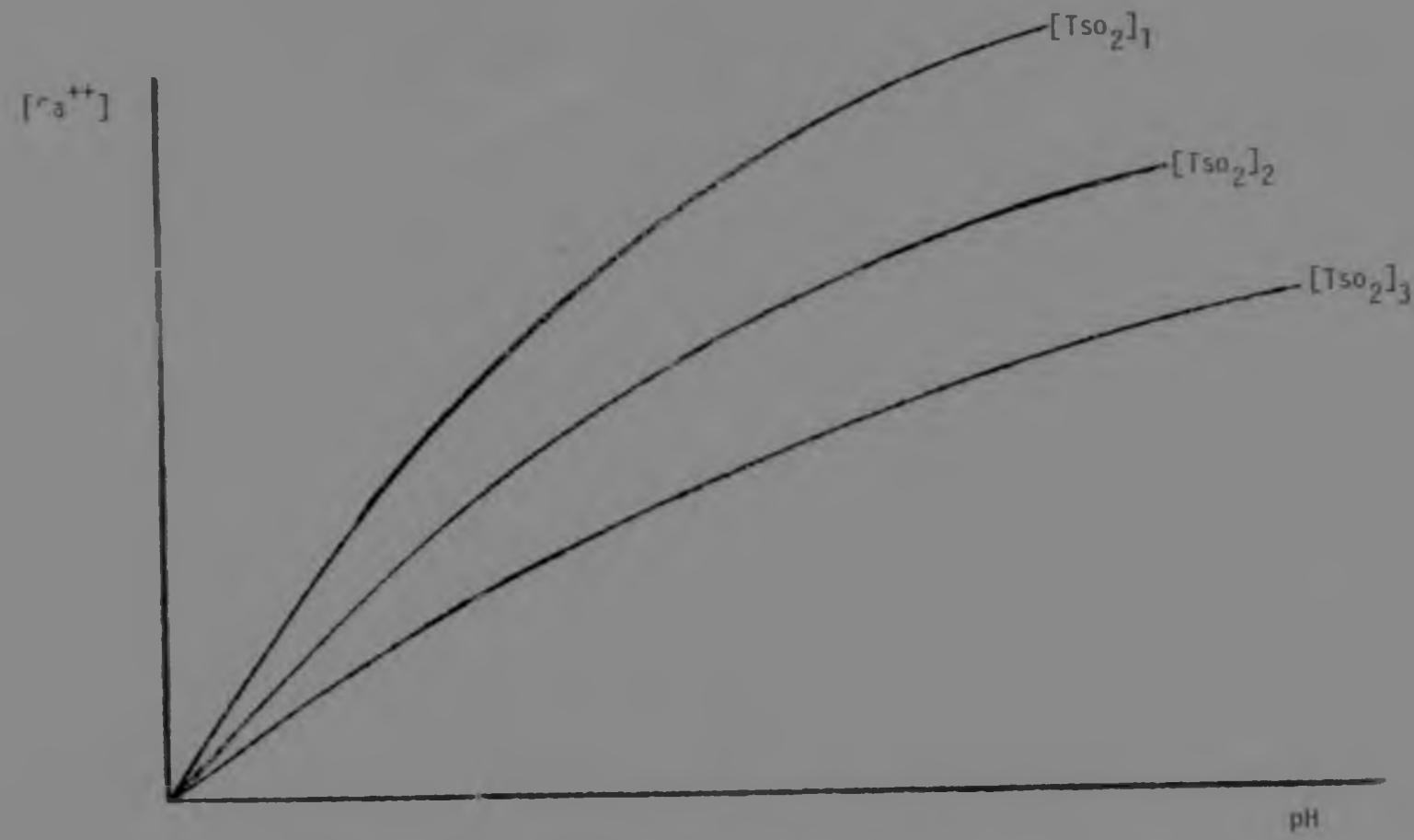

Figure 2.5. Concentraion of Ca^{++} ions as a function of pH.

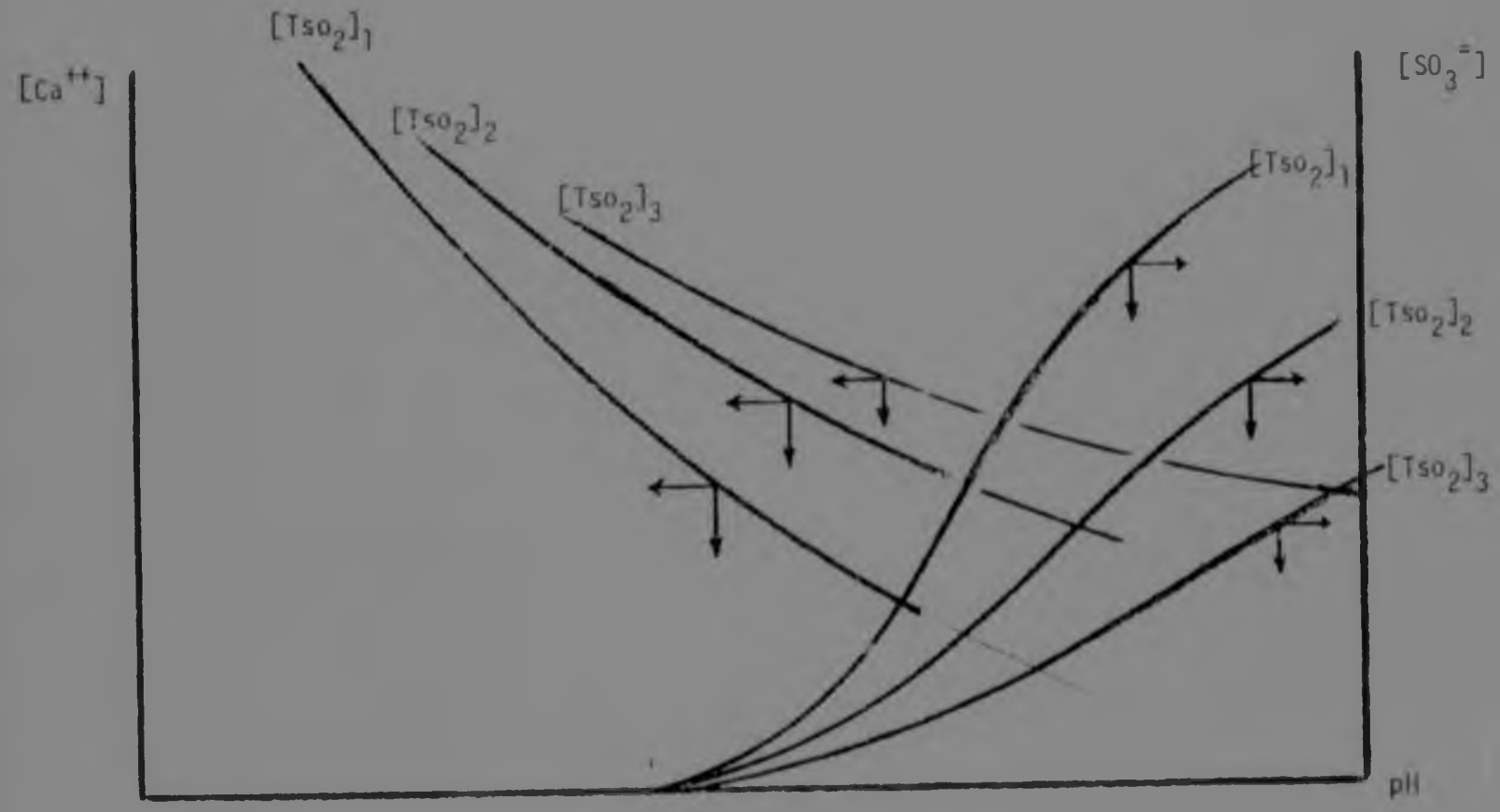

Figure 2.6. The conc.of Ca^{++} ions needed for the precipitation of $CaSO_3$, as a function of pH and $SO_3^{=}$ ions concentraion.

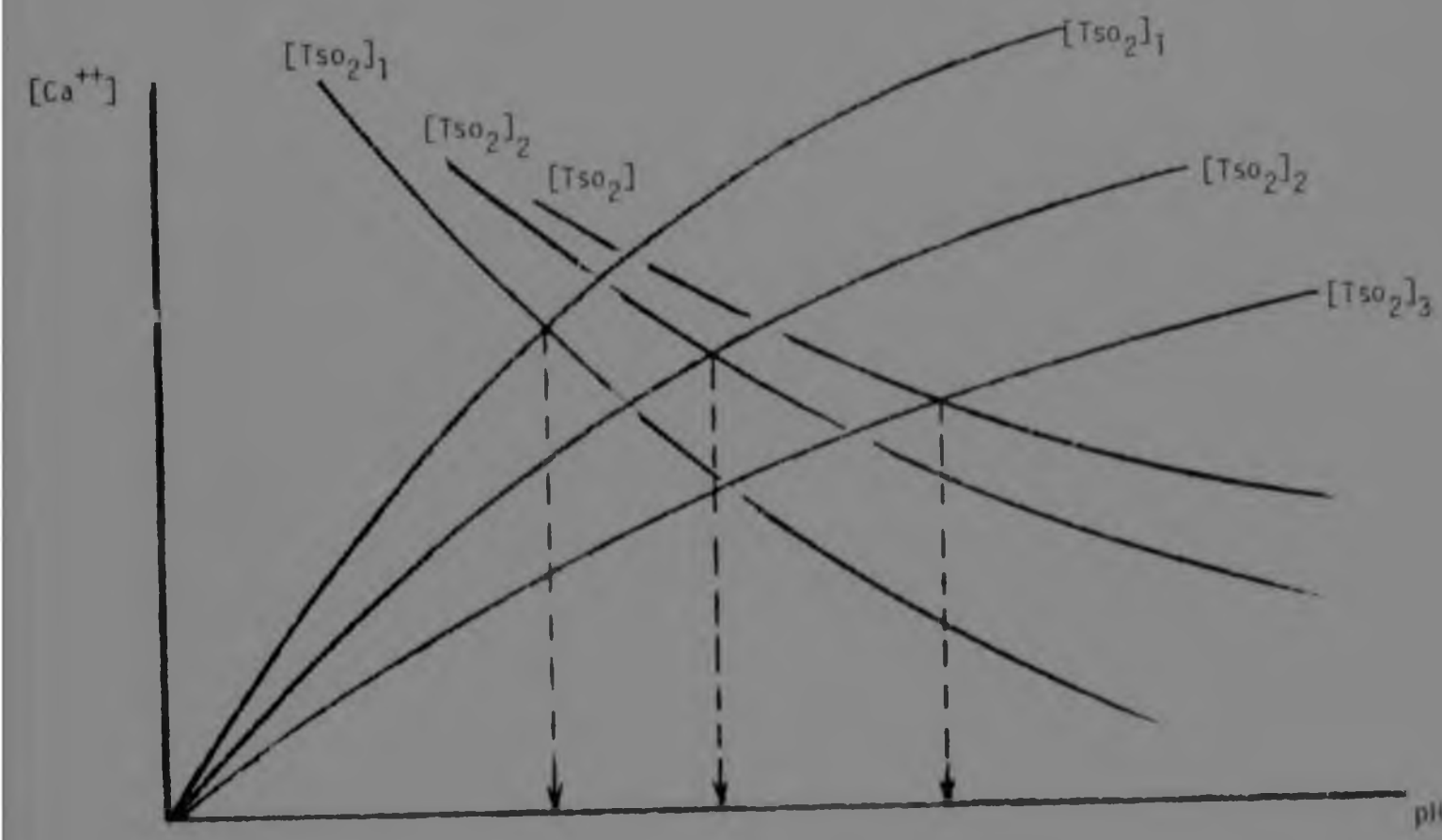

Figure 2.7. The pH at which $CaSO_3$ starts precipitating, as a function of Tso_2 and Ca^{++} concentration.

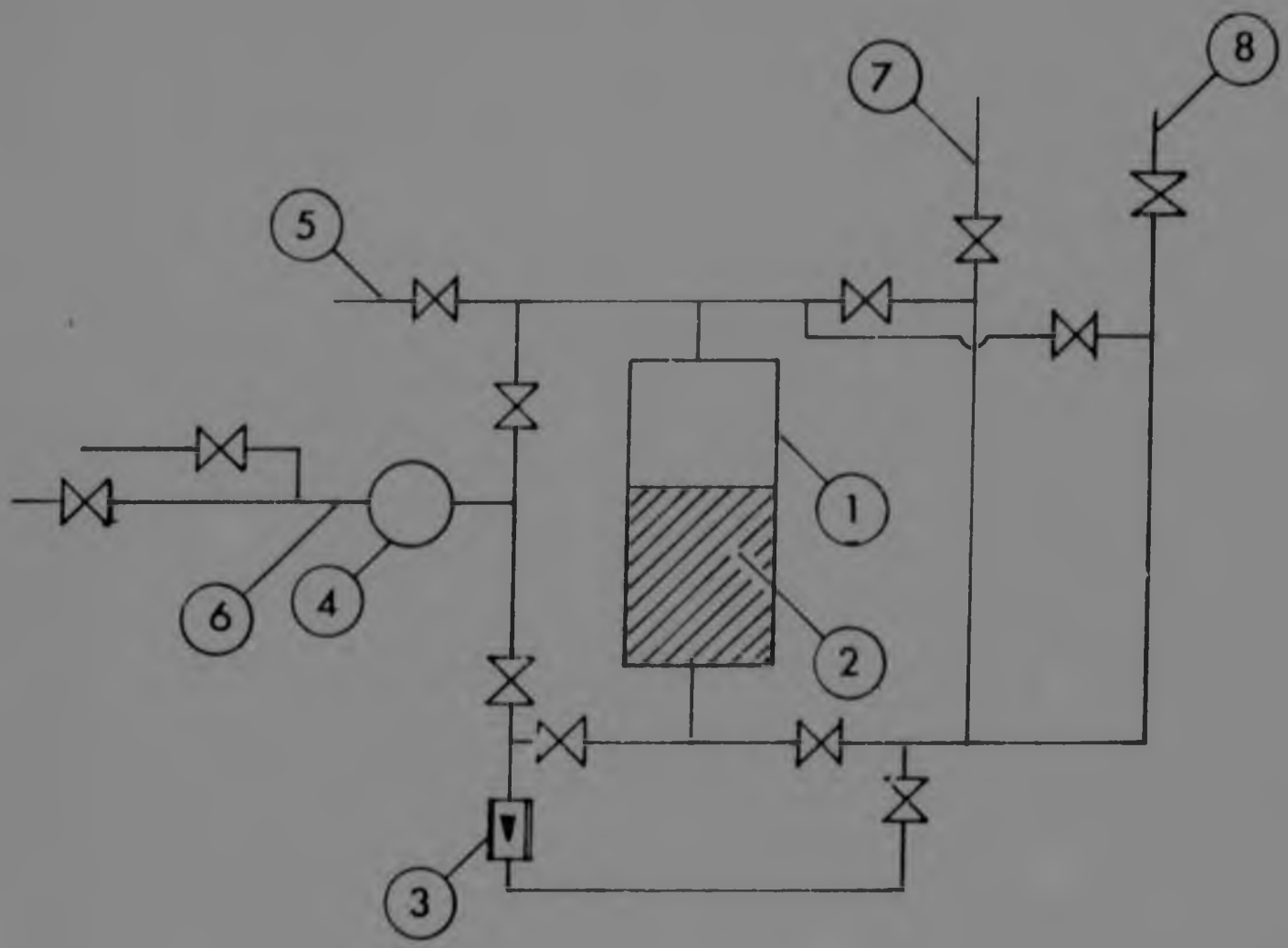

Fig.2.8. The apparatus and flow diagram for the regeneration of the weak cation resin with an aqueous solution of SO_2

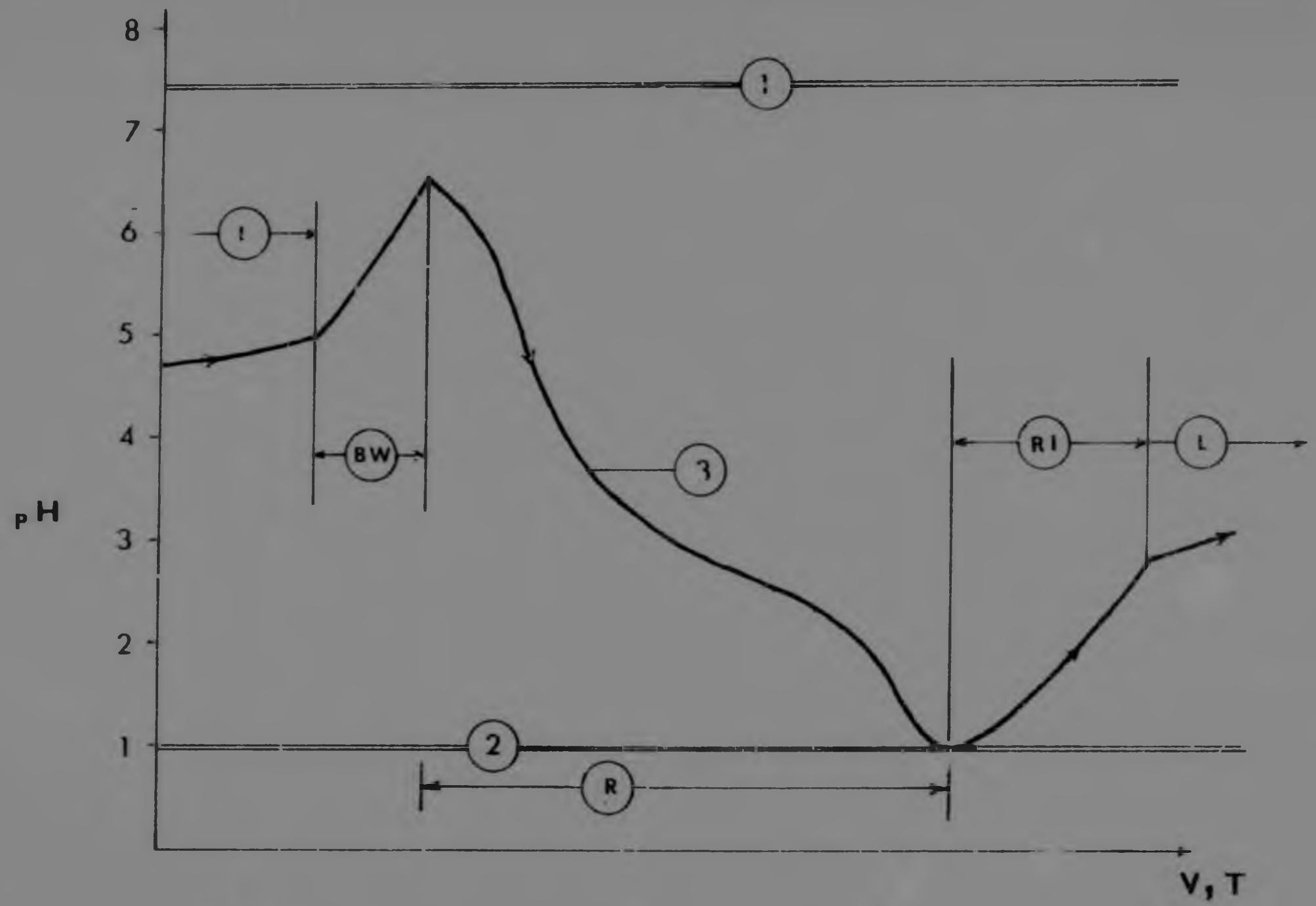

Fig 2.9. pH changes when the regeneration is conducted in one direction only

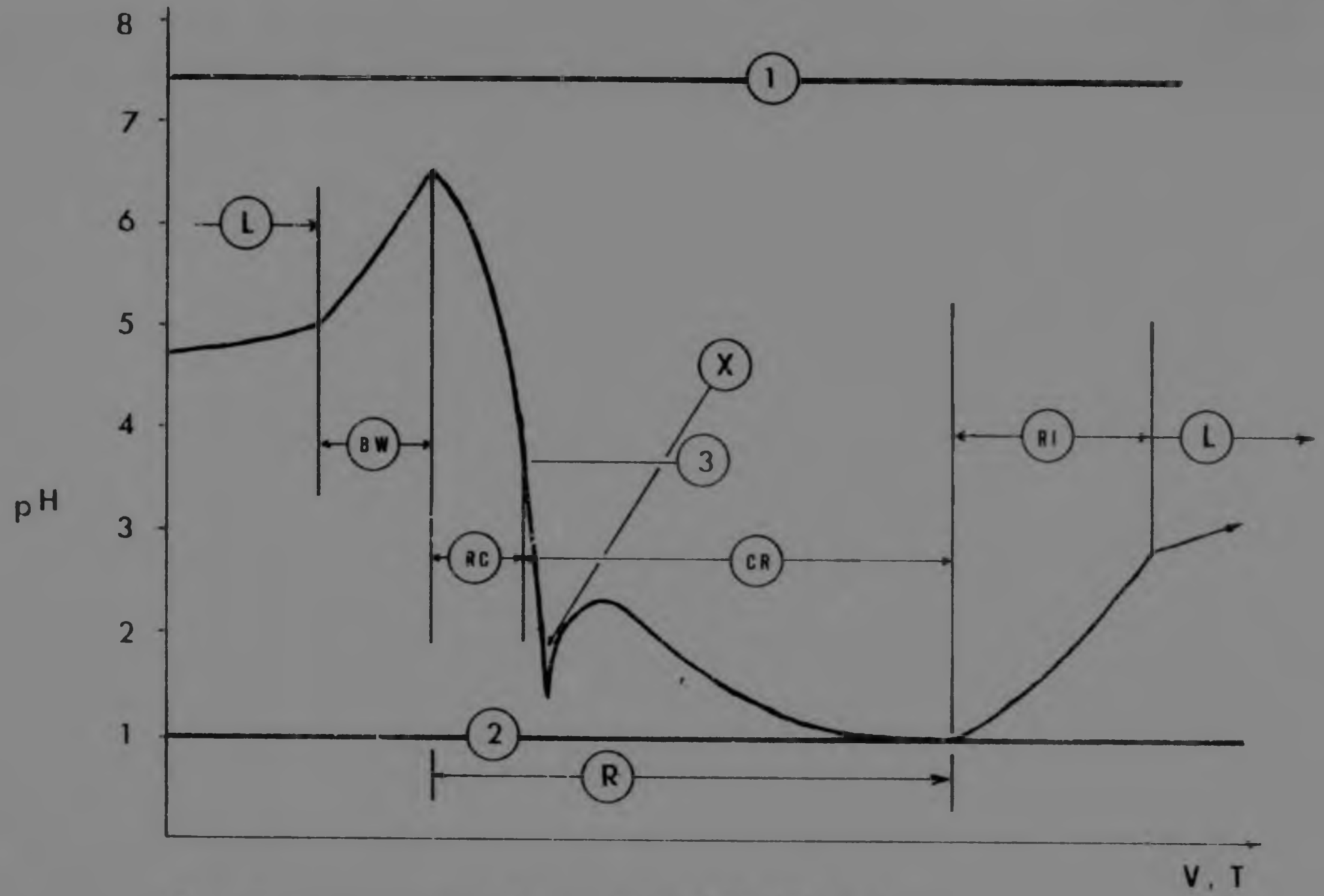

Fig. 2.10 : pH changes during the regeneration of ZEROLITE 236, loaded with Ca^{++} (and Mg^{++}, Na^{+}) with H_2SO_3

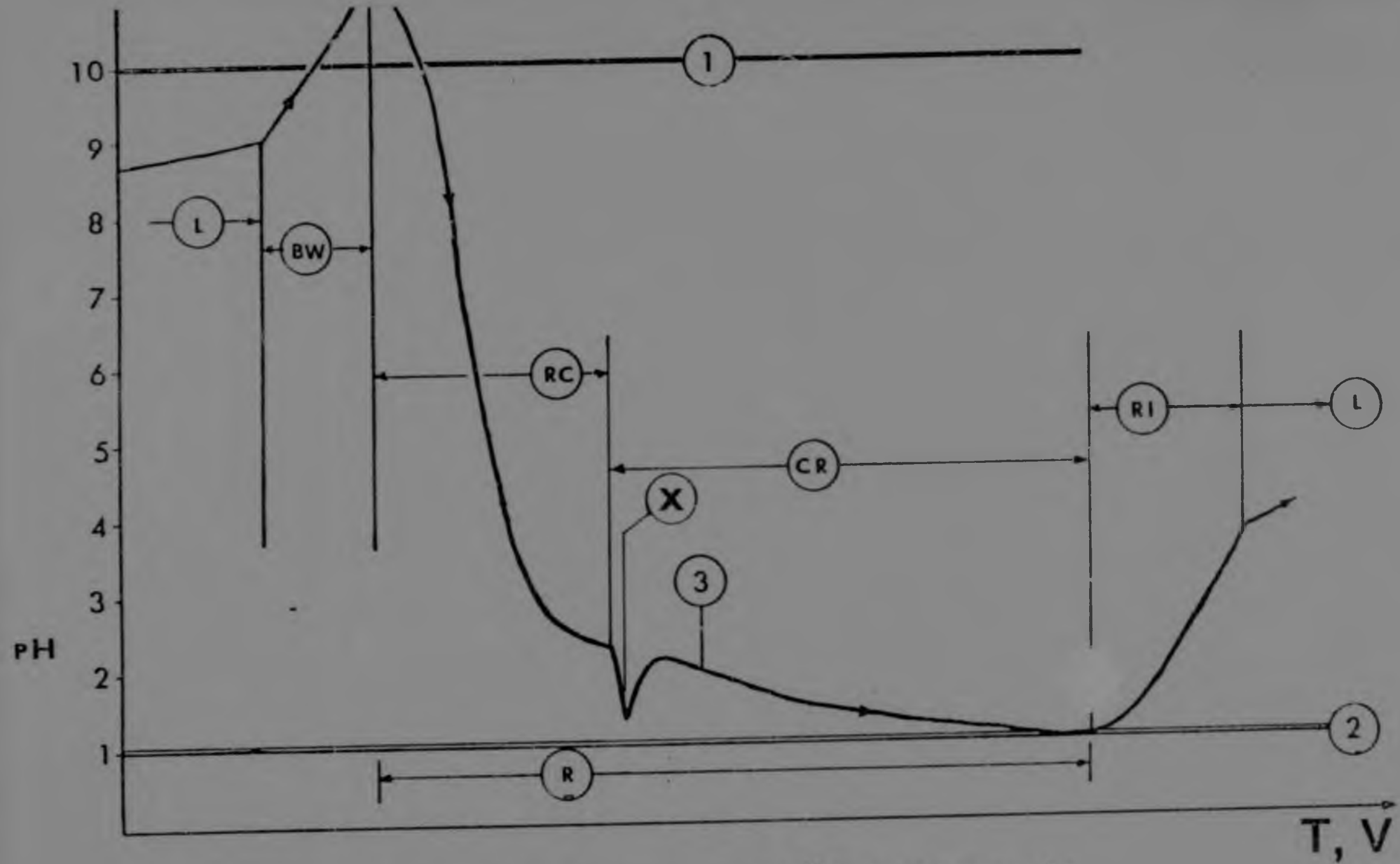

Fig. 2.11 : pH changes during the regeneration of Cu^{++} loaded with weak cation exchange with H_2SO_3

Figure 2.12. Ca^{++} break through curves.

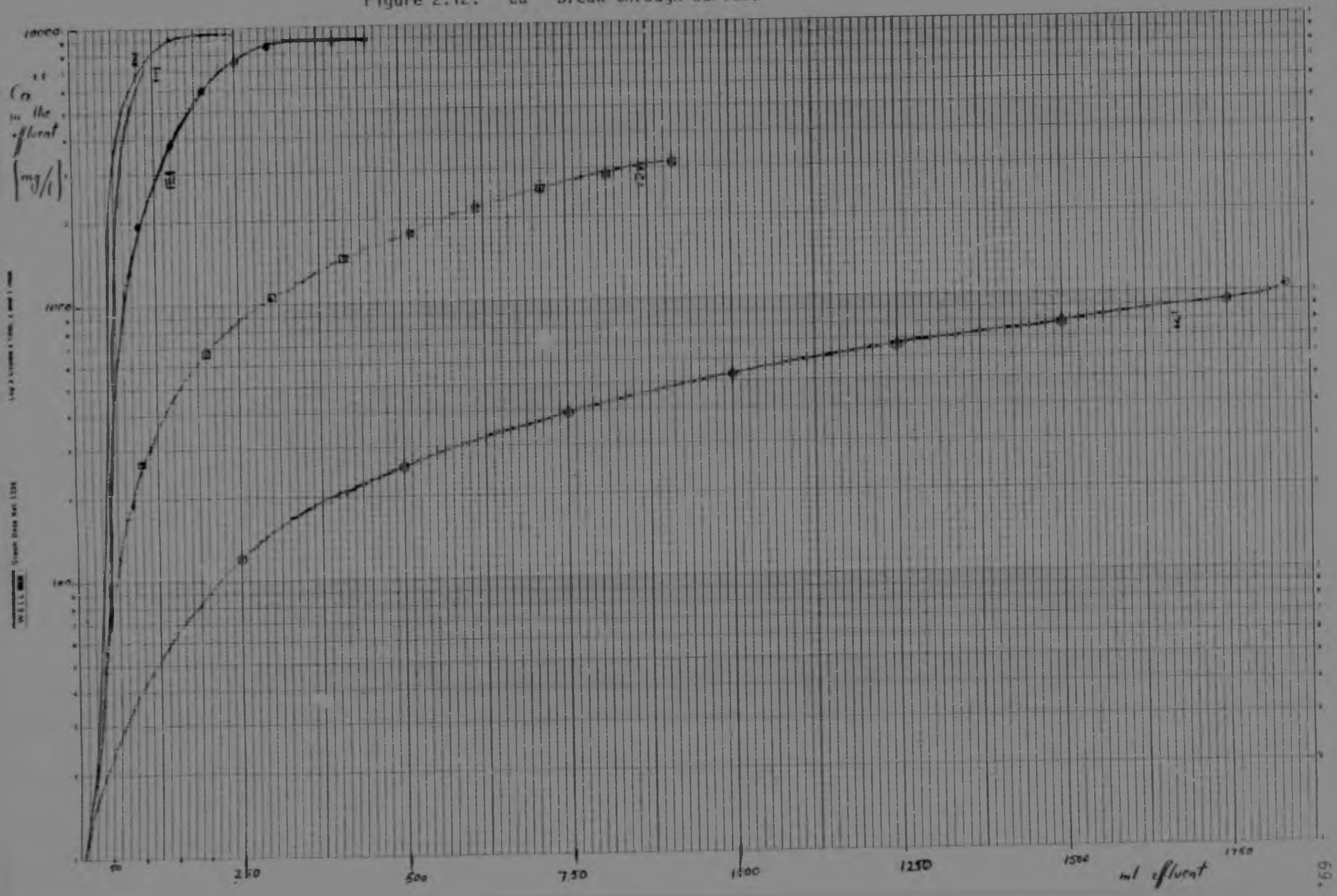

Figure 2.13. Elution efficiency and changes in pH

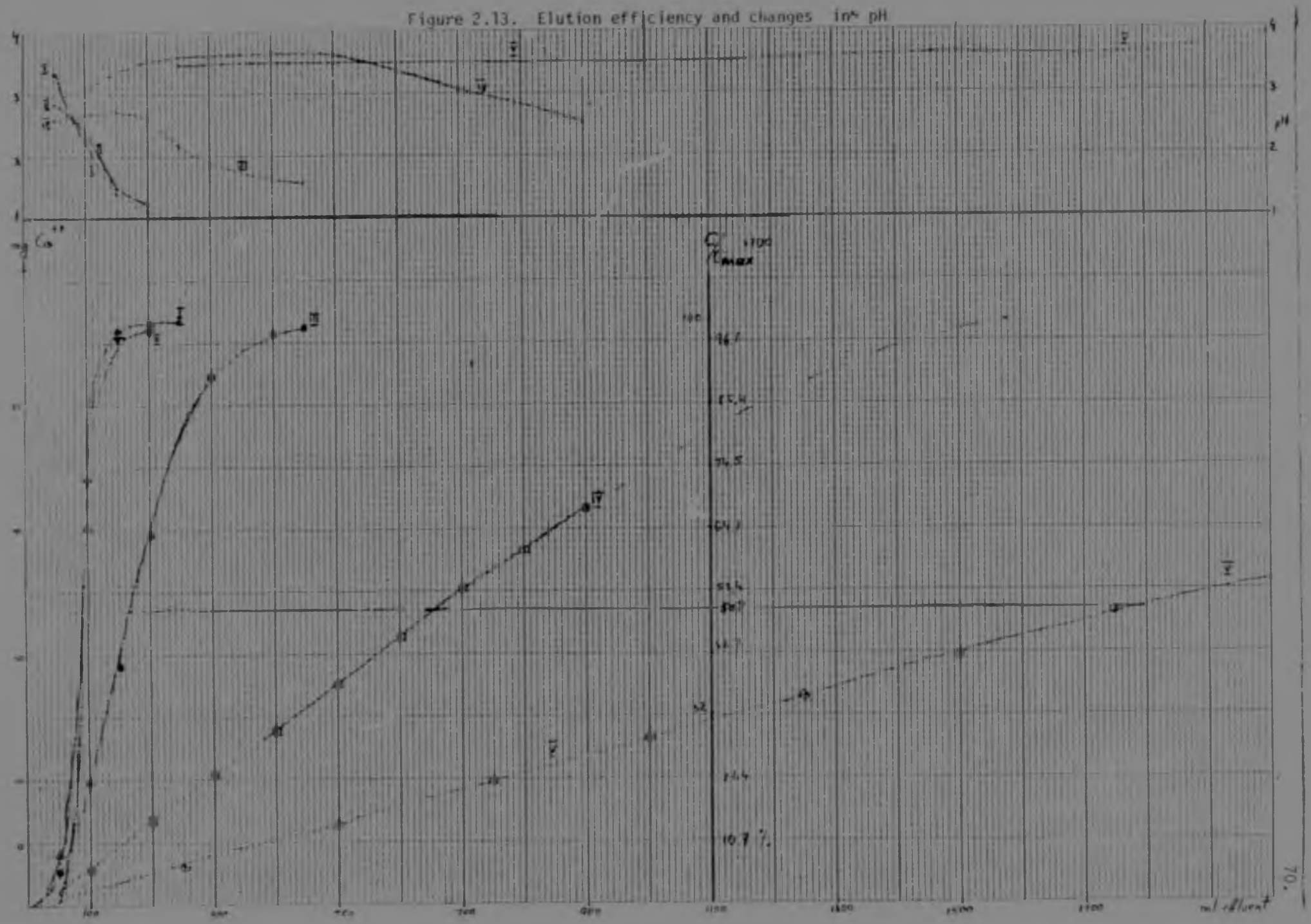

Figure 2.14 H^+ concentration in the regeneration effluent

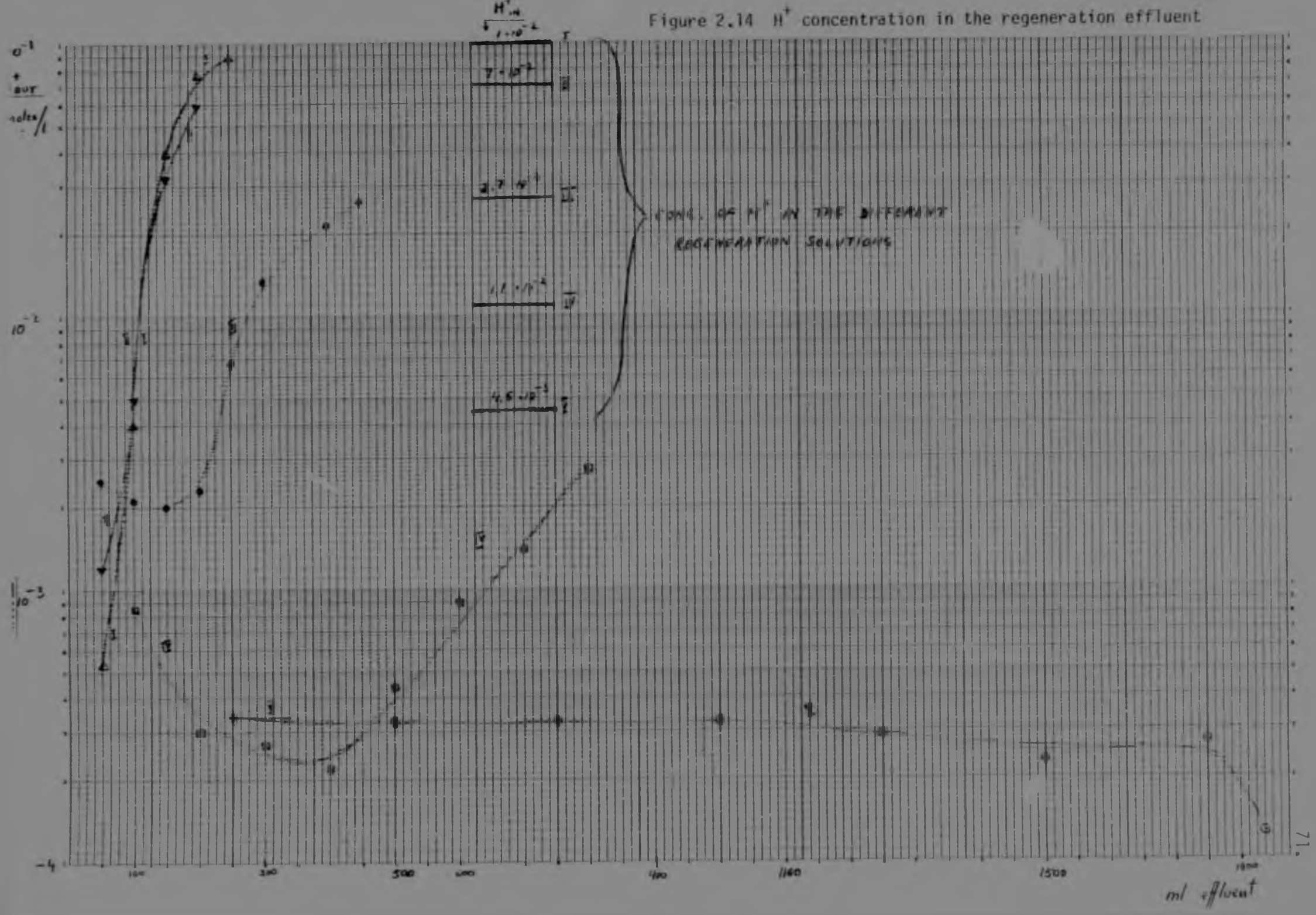

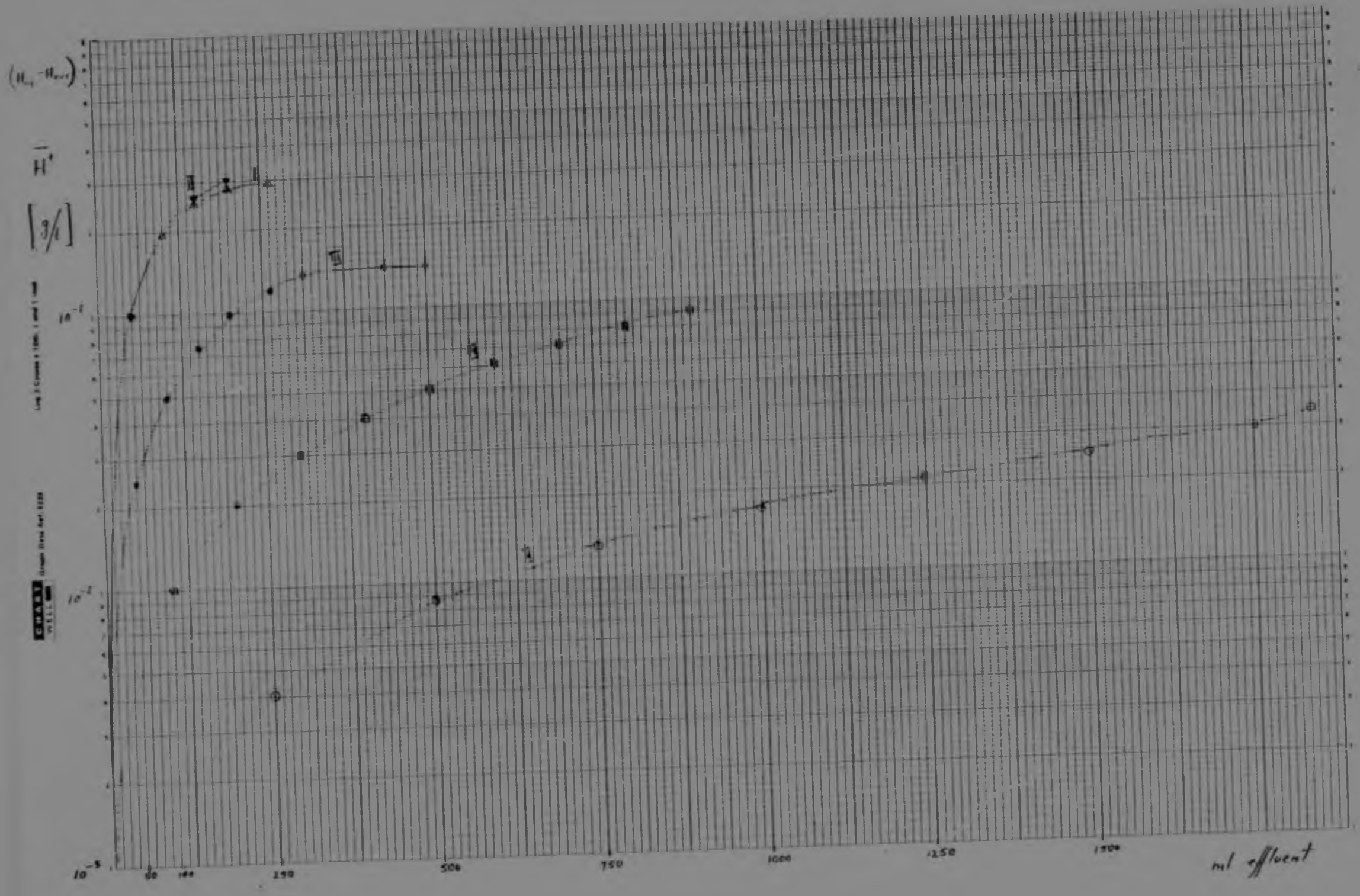

Figure 2.15 H^+ loading curves

Figure 2.16 Bed Volumes (B.V.) necessary for 50% elution, as a function of pH of the regeneration solution.

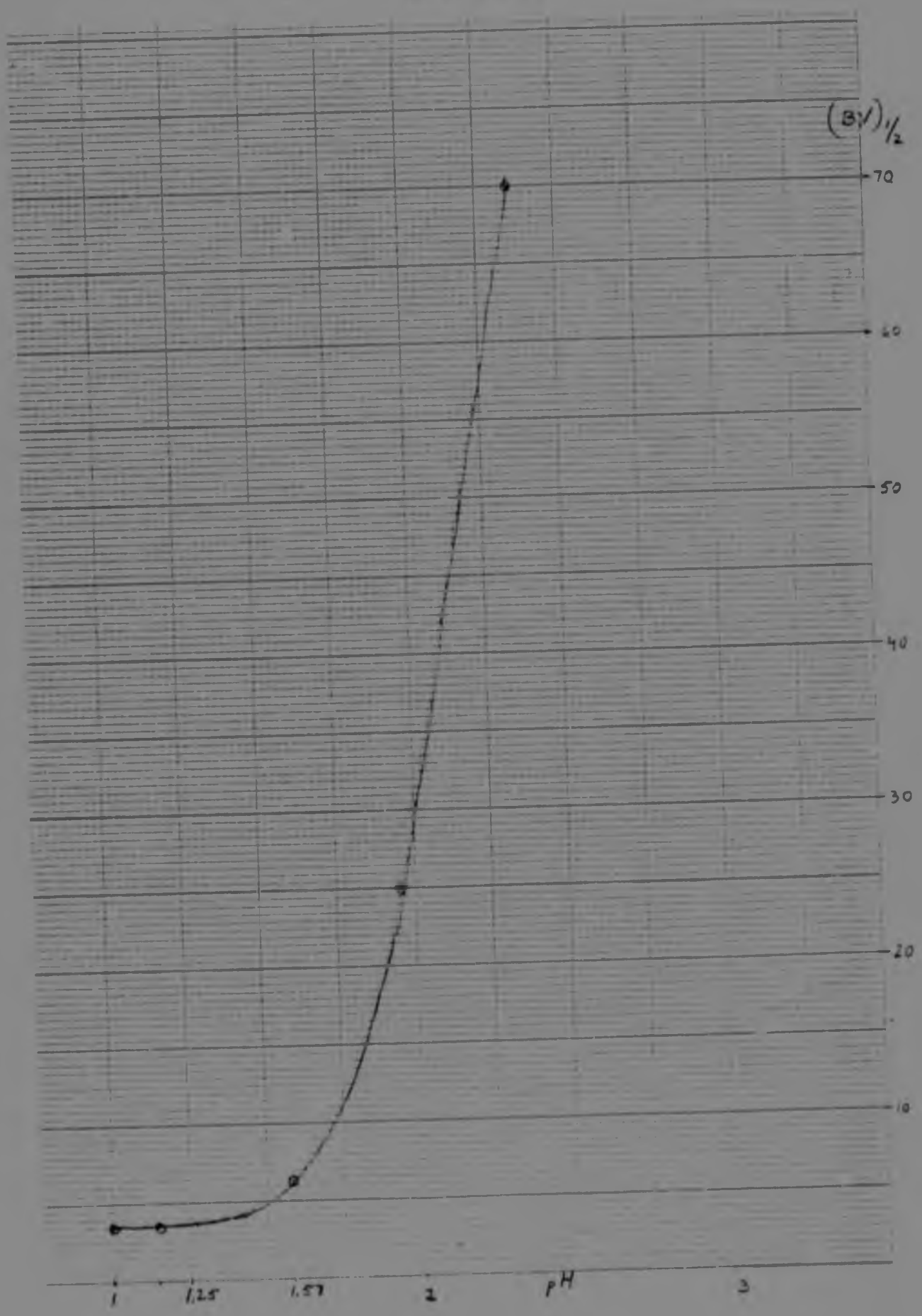

CHAPTER 3.

KINETIC EXPERIMENTS

1. INTRODUCTION

It is known that the rate of ion exchange processes are usually controlled by the rate of ion diffusion. Since the regeneration of a weak exchanger with a solution of SO_2 in water which is described in this work, has not previously been studied, it was necessary to elucidate which step governs this process. This could also help to determine the way the operating conditions of this new process can be improved and optimized.

2. THEORY

An ion exchange process is usually controlled by the rate of ion diffusion and the slowest step in the path of ion migration will control the rate of ion exchange. Figure 3.1 shows schematically the diffusion steps involved in ion exchange.

If the ion exchange process consists of exchanging ion $B^{\pm}$ from the ion exchanger with the ion $A^{\pm}$ from the solution,

$$A^{\pm} + \bar{B}^{\pm} \rightleftarrows \bar{A}^{\pm} + B^{\pm}$$

then, the ion $A^{\pm}$ must move (diffuse) through the bulk solution, the stagnant film surrounding the resin particle and through the pores of the resin to the exchange site. The displaced ion $B^{\pm}$, must follow the reverse path from the exchange site to the bulk solution (Fig.3.1). The exchange itself is usually rapid, and is not likely to be a rate controlling step.

Diffusion in the bulk solution is not usually a controlling step and the bulk solution is usually fairly homogenous from the concentration point of view. Therefore, the controlling step is likely to be either film diffusion or particle diffusion. In poorly mixed systems,

or at very slow flow-rates, the film surrounding the resin bead is very thick and the ion exchange is limited to the rate at which ions can move through this film. Under these conditions, the rate is said to be "film diffusion controlled". In this case large concentration gradients exist in the film only.

When "film diffusion" is the rate controlling step, the flux is proportional to the solution concentration and is inversely proportional to the film thickness: it is independent of the fixed-charge concentration, inter-diffusion coefficient in the bead and bead radius.

When "particle diffusion" controls the diffusion through the pores of the resin it controls the rate of ion exchange. Under these conditions effective concentration gradients exist only in the beads [Fig.3.2]. The exchange flux is proportional to the concentration of fixed charges and is inversely proportional to the bead radius. It is independent of the film thickness, solution concentration and diffusion coefficients in the film.

Since the subject of this chapter is only a general investigation on the rate controlling step of the process the mathematical development of the equations linked to those steps are not presented here.

2.1. Prediction of the rate determining step

F. Helferich [105] provides a criterion for the prediction of the rate determining step:

$$\frac{X\bar{D}\delta}{CDr_o}\left(5 + 2\alpha_B^A\right) \ll 1 \quad \text{particle diffusion control}$$

$$\frac{X\bar{D}\delta}{CDr_o}\left(5 + 2\alpha_B^A\right) \gg 1 \quad \text{film diffusion control}$$

where X = the capacity of the resin (eq/l)
C = concentration of solution (in equivalents);
$\bar{D}$ = interdiffusion coefficient in the ion exchanger;
D = interdiffusion coefficient in the film;

r_o = bead radius;

δ = film thickness;

$\alpha_B^A = \overline{C}_A C_B / \overline{C}_B C_A$ = separation factor;

where concentrations are on the molarity scale.

A further experimental method for distinguishing between particle and film diffusion control is the test called the interruption test. In this test, the elution (or loading) is interrupted for a limited period of time. This break in the process, gives time for the concentration gradients in the beads to level out. Thus, with particle diffusion control, the rate of elution or loading immediately after the process is restarted again, is greater than that prior to interruption. [Fig. 3.3]. If film diffusion is the controlling step effectively no concentration gradients exist in the resin beads only in the film. As the material held up in the film is negligible, the concentration gradient is rapidly re-established and therefore the interruption does not effect the rate of elution (or loading).

2.2. Kinetic Models

The regeneration of a weak cation resin involves the substitution of the loaded metal Me^{+} with the proton H^{+} :

$$\overline{(R\text{-}COO^{-})_2 Me^{+2}} + 2H^{+} \rightleftarrows \overline{2R\text{-}COOH} + Me^{+2}$$

The weak acid cation exchange resins have a very high affinity for the H^{+} ions, and therefore, the protonation of such a resin looks more like an irreversible reaction:

$$\overline{(R\text{-}COO^{-})_2 Me^{+2}} + 2H^{+} \longrightarrow \overline{2R\text{-}COOH} + Me^{+2}$$

In their article W. Höll and H. Sontheimer [107] described this protonation by developing a mathematical model. They verified the calculations based on the developed model by photographing the beads in different regeneration stages (Figs. 3.4, 3.5 & 3.6.)

They determined the interdiffusion coefficients and showed how they depend on the system parameters and on the properties of the resin.

In their article, they concluded that the exchange rate depends on the acid concentration of the solution. They also showed that the diffusion of H^+ ions within the resin bead is coupled with two chemical reactions:

(1) the protonation of the fixed carboxylic groups and

(2) the dissociation or acid molecules.

Both reactions are very rapid. It was also mentioned that the fixed ions at the surface of the resin, instantaneously trap the hydrogen ions, forming a thin shell with non-dissociated - COOH groups.

Since the chemical reaction is vary fast, and the diffusion of protons and counterions is slow through the pores of the resin, the unreacted core model as outlined by Levenspiel is another possibility of modelling the regeneration of the resin beads. [108].

This model suggests that the rate of elution of the resin during the regeneration can be described by

$$Z = 1\text{-}3\,(1 - X_B)^{2/3} + 2(1 - X_B)$$

where $X_B = \dfrac{C_i}{C_{max}}$ and

C_i is the concentration of the solution in mg/l at the time t_i while C_{max} is the maximum concentration obtained in that specific experiment.

Furthermore, the model suggests that by plotting Z as a function of time t, a straight line will be obtained, if the intraparticle diffusion is the rate controlling step.

On the other hand, τ which is the time for complete regeneration of the resin, can be obtained from the slope of the plot of Z versus t.

The unreacted core model suggested and developed by O. Levenspiel [108] is based on two assumptions:

(1) that the chemical reaction is very fast compared to the rate of diffusion and

(2) that the intraparticle diffusion is the controlling step. In such a case, the beads of an ion exchange are regenerated from outside to the inside, with a moving interface. (Fig. 3.2, 3.4, 3.5, 3.6).

2.3. The Intraparticle diffusion $\bar{D}$

As mentioned before, the time for complete regeneration, τ, can be obtained from the slope of the plot of Z versus t, and since

$$\tau = \frac{Xr_o^2}{6b\bar{D}C}$$

and b is the stoichiometric factor, the intraparticle diffusion coefficient $\bar{D}$ can be calculated once τ is known.

3. THE EXPERIMENTS

3.1. Aim

The experiments performed at this stage are aimed to determine the diffusion controlling step (film or particle diffusion) of the regeneration process as well as the regeneration rate. This latter is an important quantity for the designer in estimating the size of the required equipment.

3.2. Method

As described before, two possibilities had to be checked in connection with the controlling step: particle diffusion or film diffusion. Since particle diffusion depends on the bead radius, it was decided to use batches with different size beads in these kinetic experiments. Further, since film diffusion depends on the flow rate in poorly mixed systems, it was decided to use different flow rates during the experiments, as well as two different flow directions.

The conditions under which the experiments were carried out are summarised in Table 3.1.

3.3. Materials

3.3.1. Resin

The resin employed in these experiments was the same as in all the other regeneration experiments: Zerolite 236. A batch of ~150 ml. resin was screened and split into three size fractions giving 9 ml. of small beads (35-28 mesh), 56 ml of medium size beads (28-20 mesh) and 75 ml of large beads (above 20 mesh).

3.3.2. SO_2 gas was the same gas used in the previous experiments and its purity is described in Appendix A.

3.3.3. Loading solution

The resin was loaded with Ca^{++} ions, using a solution of $Ca(OH)_2$.

3.3.4. The solution initially employed for the regeneration was demineralized water, through which SO_2 gas was bubbled continuously. As each experiment was proceeding, the respective regeneration solution became more and more concentrated with Ca^{++} ions eluted from the resin, as the regeneration - effluent solution was recirculated in a closed cycle (Fig. 3.7). Even though the concentration of Ca^{++} ions increased continuously in the regeneration solution, the concentration of H^+ ions, as measured remained effectively constant. ($C_{H^+} \approx 0.1M$ since pH = 1.00)

3.4. The experimental arrangement

Fig.3.7. shows schematically the arrangement used in these experiments. The resin was held in a glass column (I.D = 1.2 cm) and rested on a sintered glass. There was another glass screen above the resin, to stop the resin escaping from the column when the flow was conducted upwards.

From Fig.3.7. it can be seen that by opening the correct valves, the regeneration could be carried out either in an up or down flow.

The regeneration solution was continuously stirred by a magnet, activated from outside by a magnetic stirrer. The regeneration solution was pumped through the column (and resin) to the storage tank by a variable displacement-piston pump the flow rate being adjusted by changing the length of the stroke.

3.5. Analysis

The samples drawn during the experiments were all 50 ml and contained Ca^{++} only. An Atomic Adsorption Spectrophotometer (Varian 1200) was employed for the Ca^{++} analysis.

3.6. The (regeneration) experiments

Seven experiments (A-G) were performed to determine the diffusion controlling step.

More than 70 samples were analysed during these experiments, and their concentration, withdrawal time, the volume passed in that period, etc., are given in Tables 3.2, 3.3, 3.4, 3.5, 3.6, 3.7 and 3.8.

The experiment was considered sufficiently complete when all the resin had regained its original shape and colour which had changed during the loading

4. RESULTS

Tables 3.2 & 3.8 give the results, as well as the calculations needed for plotting the results. The experimental results listed in the above tables, are plotted (Fig. 3.8 and 3.9) to give a graphical presentation of these results.

Fig. 3.8 shows the increase in concentration of Ca^{++} as a function of the bed volume of the regeneration solution which passed through the

bed. It can be seen, that apart from the interaption experiment there are two separate groups of curves.

This is to be expected since the experiments with small beads (curves A and F) were carried out with a bed height much smaller than the bed height in the other experiments. This was unavoidable due to the small volume fraction of small radius beads resulting from the screening process.

Therefore, the increase in concentration $C_{i/C_{max}}$ was plotted as a function of time in Fig. 3.9 and subsequently compared in Fig. 3.10.

Fig 3.10 was constructed with the experimental results, having the breakthrough concentration of Ca^{++}, plotted as a function of $t_{i/t_{\frac{1}{2}}}$, where $t_{\frac{1}{2}}$ is the time required to elute and regenerate half of the resin capacity $(\frac{C_i}{C_{max}} = 0.5)$.

Fig. 3.9 shows that the curves drawn up with the results from the experiments A and F; B and C; E and G are almost "parallel" showing a similar behaviour.

The curves become steeper and steeper as the radius of the beads decreases: the steepest curves are A and F, then C and D while E and G are the least steep curves.

Since the experiments A and F were carried out with small beads, B and C with medium size beads and E and G with large beads, this shows without any doubt that the diffusion step depends on the radius of the bead.

This figure, also shows that the increase in concentration is delayed in the experiments A, F and G, compared to the other experiments.

This delay is clearly shown in Fig 3.10 in which all the experimental results are compared on the same basis. The same figure shows also that the time to complete the elution is longer when the beads have

a big radius, compared with the beads having a small radius.

Fig. 3.8 and 3.9, show also the results of a typical interruption experiment, which looks like those in the literature (Fig.3.3.)

All the experimental results, plotted and compared in Fig.3.8 - 3.10, show a close dependancy between the elution rate and the radius of the beads.

This suggests that the rate controlling step in the regeneration is an intraparticle diffusion one for most of the time, the film diffusion step being important only at the beginning.

A further confirmation that the intraparticle diffusion is the controlling step in the new regeneration process, is given by the Fig. 3.11 which is the graph of Z (as in section 2.2) as a function of time t.

This graph shows that the theory of moving boundaries which is illustrated in Figs. 3.4, 3.5 and 3.6 and which is based on the intraparticle diffusion controlling step, fits the results reasonably well.

Fig. 3.11 thus shows that the intraparticle diffusion is a dominant controlling step in the regeneration of the large beads, while it controls only the last stage of the small beads regeneration.

As in Fig. 3.11 we have effectively got straight lines, the interparticle diffusion coefficient $\bar{D}$ can be calculated for the experiments A, F and E. Table 3.9 gives the calculated results of τ, $\bar{D}$ and X for these experiments.

5. DISCUSSION

A prediction of the diffusion controlling step could be made without

the rate experiments, by calculating the Helfferich criterion.

These calculations, done for each experiment and listed in Table 3.10, predict the same thing. There is no really effective rate controlling step, with both film and particle diffusion playing a part, though the latter is probably more important.

On the other hand, the experiments described in this chapter, showed that although both the film and intraparticle diffusion are playing a part in the regeneration elution step, the particle diffusion is the main rate controlling step, the film diffusion playing an important role in controlling the beginning of the process, especially when the beads have a small radius.

The particle diffusion coefficient, calculated in this chapter from the experimental results, is in good agreement with the value mentioned in the literature [109-111].

6. EXPERIMENTAL ERRORS

In the kinetic experiments, the estimated error on the measurements is likely to be limited by the accuracy of the concentration measurements which should be better than 5%. The times, flow rates and volumes were measured more accurately than this. The temperature fluctuation of $\pm$ 4°C around the 20°C at which the experiments were performed, could influence the kinetics of exchange itself or the diffusion of different ions, though these are not usually very temperature dependent.

There is no reason to believe from the results themselves, that the accuracy of the results is worse than 5%, though the diffusion constants derived from the model differ by a factor of 3.

Exp.	Flow rate [ml/min]	Flow rate [B.V./min]	Size r_o [cm]	Up/Down Flow	Capacity [meq/ml]	Diffusion control calc.	Quantity of resin in the experiment [ml_r]	$t_{\frac{1}{2}}$ [min.]
A.	12	2.4	0.02	Down	0.5	0.54	5	11.7
B.	12	0.5	0.03	Down	1.2	0.95	25	18.5
C.	16	0.7	0.03	Up	1.2	0.95	25	13.5
D.	12	0.5	0.04	Down	0.9	0.50	25	
E.	16	0.7	0.04	Up	1.0	0.54	25	11.7
F.	10	3.0	0.02	Up	0.5	0.54	3.5	9.5
G.	10	0.5	0.04	Up	1.1	0.62	22	10.3

Table 3.1 The Conditions under which the Kinetic experiments were carried out.

Sample No.	Ci[mg/l]	t[min] time from start	Volume passed[ml]	Bed Volume passed	Ci/Cmax	t/t½
1A	0	1	12	2.4	0	0.18
2A	0	3	37	7.4	0	0.26
3A	0	5	61	12.3	0	0.43
4A	4	7	[illegible]	17.3	0.04	0.60
5A	30	9	111	22.2	0.29	0.77
6A	51	13	160	32.1	0.55	1.11
7A	80	17	210	42.1	0.78	1.45
8A	93	21	259	52.0	0.90	1.79
9A	101	25	309	62.0	0.98	2.14
10A	103	29	358	72.0	1	2.48
11A	103	33	408	81.6	1	2.82

Table 3.2 - Exp. A: Downflow experiment with small beads of ZEOLITE 236 loaded with Ca^{++}

Sample No.	Ci[mg/l]	t[min] time from start	Volume passed [ml]	Bed Volume passed	Ci/Cmax	t/t½
1B	2	2	24	1.0	0.008	0.10
2B	8	6	74	3.0	0.33	0.32
3B	33	10	123	5.0	0.14	0.54
4B	69	14	173	7.0	0.29	0.75
5B	109	18	222	8.9	0.46	0.97
6B	161	22	272	10.9	0.67	1.2
7B	200	28	346	13.8	0.83	1.51
8B	221	34	420	16.8	0.92	1.83
9B	229	40	494	19.8	0.96	2.16
10B	237	46	569	22.8	0.99	2.48
11B						

Table 3.3. Exp. B: Downflow experiment with medium size beads of ZEROLITE 236 loaded with Ca^{++}

Sample No.	Ci[mg/l]	t[min] time from start	Volume passed[ml]	Bed Volume passed	Ci/ Cmax	t/ $t_{\frac{1}{2}}$
1C	0	1	16	0.7	0.00	0.07
2C	11	5	82	3.3	0.16	0.37
3C	59	9	148	5.9	0.25	0.61
4C	111	13	214	8.6	0.46	0.96
5C	155	17	280	11.2	0.65	0.26
6C	197	21	346	13.8	0.82	1.55
7C	223	27	412	16.5	0.93	2.00
8C	233	33	549	21.7	0.97	2.44
9C	239	39	642	25.7	1.00	2.90

Table 3.4 Exp C: Upflow experiment with medium size beads of ZEOLITE 236 loaded with Ca^{++}

Sample No.	Ci[mg/l]	t[min] time from start	Volume passed$_{[ml]}$	Bed Volume passed	Ci/ Cmax	t/ $t_{\frac{1}{2}}$
1C	0	1	16	0.7	0.00	0.07
2C	11	5	82	3.3	0.16	0.37
3C	59	9	148	5.9	0.25	0.61
4C	111	13	214	8.6	0.46	0.96
5C	155	17	280	11.2	0.65	0.26
6C	197	21	346	13.8	0.82	1.55
7C	223	27	412	16.5	0.93	2.00
8C	233	33	549	21.7	0.97	2.44
9C	239	39	642	25.7	1.00	2.90

Table 3.4 Exp C: Upflow experiment with medium size beads of ZEOLITE 236 loaded with Ca^{++}

Sample No.	Ci[mg/l]	t[min] time from start	Volume passed [ml]	Bed Volume passed	Ci/ Cmax
1D	0	2	25	1.0	0.00
2D	0	6	74	3.0	0.00
3D	23	10	124	5.0	0.11
4D	35	16	198	8.0	0.17
5D	48	18	223	8.9	0.24
6D	59	22	272	10.9	0.29
7D	70	28	346	13.9	0.35
8D	81	34	421	16.9	0.4
9D	85	40	495	19.8	0.42
10D	91	46	569	22.8	0.45
11D	97	52	643	25.8	0.48
		Interruption for two weeks			
12D	137	(4)56	693	27.8	0.68
13D	169	(9)61	755	30.2	0.84
14D	200	(15)67	829	33.1	1.00
15D	200	(21)73	903	36.1	1.00
16D	200	(27)79	977	39.0	1.00
17D	200	(33)85	1051	42.0	1.00

Table 3.5.Exp.D Downflow experiment with big beads of ZEROLITE 236 loaded with Ca^{++}

Sample No.	Ci[mg/l]	t[min] time from start	Volume passed[ml]	Bed Volume passed	Ci/Cmax	t/t½
18	3	2	33	1.3	0.01	0.1
28	40	7	98	4.0	0.23	0.57
38	87	10	166	6.8	0.40	0.85
48	129	14	231	9.2	0.60	1.20
58	157	18	296	11.9	0.70	1.52
68	175	20	362	14.5	0.81	1.85
78	191	28	461	18.5	0.89	2.40
88	201	34	566	22.4	0.93	2.90
98	210	40	699	26.4	0.98	3.42
108	215	46	758	30.3	1.00	3.93

Table 3.6. Exp. 8: Upflow experiments with big size beads of ZEROLITE 236 loaded with Ca^{++}

Sample No.	Cl[mg/l]	t[min] time from start	Volume passed[ml]	Bed Volume passed	Cl_t/C_{max}	$t/t_{\frac{1}{2}}$
1F	0	2	21	5.9	0.0	0.21
2F	0	4	41	11.8	0.0	0.42
3F	0	6	62	17.7	0.0	0.63
4F	3	8	83	23.6	0.3	0.84
5F	17	12	124	35.5	0.7	1.26
6F	23	16	166	47.3	0.9	1.68
7F	23	20	207	59.1	1.0	2.1
8F	23	24	248	70.9	1.0	2.1
9F	23	28	289	82.8	1.0	2.5
10F	23	32	331	94.8	1.0	

Table 3.7.Exp.7: Upflow experiment with small beads of ZEOLITE 2W4 loaded with Cu^{++}

Sample No.	Ci[mg/l]	t[min] time from start	Volume passed [ml]	Bed Volume passed	Ci/ Cmax	t/ $t_{\frac{1}{2}}$
1G	0	2	20	0.9	0	0.09
2G	3	7	72	3.3	0.015	0.34
3G	29	11	113	5.2	0.15	0.54
4G	61	15	155	7.0	0.31	0.74
5G	90	19	196	8.9	0.45	0.93
6G	135	26	269	12.2	0.68	1.28
7G	163	32	331	15.0	0.82	1.58
8G	180	38	393	17.9	0.91	1.87
9G	190	44	455	20.7	0.96	2.16
10G	194	50	517	23.5	0.98	2.46
11G	198	56	579	26.3	1	2.75

Table 3.8. Exp. G Upflow experiment with big beads of XEROLITE 236 loaded with Ca^{++}

Table 3.9.

The values of τ and $\bar{D}$ for three experiments

Exp	τ (min)	$\bar{D}$ (cm^2/sec)	X(eq/l)
A	19	0.95×10^{-5}	0.49
F	16	1.06×10^{-5}	0.49
E	43	3.36×10^{-5}	0.99

Experiment	$\frac{X}{r_o}\frac{\bar{D}}{D}\frac{\sigma}{C}(5 + 2\alpha_B^A)$
A.	0.54
B.	0.95
C.	0.95
D.	0.50
E.	0.54
F.	0.54
G.	0.62

Table 3.10. Helfferich Diffusion Criterion Expression

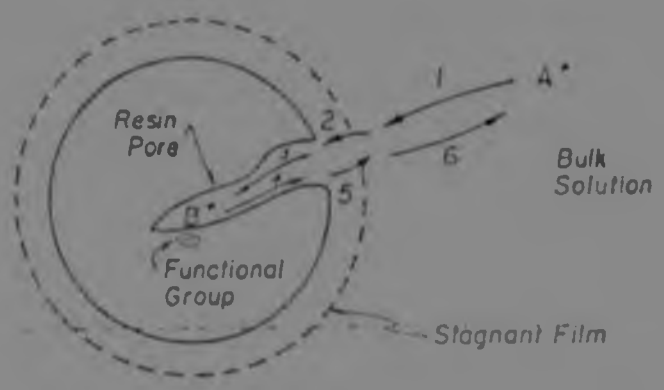

Fig. 3.1. A SCHEMATIC DIAGRAM SHOWING THE TRANSPORT STEPS INVOLVED IN ION EXCHANGE.

1 AND 6--BULK CONVECTION: 2 AND 5--FILM DIFFUSION: 3 AND 4--PORE DIFFUSION.

Source [103]

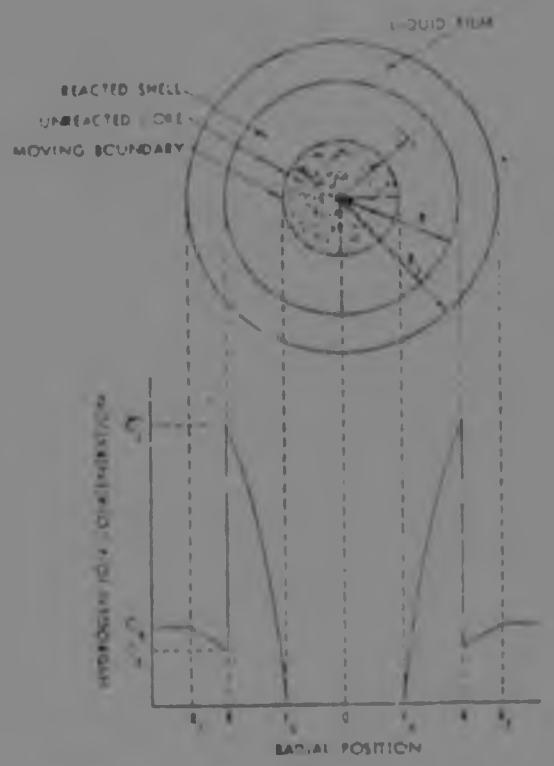

Fig. 3.2. Theoretical concentration profile

Source [104]

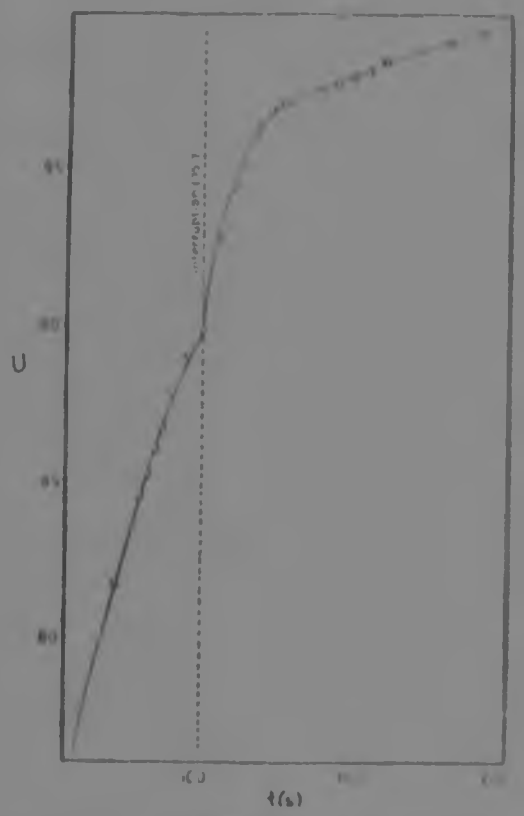

Fig. 3.3. Typical interrupted test. Resin Kastel A 500; [illegible]

Source [106]

Fig.3.4. Visible boundaries in IRC 84 at different hydrogen ion concentrations. Above: $c_{H^+} = 1N$ Below: $c_{H^+} = 0.01\ N$

Source [107]

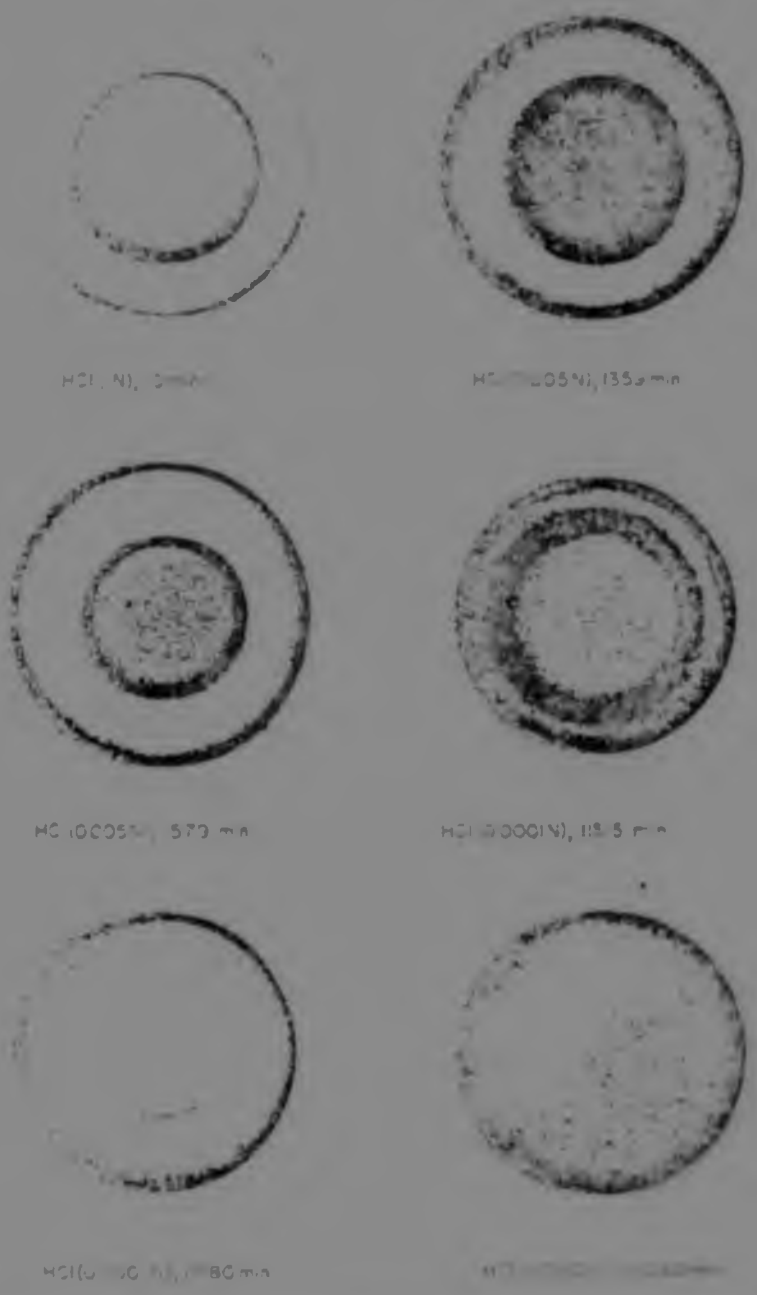

Fig. 3.5.

Source [107]

Fig.3.6.

Source [107]

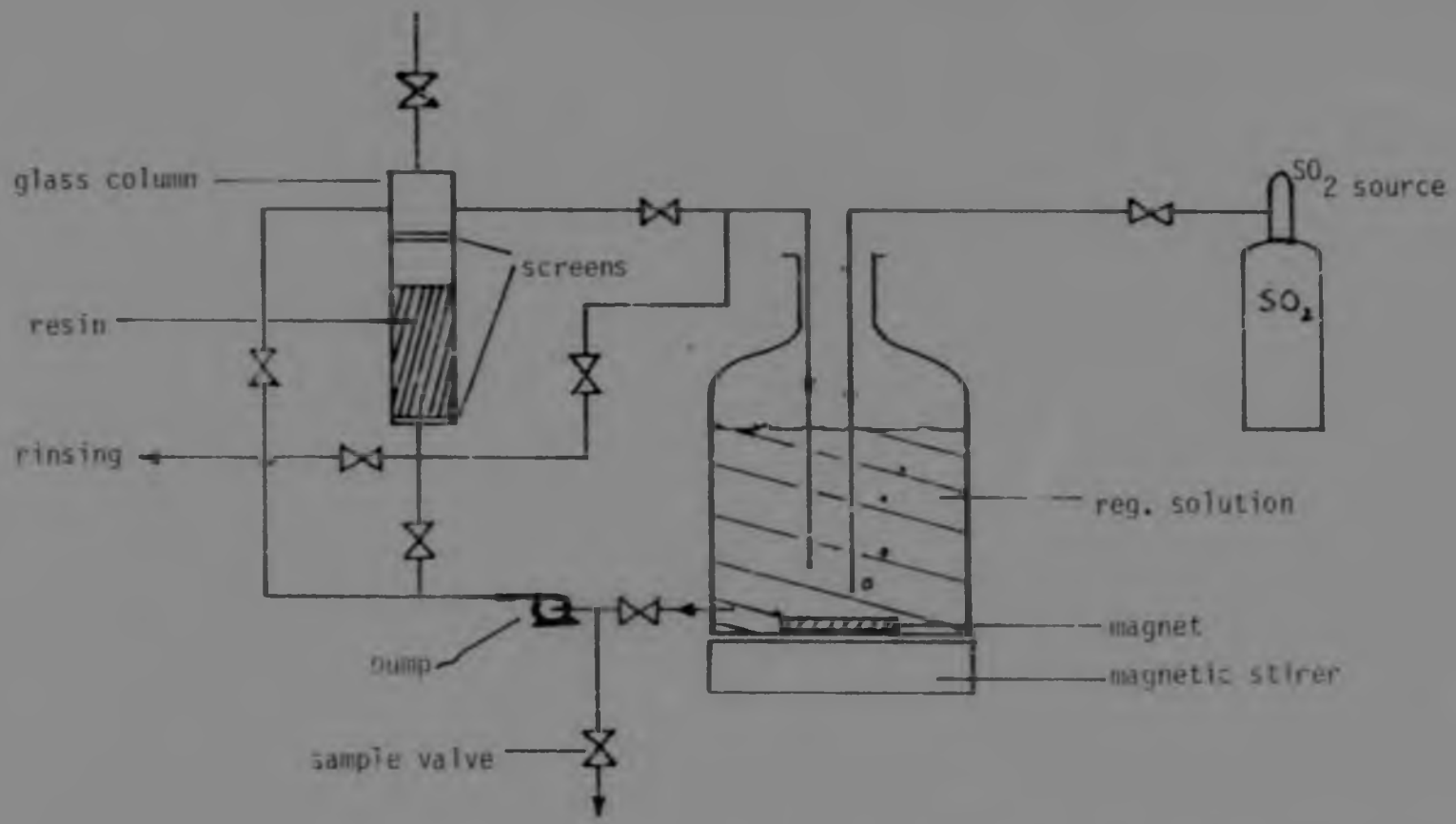

Fig.3.7 The arrangement used for the Kinetic experiments.

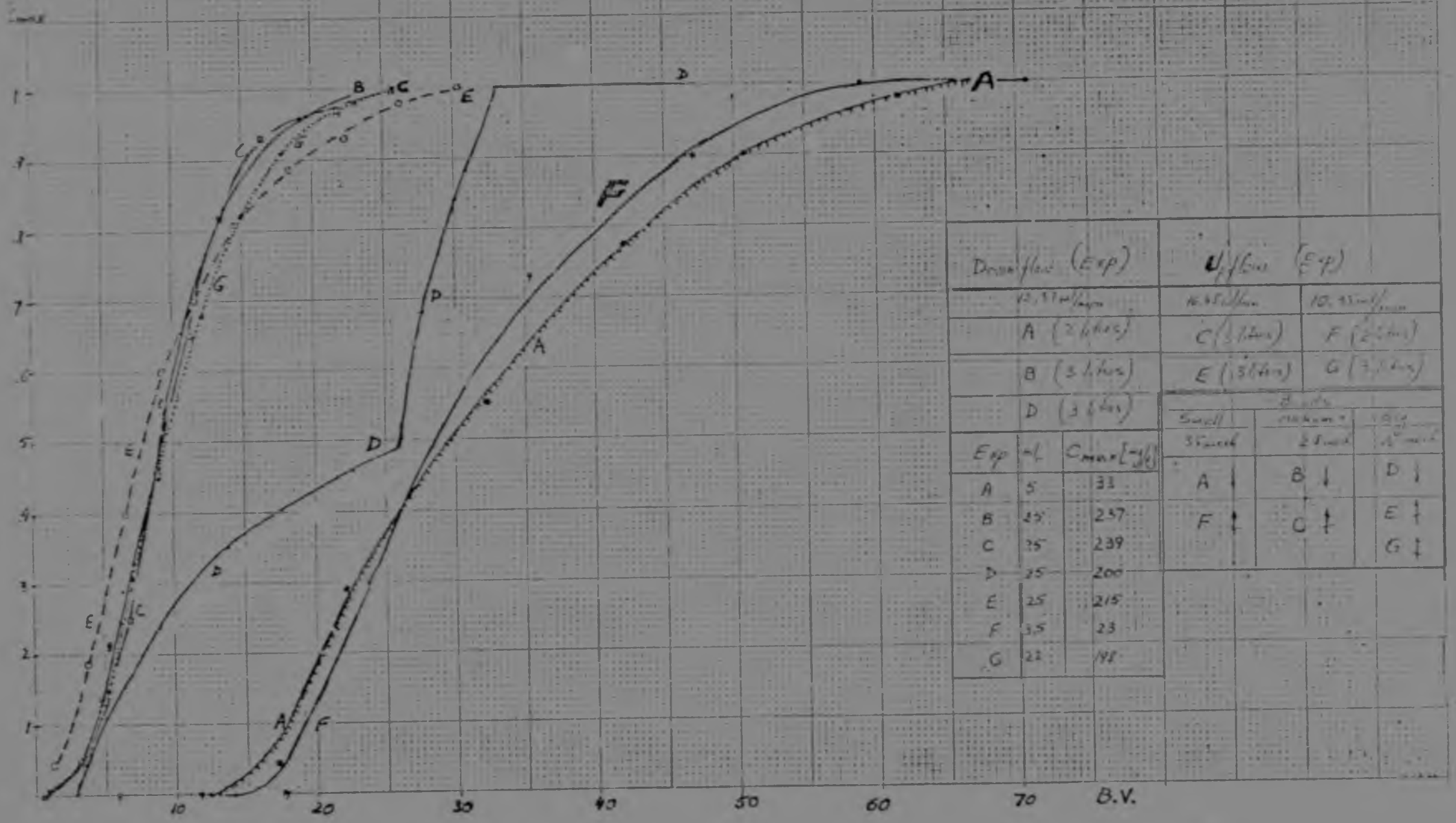

Drawdown (Exp)			Uptake (Exp)	
12.33 milliequiv/liter			10.65 milliequiv/liter	10.33 milliequiv/liter
A (2 l/hour)			C (3 l/hour)	F (2 l/hour)
B (3 l/hour)			E (3 l/hour)	G (7 l/hour)
D (3 l/hour)				
Exp	-L	C_{max} [-yl]		
A	5	33		
B	45	257		
C	35	239		
D	25	200		
E	25	215		
F	35	23		
G	22	141		

Small	Medium	Big
35 mesh	28 mesh	16 mesh
A ↓	B ↓	D ↓
F ↑	C ↑	E ↑
		G ↑

Fig. 3.8. Kinetic experiments: Concentration of the eluted Ca^{++}, as a function of Bed-Volume of regeneration solution which passed through the resin.

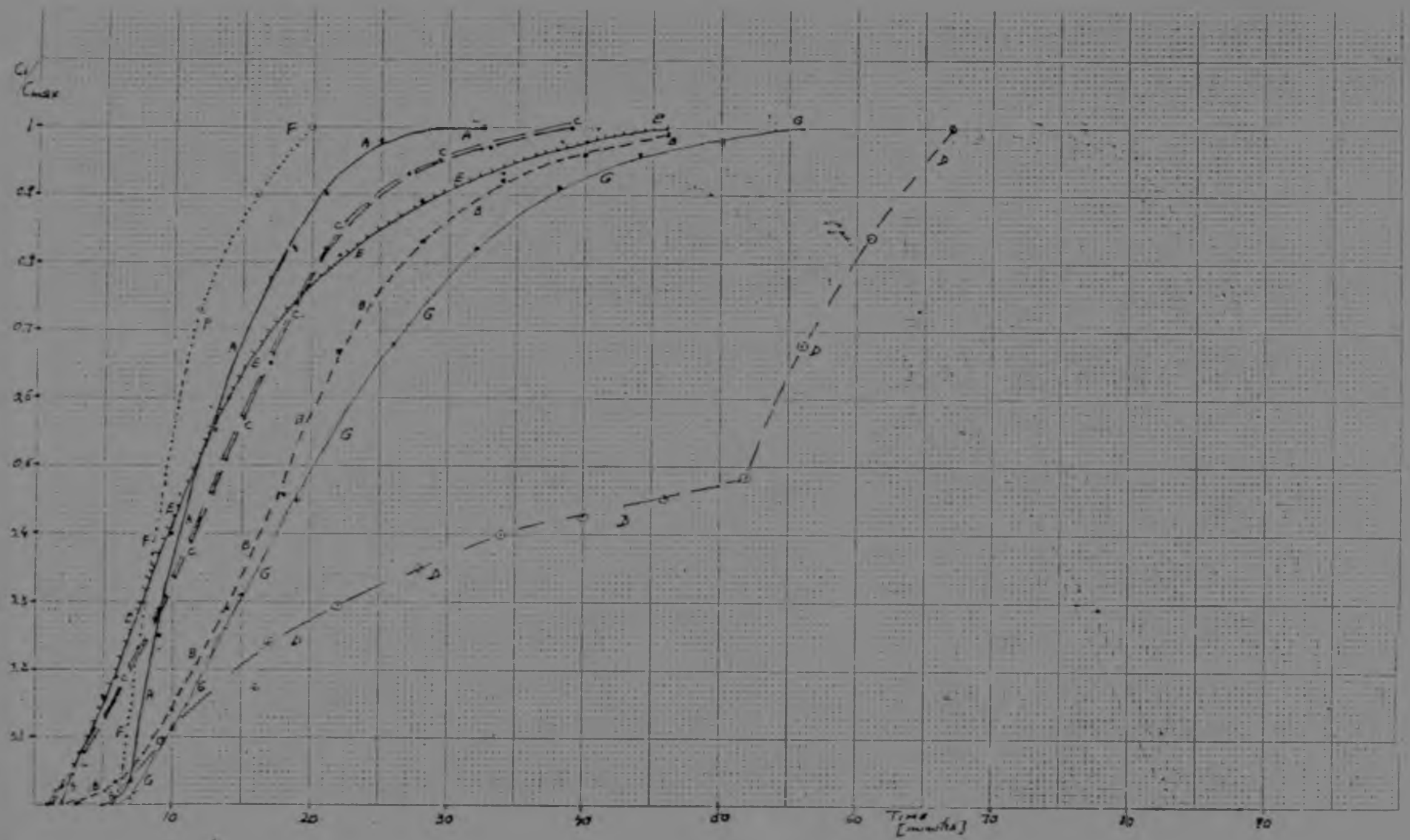

Fig. 3.9. Kinetic experiments: Concentration of the eluted Ca^{++} as a function of time.

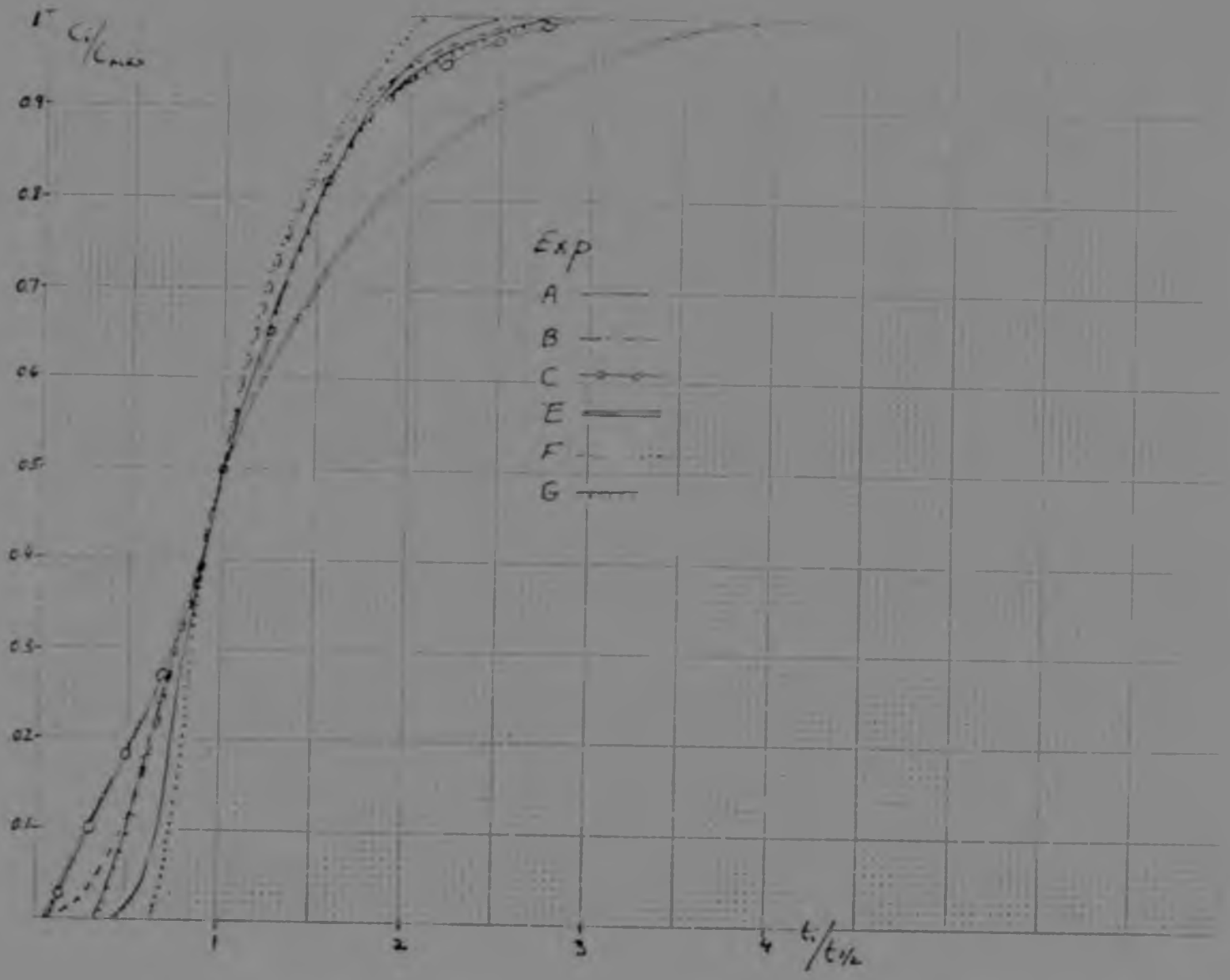

Fig.3.10 Kinetic experiments : Concentration of the eluted Ca^{++} as a function of relative time: ti/t_i

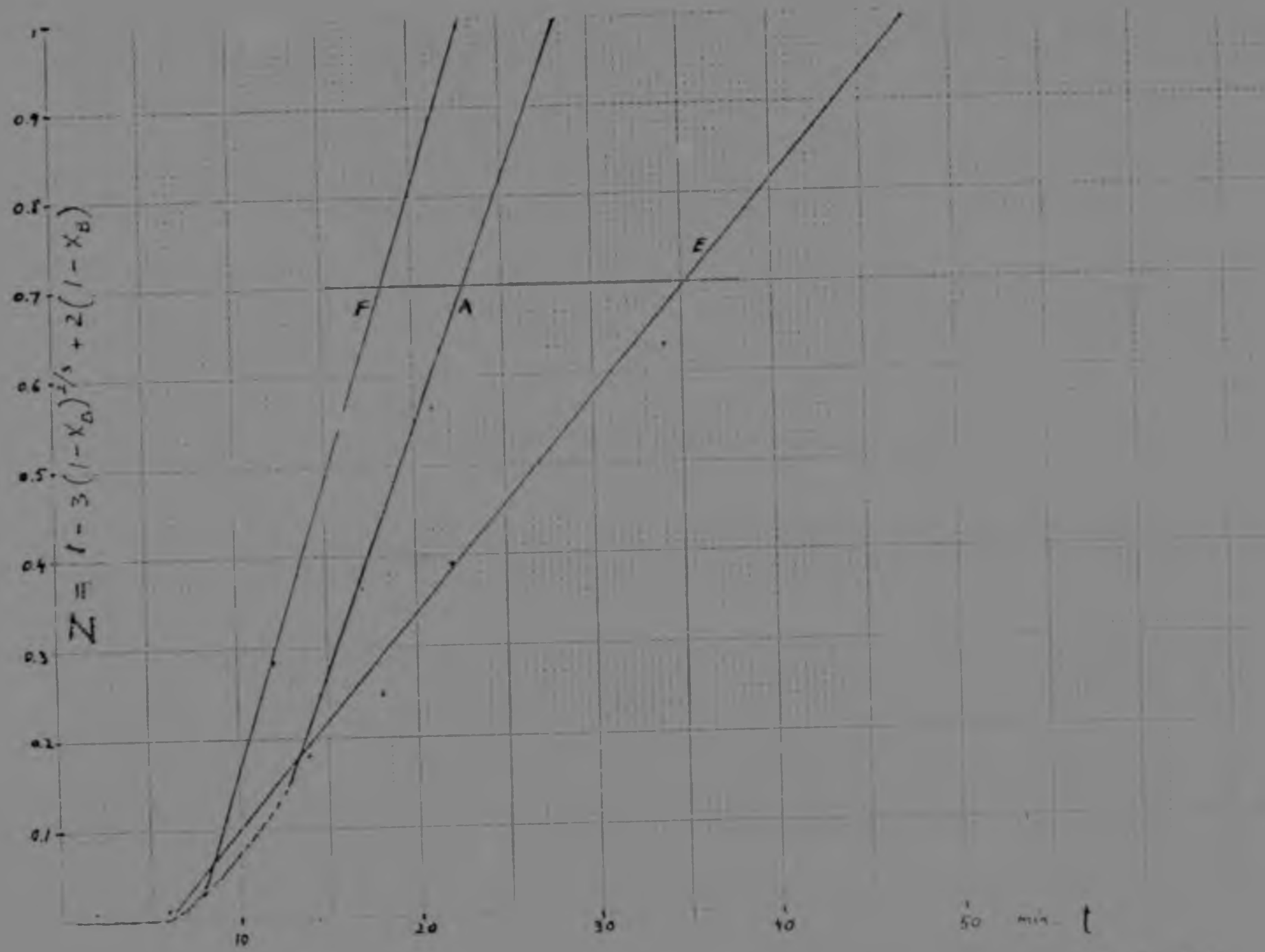

Fig. 3.11. Levenspiel criterion plotted for three Kinetic experiments : A, F and E.

CHAPTER 4

INDUSTRIAL APPLICATIONS

1. LITERATURE SURVEY

The problem of sulphur dioxide removal from waste gases of power plants and other industrial sources has been around for the last half century. However, it is only in this decade that SO_2 removal has become a major issue and has been widely recognised that the emission of SO_2 from fossil fuel combustion and other industrial sources represents a serious threat to the environment. Although a great deal has been done to learn about the nature of this pollutant and some progress has been made, the effects of SO_2 on health, property and vegetation are not well understood. However the damage to health and property caused by SO_2 in the atmosphere is estimated to be very costly.

The possible health hazard has been the subject of many medical investigations such as that carried out some time ago in South Africa [112]. Thus, sulphur dioxide from flue gases is a pressing ecological problem, particularly now that the energy crisis has accelerated the use of high sulphur fuels [113, 114].

The elimination of SO_2 from stack gases has been the subject of a large amount of research. SO_2 has been adsorbed, with different levels of success, in many instances from alkalized alumina [115], to limestone and magnesium dolomite [116] or on limestone slurry alone [117] and fly ash [118].

Many processes and systems [119 - 126] have been designed to cope with the increasing amount of SO_2 in the waste gases released into the atmosphere. These systems have been developed into pilot plants and a few into full scale plants, so that since 1931 when the first SO_2 removal plant was put into operation [127] more than 100 SO_2 removal processes have been operational in the U.S.A. alone! A list of flue gas desulphurisation (F.G.D) systems in operation in industrial boilers in the U.S.A. is given in Table 4.1. The flow sheets of the main F.G.D. processes mentioned above are given in Figs. 4.1 to 4.13.

Another method of SO_2 removal which is in the research stage is the use of ion exchange resins for SO_2 removal. Much work has been carried out to establish the removal efficiency of SO_2 by micro-reticular anion exchange resins [86] macroporous anion exchange resins [87, 88, 89] and ordinary anion exchange resins [90 - 94].

All the suggested processes for waste gas desulphurization can be classified into two basic cateogries: throwaway processes and recovery processes. In each category one can make additional classifications of wet or dry and catalytic or non catalytic processes. Technolcgies for SO_2 removal are summarised in Fig. 4.14.

Generally speaking, two basic challenges face the designer and user of an SO_2 removal system: 1. efficient and reliable removal of SO_2 to prevent it reaching the atmosphere and 2. provision of some means whereby the captured sulphur or its compounds can be used or recovered for further use in an industrial process.

Most of the processes designed and used in practice as well as most of the literature dealing with the subject of desulphurisation [128, 129, 131-133] advise on the best way of achieving a high removal efficiency, leaving the subject of wastes from such a process to the free imagination of the designer.

The first desulphurisation plant [127] was very simple. It used water from the river Thames to scrub the SO_2 from flue gases, discharging the effluents into the same river, downstream!

The efficiency of the process was 95%, and since then, the main development in wet scrubbing systems has consisted in choosing the chemical which, when added to the water, will increase the removal efficiency. As a result of adding these chemicals, the subject of scrubbing effluents treatment cannot be ignored Developments have been made in the direction of recovery of the chemicals originally added or the treatment of these effluents for dumping purposes [134 - 140].

Not much thought has been given to the idea of using these effluents [141]. Actually, some of this potential has been almost completely

destroyed by adding chemicals to the scrubbing water. An aqueous solution of SO_2 without any added chemicals have found applications in regenerating weak cation exchange resins loaded with monovalent cations [142] and for regenerating strong cation exchangers in combination with aldehydes or ketones [143, 144] which were added to lower the pH and thus to enable the regeneration to take place.

Workers do not seem to have considered the use of SO_2 as a gas or in an aqueous solution, (without the addition of aldehydes or ketones) for the regeneration of weak (or strong) cation exchange resins loaded with Ca^{++} or Mg^{++} cations.

Summarising it can be concluded that by introducing chemicals into the wet scrubbing systems, the process designers have almost forgotten one of the two challenges mentioned previously: provision of some means whereby the captured sulphur or its compounds can be used or recovered for an industrial process.

A new look at wet scrubbing systems with a particulate look at the potential use of the wastes of such systems is therefore necessary.

2. ION EXCHANGE AND THE UTILIZATION OF THE F.G.D. SCRUBBING WATER

Although the percentage of SO_2 in the flue gases is very small in comparison with the amount of CO_2, SO_2 is the only one which effectively dissolves in the scrubbing water. This is as a result of two effects: the high temperature and the low pH caused by the dissolved SO_2.

Compared with CO_2, SO_2 is very soluble in water (Table C3) (≈ 100 times more soluble,) and therefore, most of the SO_2 dissolves in the scrubbing water and partially ionizes. This lowers the pH of the solution suppressing the ionization of the CO_2 and so its overall solubility. As the solubility of both gases decreases with temperature, and since the flue gases have quite an elevated temperature, only a small part of the CO_2 dissolves during the scrubbing process.

The effluent from an FGD system which uses pure water for scrubbing, has a low pH. Having a low pH the obvious use for this solution is in the

regeneration process of cation exchange resin and since the pH is not too low, only the regeneration of a weak cation resin should be suitable. Such an application has been previously realised [142] and patented. By thinking of the entire system in which the FGD process is incorporated, it becomes obvious that the most suitable application for the low pH scrubbing effluents is the regeneration of the weak cation resins used in the system for the treatment of the raw water! Thus the scrubbing effluents can regenerate the loaded weak cation resins used in the water treatment, and by doing this the treatment cycle is closed for the system: Raw water is treated by weak cation exchange resins, the water is made into steam by burning fossil fuels which are transformed into gases releases into the atmosphere. The SO_2 from these gases is scrubbed with raw water and the effluent is used in the regeneration of the resin before itself being treated.

Fig. (7.15) shows the suggested integration of the regeneration process in the water and waste-gases treatment circuit of a power station.

In a power station which uses steam [23] to move turbines [22] or for any other process [22] the water [1] is usually treated (among other things) by a weak acid cation exchanger [2] to remove part of the hardness.

The partially "soft" water [3] is then transformed into steam [23] in the boiler [5] by burning fuel [6] in excess of air [7]. The waste gases [8] resulted, must be treated before their release into the atmosphere. They are scrubbed with water [11] in the absorption column[9] and the treated gases [10] can be released into the atmosphere.

The gases [8] can be cooled down before scrubbing with the partially "soft' water [3] in the heat exchanger [4]. [21] is the condensate.

The solution resulting from scrubbing [16] is used to regenerate the weak cation exchange resin [2] because it contains mainly H_2SO_3.

The excess of this solution can be passed directly for treatment [25].

The effluent from the regeneration [20] is treated with $Ca(OH)_2$, CaO or $CaCO_3$ [29] until the pH rises to $\sim$ 9. The slurry is allowed to settle in the settler [15] from which the clear solution [13] can be recycled [12] to the scrubbing solution [11] or to the feed water [1]. The precipitates [14] can be decomposed [17] by heat into CaO, or $Ca(OH)_2$ and SO_2 [19].

The solids [18] can be used again in the effluent treatment and the SO_2 [19] can be used in a sulphuric acid plant, and for lowering the pH of the regeneration solution [16] to the required level [pH1-1.6].

3. INDUSTRIAL SIZES

To further explain the suggested integration of the regeneration process in the water and flue gases treatment, a full size absorption tower and a water treatment unit are designed. The design of the absorption tower is done in Appendix C, while the ion exchange unit is sized in Appendix D.

The values of the volumetric flow rates of flue gases and water used in this design, are the same as those treated at the Japanese FGD unit at Toyamo-Shinko power plant which treats flue gases from a 250 MW utility boiler (Fig.4.9) [122], though their process is of course different.

The designed features of the scrubbing tower and the ion exchange column are summarised in Tables 4.2 and 4.3 respectively.

4. IS THE INTEGRATION FEASIBLE?

Going back to the "old fashioned" scrubbing process in which water (only) was used in the process of SO_2 removal from flue gases, the integration suggested is an unconventional step, which must be evaluated on its own merits before being implemented.

The success of regenerating a weak cation resin loaded with Ca^{++} cations is actually the key to the integration proposed. The

regeneration process has been described in the chapters preceding this one and therefore, the actual regeneration of a weak cation exchange resin loaded with Ca^{++}, using a solution of SO_2 in water, is not in doubt.

The only question arising in connection with the regeneration is the pH of the solution which must be quite low. The efficiency experiments showed that as the pH of the regeneration solution increases, the volume of that solution needed increases as well, transforming an efficient regeneration process (at pH 1-1.2) into an inefficient one (above pH 1.5).

Since the concentration of SO_2 in the scrubbing effluents is very low, the pH is probably about 2.5 which is not enough for an economical regeneration process. This problem can be solved by lowering the pH of the effluent before it reaches the ion exchange unit, by bubbling SO_2 through it until the required pH value is achieved. This additional adsorption of SO_2 into the effluent solution, can be accomplished in a closed system by using the device described in the S.A. Patent 781211 [145] intended for this purpose.

The SO_2 is supplied from the treated effluents, after their decomposition into oxides and SO_2, as suggested in Fig. 4.15.

The SO_2 scrubbing process together with the regeneration process for the weak cation exchanger, integrated in a single system as suggested before (Fig.4.15) can now be compared with other scrubbing processes, as well as with other regenerants.

A brief comparison of this new approach with one of the most used methods for SO_2 scrubbing from flue gases ($Ca(OH)_2$- lime slurry adsorption) and with the most employed regenerants for the cation resins (H_2SO_4 or HCl), reveals that the scrubbing efficiency of SO_2 with water only, is ≈ 95% (proved at Battersea Power Station) while the lime slurry adsorption increases the efficiency by only 3 to 4%. On the other hand, large quantities of water have to be handled in comparison with relatively low quantities of lime slurry theoretically needed. In practice the quantities of lime slurry necessary to

efficiently remove the SO_2 from the flue gases become very large since CO_2 is also absorbed, and its concentration is far greater than that of SO_2 :

eq.1. $SO_2 + Ca(OH)_2 \rightarrow CaSO_3 \downarrow + H_2O$

eq.2 $CO_2 + Ca(OH)_2 \rightarrow CaCO_3 \downarrow + H_2O$

The same comparison shows that the effluents from the FGD with water can still be used, which is not the case with the effluents from FGD which contain chemicals (lime, $CaCO_3$, $CaSO_3$).

From the regeneration of the weak cation resin point of view, only dilute solutions of H_2SO_4 can be used since high concentrations will precipitate the $CaSO_4$ in the resin bed, which means that large volumes of diluted acid are still needed.

The treatment of the regeneration effluent (with $Ca(OH)_2$ for example) will not bring any change in the solubility of the calcium salts, eluted from the resin, since $Ca(OH)_2$ is less soluble than $CaSO_4$, the solubility sequence being :

$$CaSO_4 > Ca(OH)_2 > CaSO_3 > CaCO_3$$

Therefore no use of this effluent can be expected. Its disposal is very difficult since all the calcium salts are in solution!

Similar results for the regeneration of the weak cation resin with HCl will occur, the only difference being that smaller and more concentrated amounts of acid can be used:

Calcium salts will thus remain in solution whether the effluent is treated with $Ca(OH)_2$ or not.

Yet, by using an aqueous solution of SO_2 for the regeneration of the weak cation exchanger, the regeneration effluent contains besides $SO_3^=$ and HSO_3^- ions, Ca^{++} cations, having the special feature that it contains the only combination of cations and anions which requires

only an increase in the pH level for its precipitation into a highly insoluble form.

The only question which must still be answered is the quantity of SO_2 needed to be added to the FGD effluent to lower its pH to a level considered to be adequate for its economical use as a regenerant for the weak cation exchanger. Chapter 2 showed that the desired pH should not be higher than 1.6 and the corresponding amount of SO_2 in water which produces such a pH is 0.16 moles SO_2/litre, or 10.24 g SO_2/l.

The FGD effluent leaving the scrubbing tower (designed in Appendix E) has a concentration of 'g SO_2/l which means that an additional 10g SO_2/l will be needed to ensure the correct pH. This additional SO_2 can be provided from pressurized cylinders at the beginning, but can be recycled from the decomposed $CaSO_3$ at a later stage, as suggested.

It can be summarised that if SO_2 has to be removed in a plant, where there is a weak acid cation exchange unit, it might well be preferable to scrub the SO_2 with water and to use the scrubbing effluent for the regeneration of the ion exchange unit, rather than scrubbing the SO_2 with a slurry of $Ca(OH)_2$ or any other solution. The scrubbing of SO_2 with water and the use of the scrubbing effluents for regeneration purposes are both possible processes and their integration is desirable.

User/location	Supplier	Capacity: MW	Capacity: Gas volume	Waste product disposal
Canton Textile Mills, Inc.[1] Canton, Ga.	FMC Environmental Equipment Div.	10	42,000 acfm	Na_2SO_3/Na_2SO_4 liquor to lined holding ponds
Caterpillar Tractor Co. Joliet, Ill.	Zurn Industries, Inc.	18[2]	1 43,500 acfm	More than 60% solids. $CaSO_4$ sludge pond-dried for landfill.
Caterpillar Tractor Co. Mossville, Ill.	FMC Environmental Equipment Div.	57[3]	240,000 acfm	$CaSO_3$ (more than 60%) sludge to landfill.
FMC Corp. (soda-ash plant) Green River, Wyo.	FMC Environmental Equipment Div.	150[3]	–	Liquor (Na_2SO_3/Na_2SO_4) to collection pond for future landfill.
GM/Delco Moraine Div. Dayton, Ohio	Entoleter, Inc.	24[2]	55,440 scfm	Onsite clarification and dewatering facility receives Na_2SO_3/Na_2SO_4 liquor at 35 gpm
GM Chevrolet Parma Plant Parma, Ohio	GM Environmental Design, Koch Engineering Co., fabrication	32[3]	60,000 acfm	$CaSO_3/CaSO_4$ (more than 50% solids) sludge to drying pond and eventual landfill.
GM Truck & Coach Plant Pontiac, Mich.	Peabody Process Systems	26	55,000 scfm	Landfill receives dewatered 5% solids slurry.
GM Corp. St. Louis, Mo.	Combustion Equipment Associates, Inc.	25[2]	–	Na_2SO_3 is oxidized to Na_2SO_4, then pH is neutralized; eventually to city sewer.
GM (Chevrolet Motor Div.) Tonawanda, N.Y.	FMC Environmental Equipment Div.	32	146,800 acfm	Sanitary landfill receives flyash and dewatered Na_2SO_3/Na_2SO_4.
Georgia-Pacific Paper Co. Crossett, Ark.	Neptune AirPol, Inc	96	320,000 acfm	pH neutralized for discharge to city sewer.
Great Southern Paper Co. Cedar Springs, Ga.	Neptune AirPol, Inc	100[4]	700,000 acfm	Clarification, ponding, eventual discharge to river.
ITT Rayonier, Inc. Fernandina Beach, Fla.	Neptune AirPol, Inc	120[3]	–	Clarification, ponding, eventual discharge to river.
Mead Corp. Stevenson, Ala.	Neptune AirPol, Inc	60[2]	175,000 acfm	Pulp mill uses recovered solution as makeup to cooking liquor.
Nekoosa Edwards Paper Co. Ashdown, Ark.	Neptune AirPol, Inc.	52	55,000 lb/h steam	SO_2 recovered from Na_2SO_3/Na_2SO_4 for recycling in pulping process.
Rickenbacker Air Force Base Columbus, Ohio	Research Cottrell/ Bahco	20	55,000 scfm	Lined pond receives unstabilized calcium sulfite/ calcium sulfate sludge.
St. Regis Paper Co. Cantonment, Fla.	Neptune AirPol, Inc	60	175,000 acfm	Onsite sewage treatment plant receives discharged sludge.

All scrubbers in this table use an aqueous scrubbing liquor with an alkaline reagent. All are capable of removing both SO_2 and particulates from flue gas that is generated by burning fossil fuels.

Capital costs have not been included because they are often incomplete. For example, some data include costs of site acquisition and preparation, while others do not. Some data include developmental or construction cost while others cover only the cost of hardware.

Capacity ratings in MW (megawatt) equivalent.

All systems in this table are operating satisfactorily, and have availability rates (when reported) in the range of 90% to 100%.

1 This installation, in addition to removing SO_2 and particulates, uses a very high pH effluent from the dye house as a scrubbing liquor. It neutralizes that effluent in the acid environment of the scrubber, and thereby reduces disposal problems.
2 Total of two boilers.
3 Total of four boilers.
4 Total of two boilers and two scrubbers.

Table 4.1. Data for flue-gas-desulfurization systems in operation on industrial boilers

Source [128].

TABLE 4.2.

SO_2 SCRUBBING TOWER

Flue Gases flow rate		467 000 m^3/h
Water flowrate (scrubbing solution)		6143 m^3/h
Gas concentration of SO_2	(IN)	0.3%
	(OUT)	0.01%
Water concentration with SO_2	(IN)	0
	(OUT)	0.1%
Packing		Random rings (2m x 2in x 3/16in)
Area of cross section		253 m^2
Height		8 m
Pressure drop		10 m atm
Materials of construction		316L stainless steel and Incoloy 825

TABLE 4.3.

Weak cation exchange unit

Water flow rate		90 gal/min or 20.44 m^3/h. or 20 $m^3/m^3_r h$
Concentration	IN	17.2 meq/l (Ca^{++} and Mg^{++})
	OUT	8.2 meq/l (Ca^{++} and mg^{++})
Packing		Weak acid cation exchange resin beads in H^+ form.
Diameter		1 m
Resin volume		1.27 m^3
Height	(Unit)	2.6 m
	(Resin)	1.5 m
Pressure drop		0.9 - 1.1 bar
Material of contractions		316L stainless steel lined with Non corrosive material or fibre glass reinforced polyester.

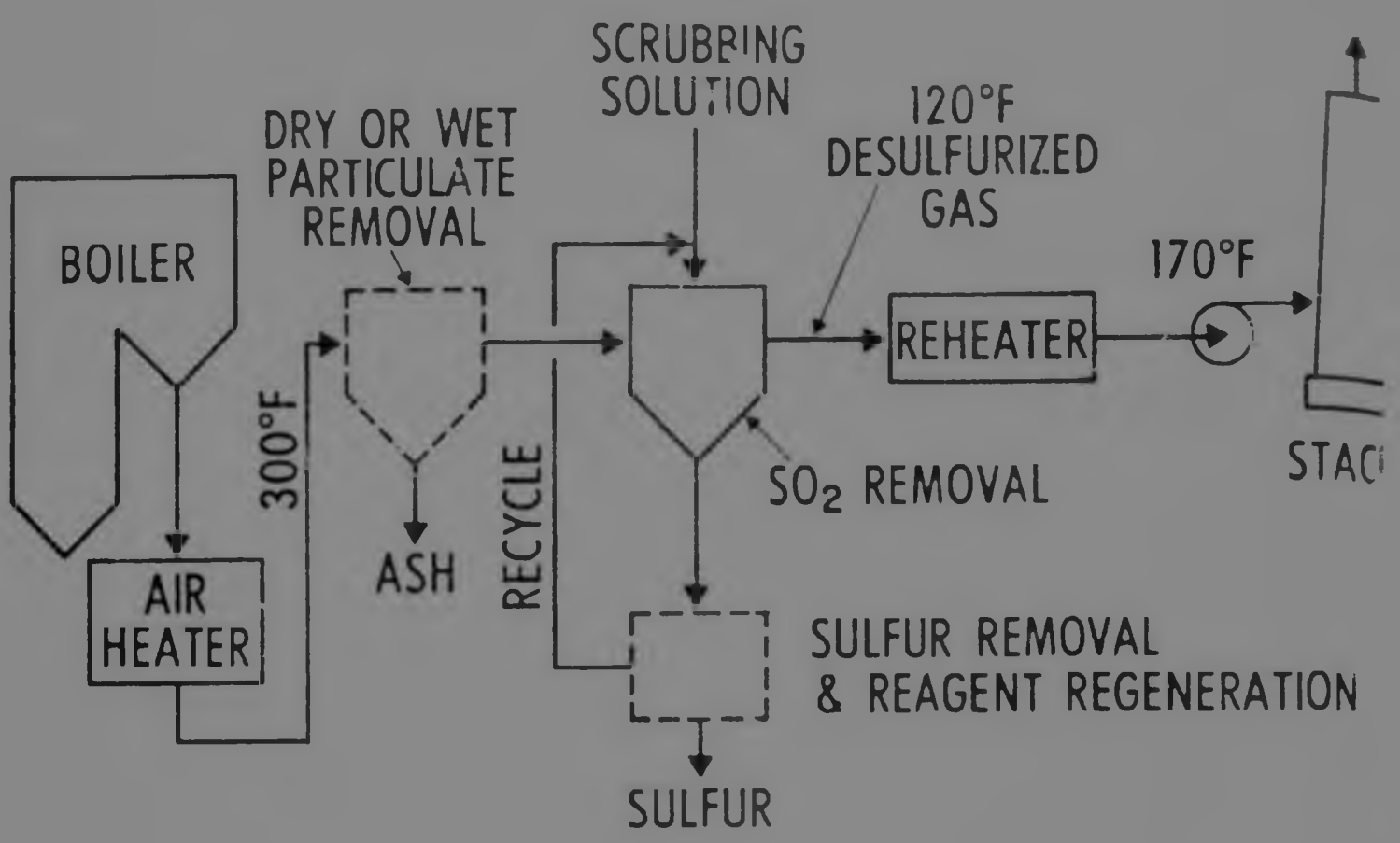

Fig. 4.1. Generalized wet system for SO_2 removal. Source [126]

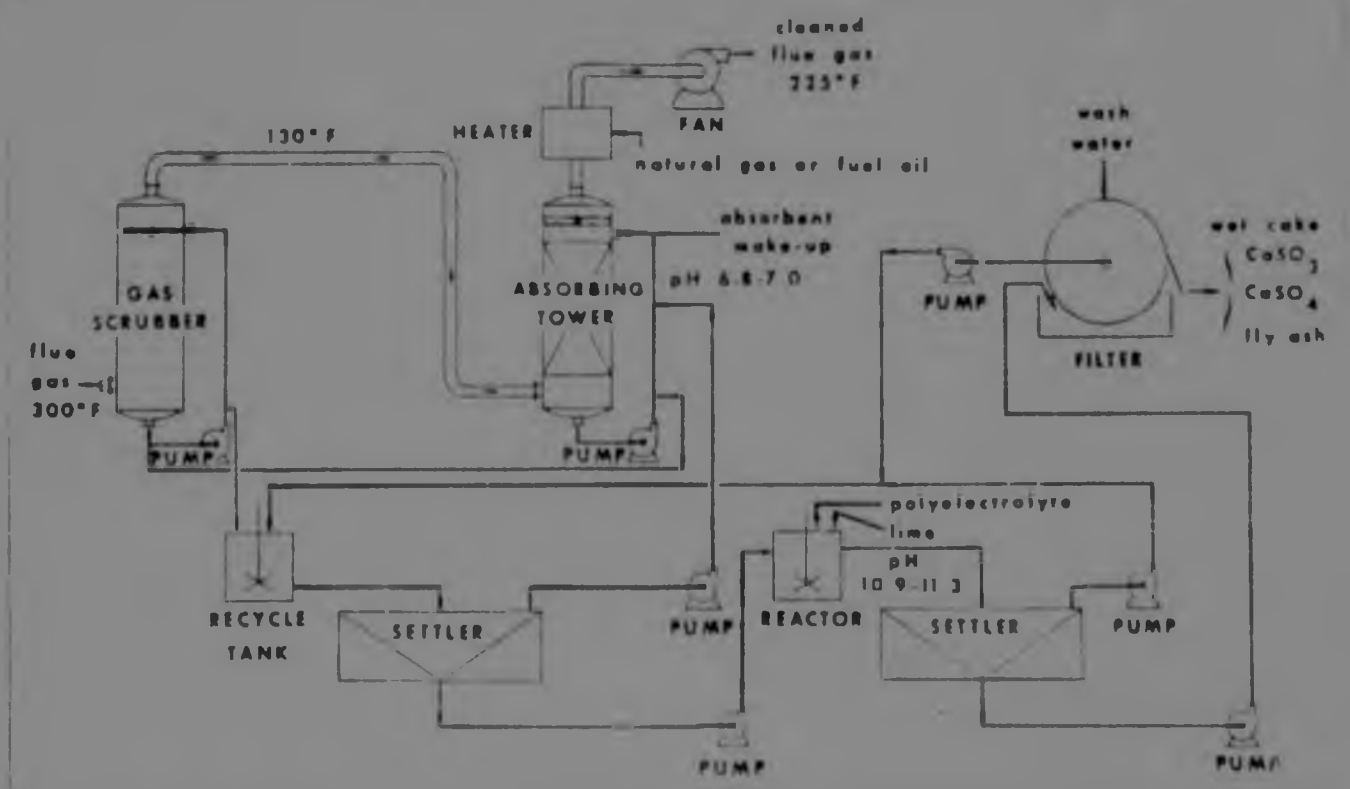

Fig. 4.2. CALSOX process for SO_2 removal. Source [129].

Fig. 4.3. Cominco process recovers SO_2 and yields $(NH_4)_2SO_4$ byproduct

Source [124]

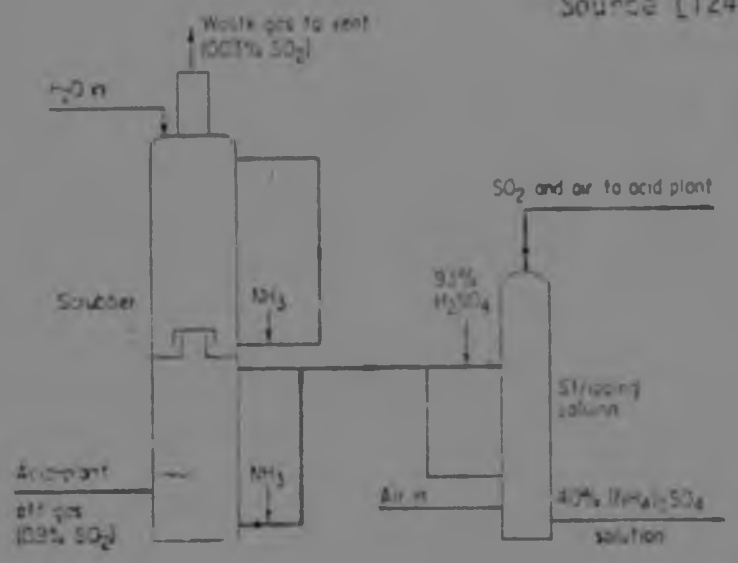

Fig. 4.4 .Battersea process wrings SO_2 from exhaust gases

Source [124]

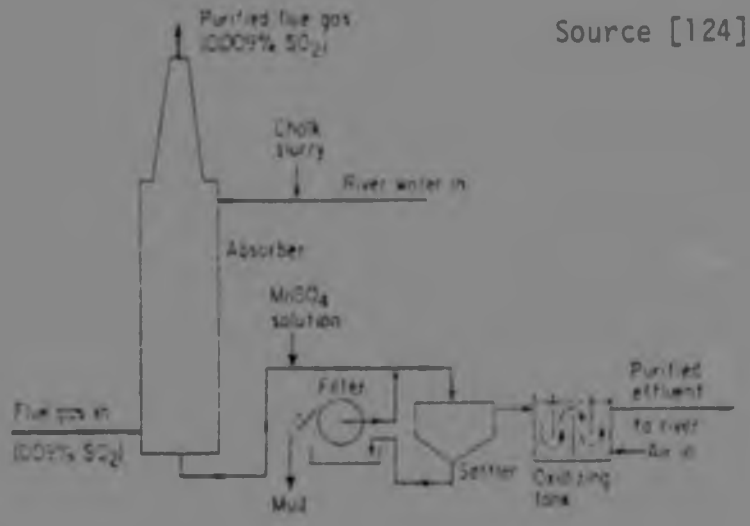

Fig.4.5. Zinc Oxide process Flue gas vented but SO_2 liquefied

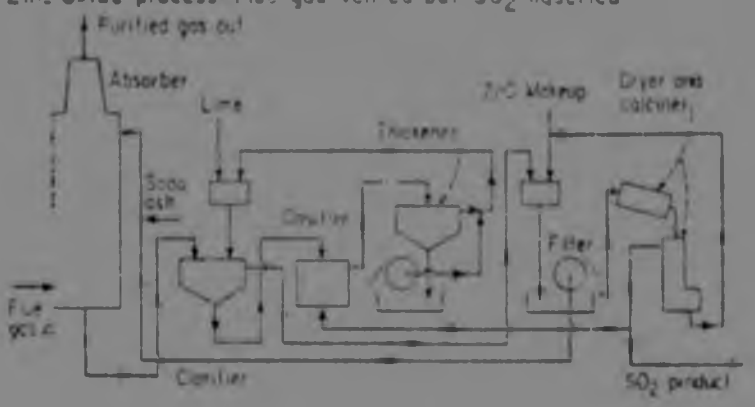

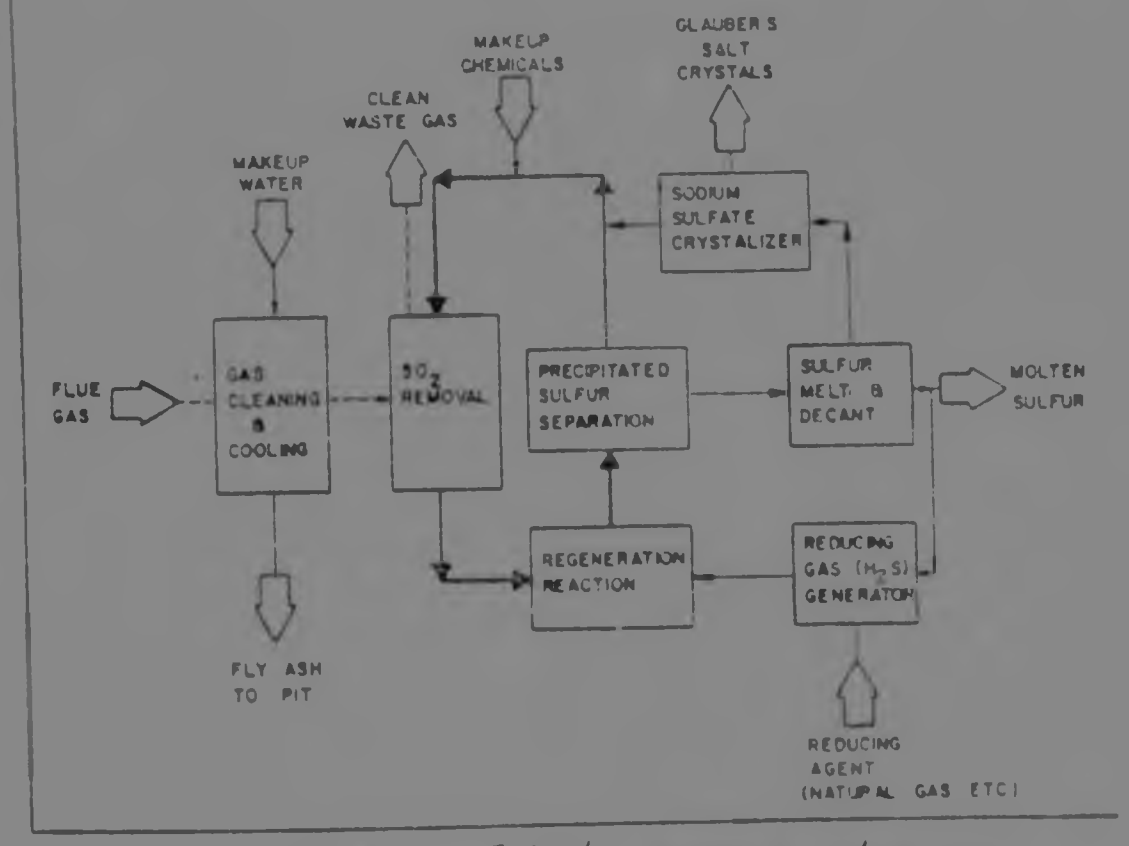

Fig. 4.6. Citrate process diagram

Source [119]

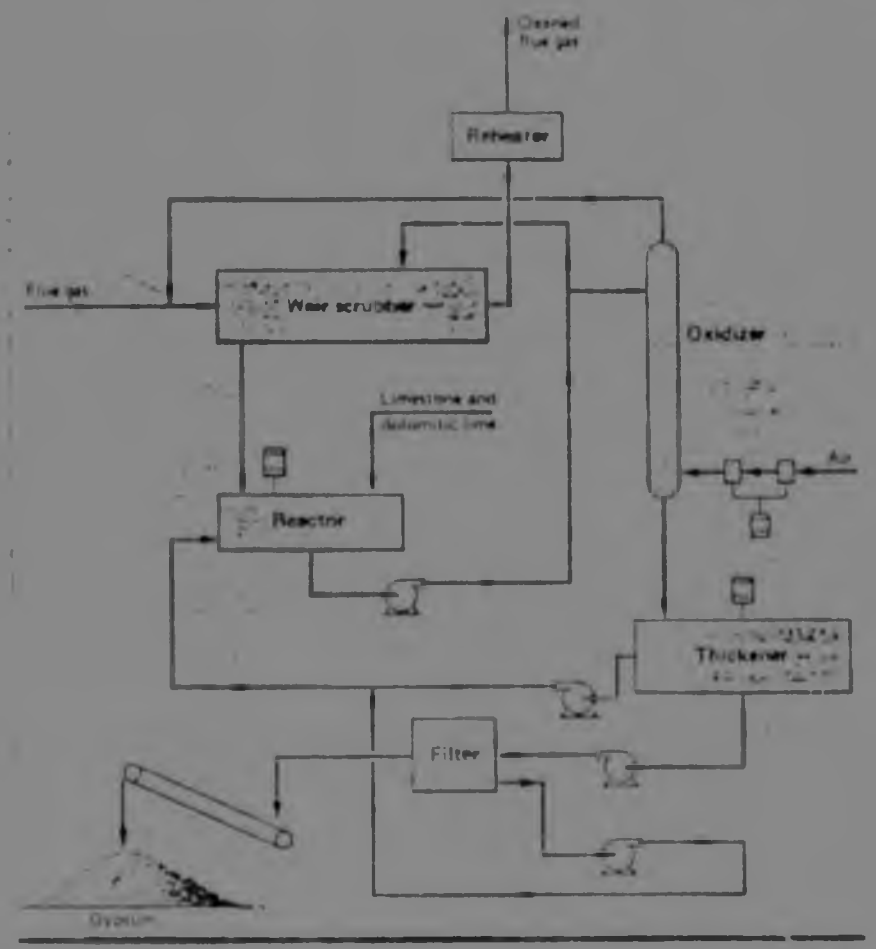

Fig. 4.7. Pullman Kellogg's magnesium-promoted limestone scrubbing system

Source [116]

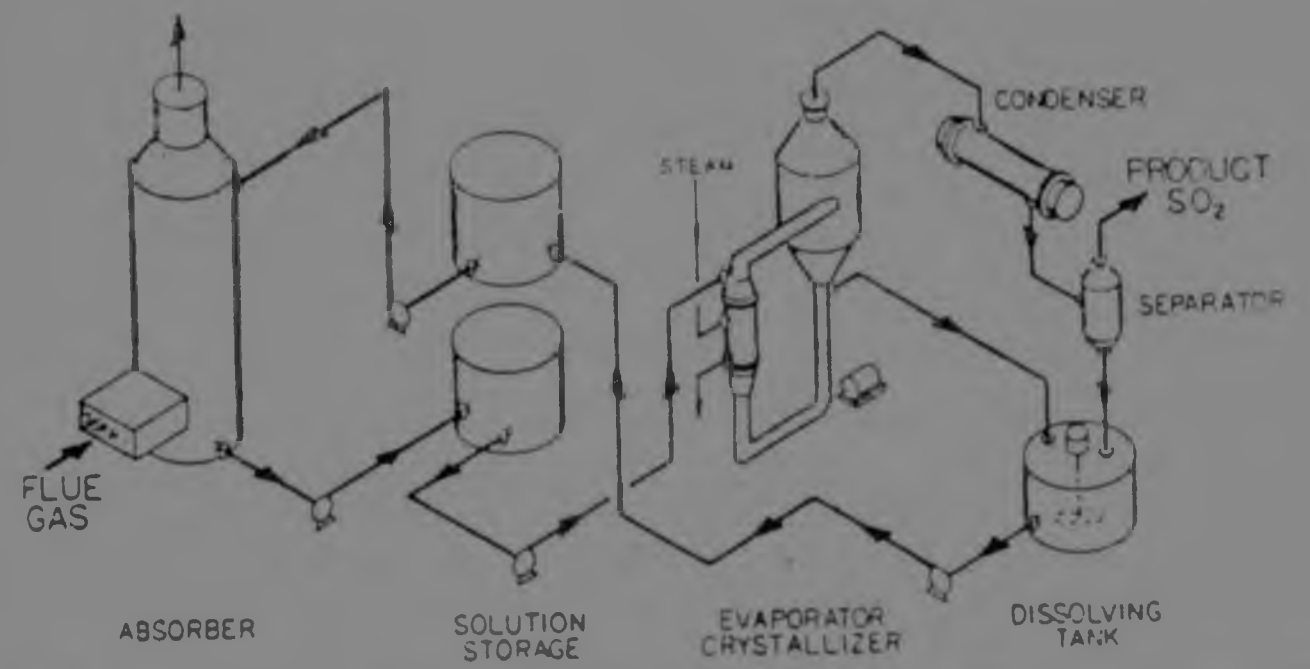

Fig. 4.8. Basic flow diagram of the Wellman-Lord sulfur dioxide recovery process.
Source [130]

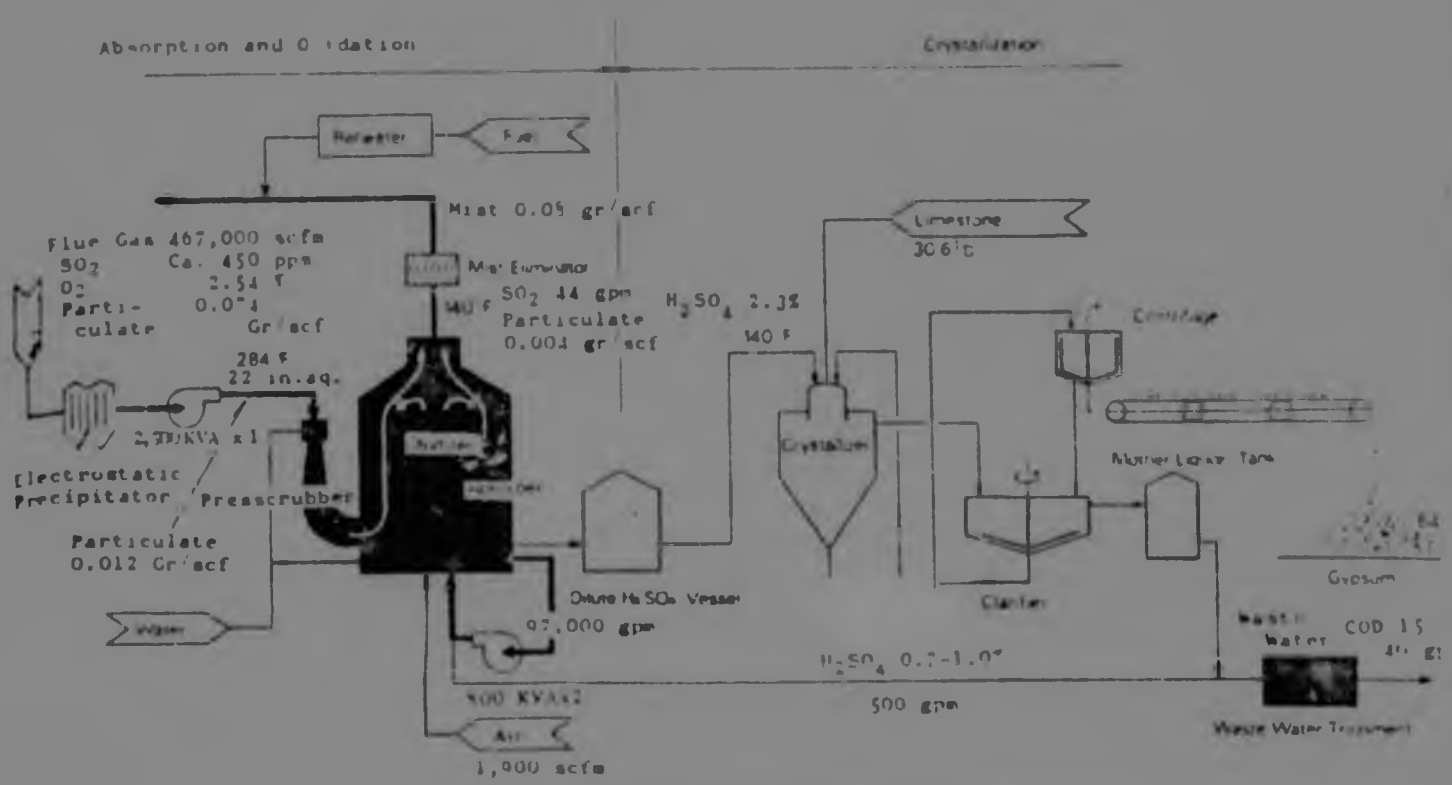

Fig. 4.9. Process flow sheet of the Chiyoda process.

Source [122]

Fig.4.10. Xylidine-water mixture absorbs SO_2 in Sulphidine process

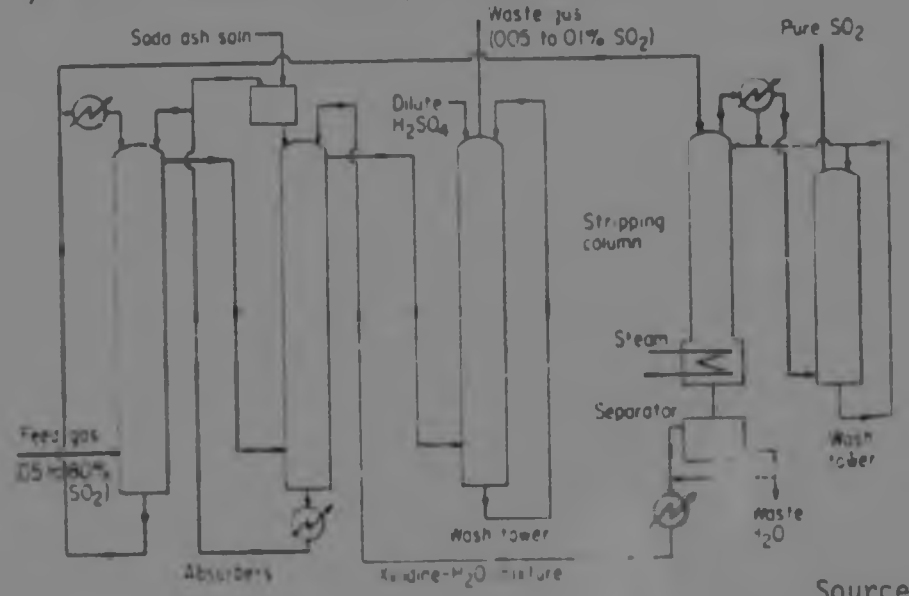

Source [124]

Asorco process for recovering SO_2 represents an improvement over the Sulphidine process

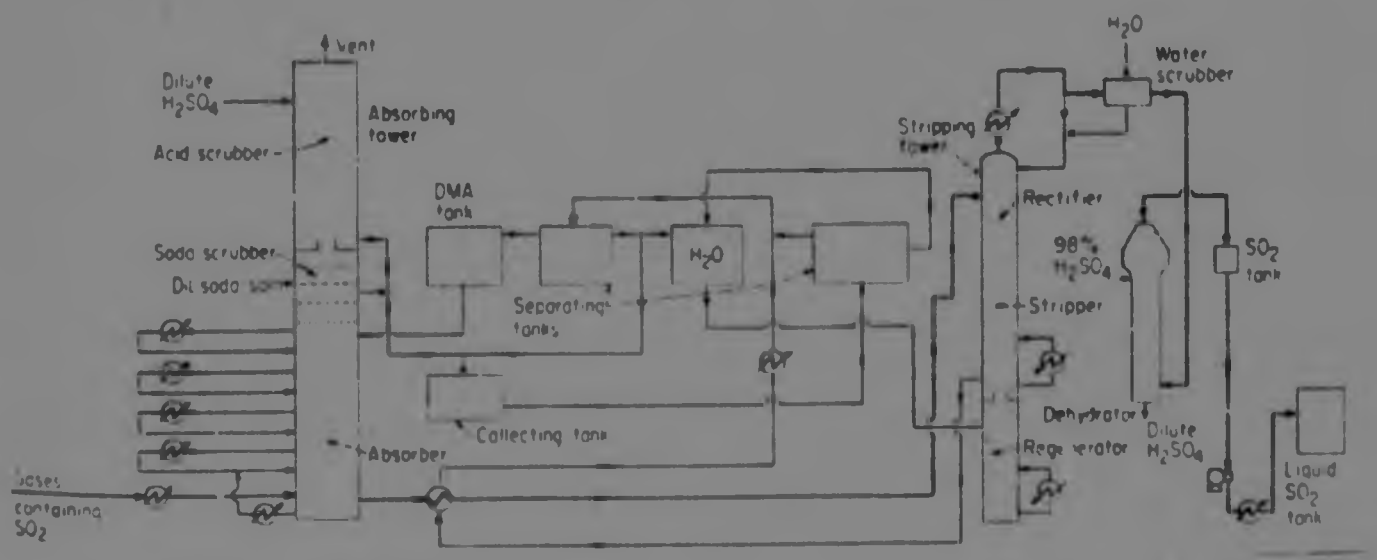

Fig. 4.11 Source [124]

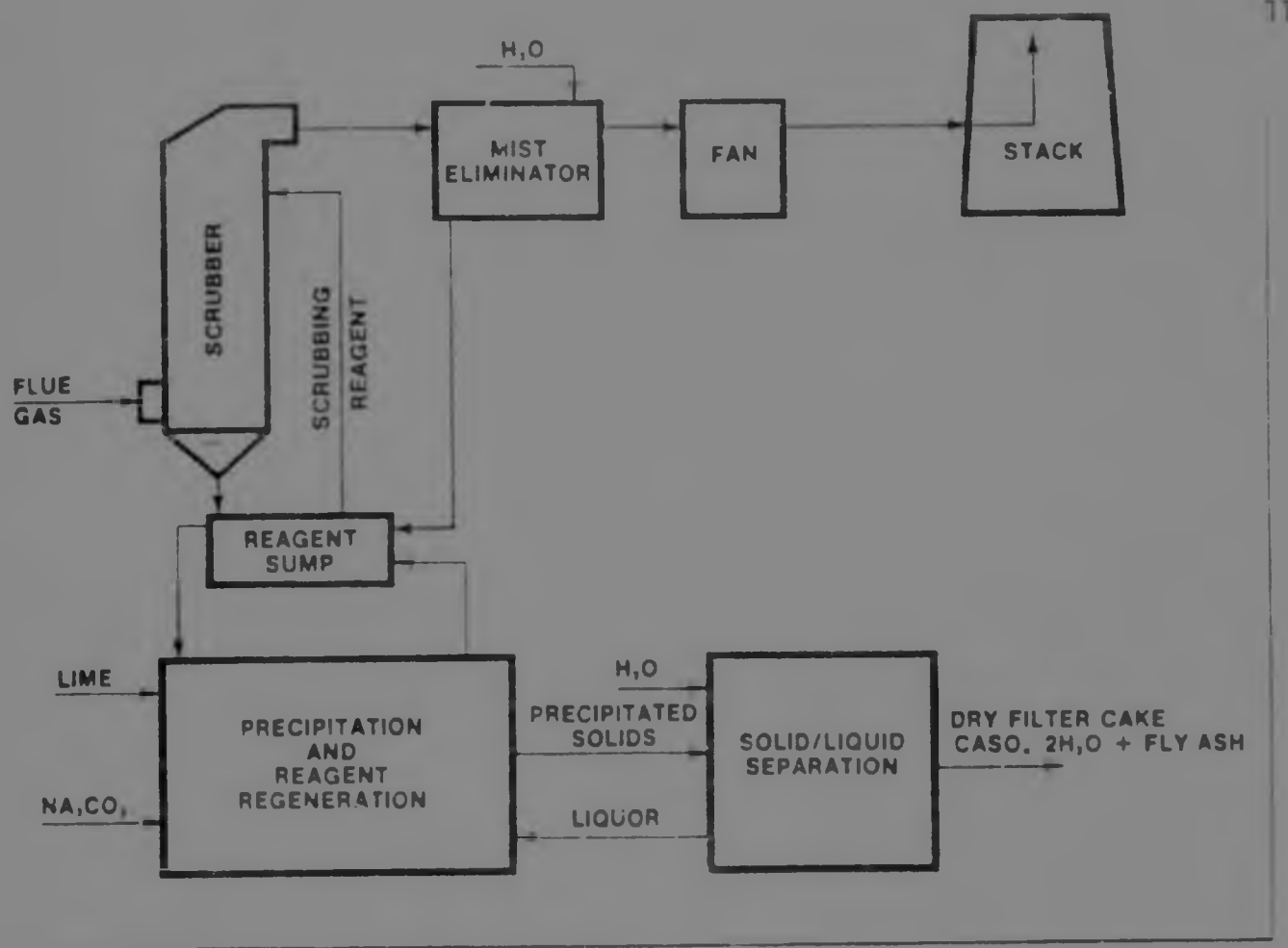

Fig.4.12 Envirotech Double-Alkali SO_2 Removal System, basic concept.
Source [126]

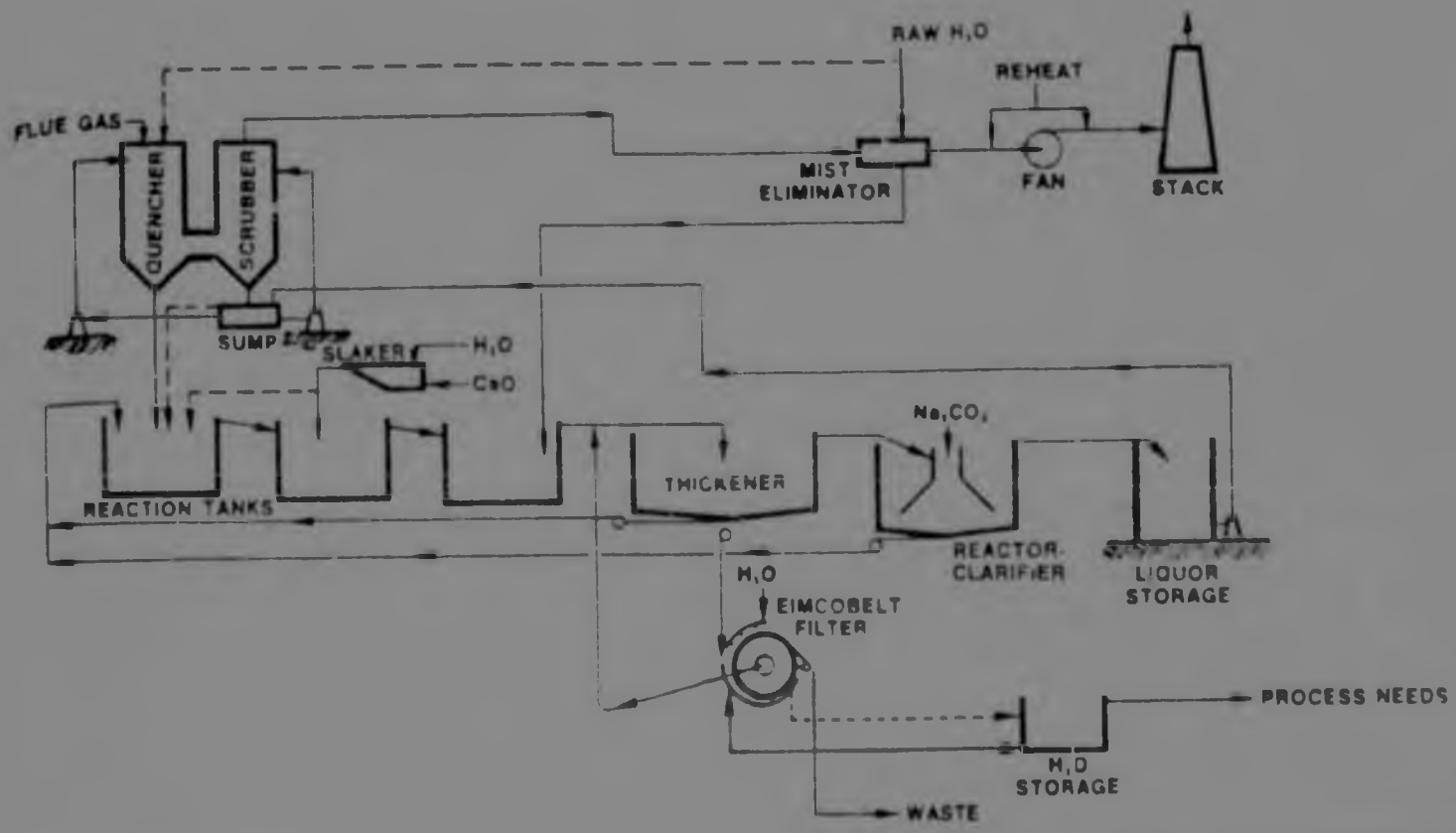

Fig.4.13 Envirotech Double-Alkali SO_2 Removal System. Source [126]

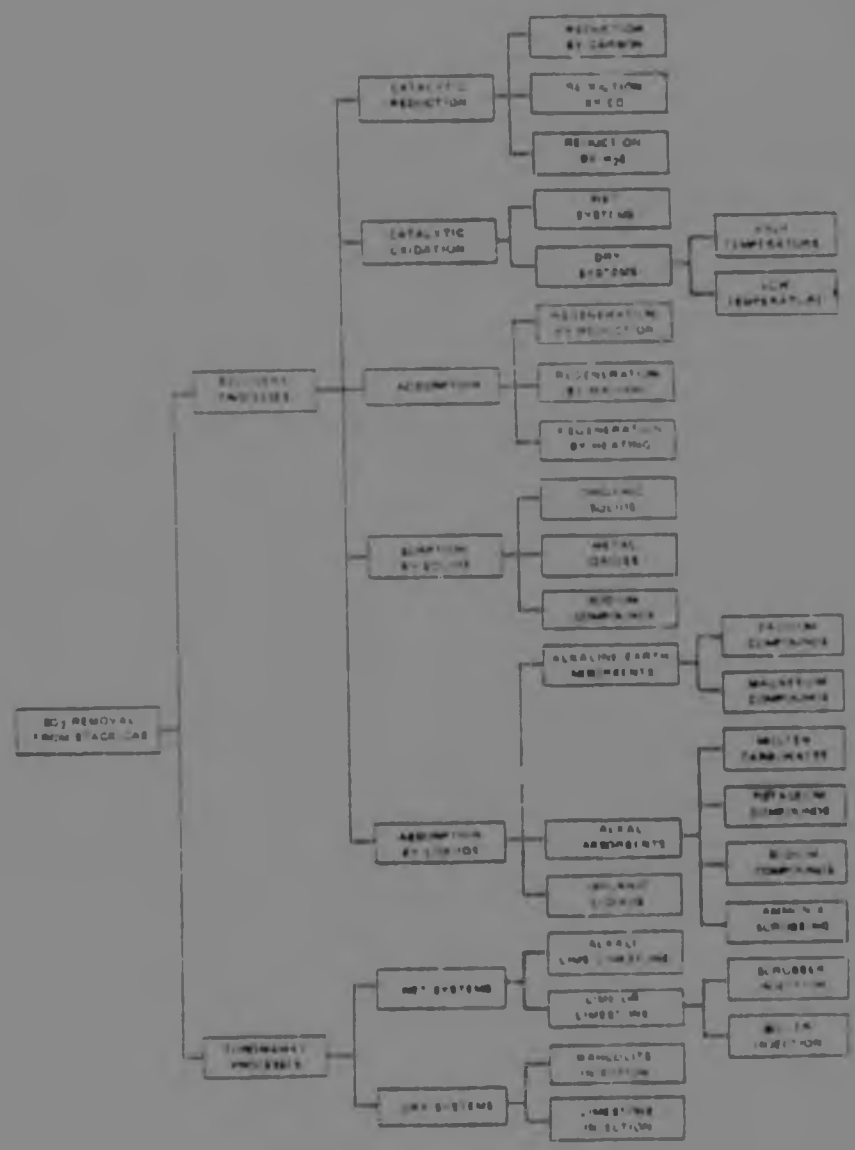

Figure 4.14 Technologies for the removal of sulfur dioxide from stack gas.

Source [131].

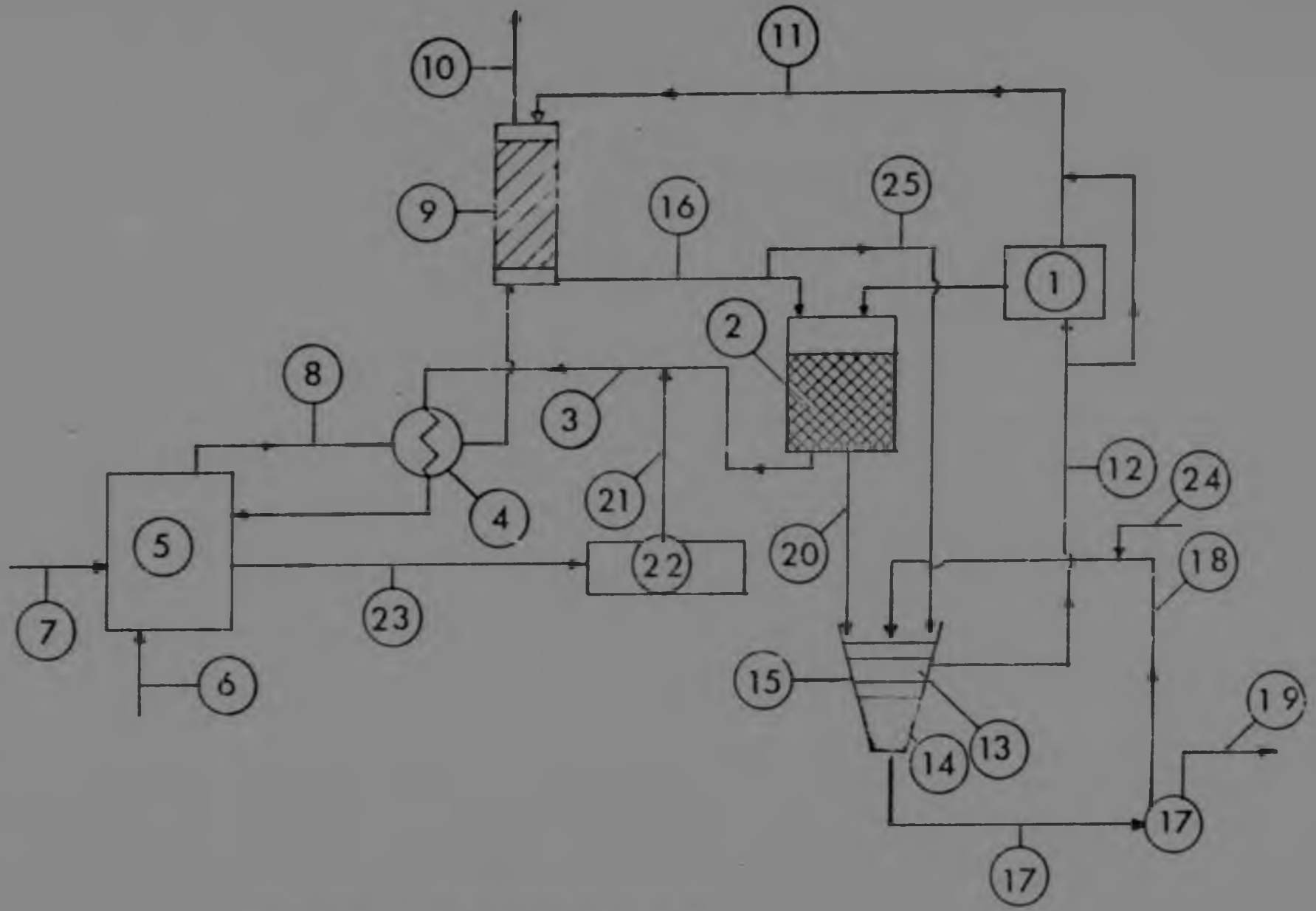

Fig. 4.15. An integrated system for water and SO_2 treatment

CHAPTER 5.

GENERAL DISCUSSION AND CONCLUSIONS

This thesis concentrates on experiments carried out for the development of a new regeneration process and on the applications of the new process.

The first chapter contains a general description of weak ion exchange resins and attention is drawn to the role that weak resins play in the field of ion exchange. The role of weak acid cation exchangers is emphasized in connection with water treatment and the latest processes based on this type of resin are discussed. The chapter also reviews the main problems connected with ion exchange regeneration, and the direction that new developments are likely to take: a broader use of weak resins, and the need to find cheaper regeneration agents.

Bearing this in mind, a new type of regenerant is suggested, which can be used for the regeneration of a weak cation resin. This is very much cheaper than the conventional regenerants and at the same time could ease pollution problems. The regenerant suggested is a solution of SO_2 in water.

The preliminary investigation into the regeneration of a weak cation exchanger with a solution of SO_2 in water, revealed that such a regeneration is possible. The question of interference by $CaSO_3$ precipitation was also investigated.

1. If Ca^{++} precipitates as $Ca\ SO_3$ (at high pH only) it precipitates <u>outside</u> the resin beads, and can be washed away.

2. On the other hand, $Ca\ SO_3$ is soluble at low pH and it can therefore be eluted as a solution during the regeneration.

It was also found that the Cu^{++} loaded weak cation resin (Zerolite 236) could also be regenerated using the same SO_2 in water solution.

During the preliminary investigation, five methods were developed and applied for ensuring the end of the loading/regeneration step, and for checking the type of precipitates (if any) obtained. Three of those methods (monitoring the pH of the effluents, colouring the resin with methyl red and the P.R. tests) were applied in the more comprehensive experiments which followed the preliminary investigation, and two of them became part of the new procedure for regeneration.

(a) Colouring the resin with methyl red is part of the regeneration procedure developed for the regeneration of Cu^{++} loaded weak cation exchange resins.

(b) The equalization of pH values of the inlet and outlet regeneration solution denotes the end of the regeneration.

The preliminary investigations were successful and therefore, further experiments were carried out.

These experiments showed that:

(1) The regeneration of a weak cation resin loaded with Ca^{++}, Mg^{++}, Na^{+} or Cu^{++} using a solution of SO_2 in water, is a feasible process.
(2) The process is efficient.
(3) The procedure is simple.
(4) The process is easy to control.
(5) The newly employed regenerant has no negative effects on the loading capacity of the resin.
(5) Demineralized, soft or hard water can be equally well employed.
(7) The pH has a drastic effect on the efficiency of regeneration and an upper limit of pH = 1.6 is suggested.

Since the loading solution can also be used as a regeneration solution with the addition of SO_2) the necessity of providing a special solution for regeneration is avoided.

In the case of Cu^{++} loaded resin, a high concentration of Ca^{++} ions in the regeneration solution can adversely effect the regeneration but the effect is small.

During the same experiments it was shown that the effluents from the regeneration can be successfully treated and the solution recycled.

Theoretical calculations predicted that ion exchange during the regeneration is controlled by the intraparticle diffusion step, the film diffusion step playing an important role at the beginning of the process.

The Kinetic experiments, confirmed as a whole the predictions made about the diffusion controlling step, and led to the calculation of the intra-particle diffusion coefficient $\bar{D}$ for the new regeneration process.

The value obtained for $\bar{D}$ is in good agreement with the values reported in the literature.

A new type of flow meter which can handle a large range of flow rates, has no moving parts and is very easy to build, was developed and tested.

This work was carried out, bearing in mind the modern problems of air and water pollution, and the dramatic increase in raw material prices.

It does not only provide the necessary information for further development of the new regeneration process, but it also suggests the way this process could be applied.

Two appendices were devoted to the design of equipment needed for the suggested integration of SO_2 scrubbing and water treatment.

The required sizes compare favourably with the sizes reported in the literature: the ion exchange unit is of medium size while the scrubbing tower, which seems to be very large, compares favourably with a scrubbing tower designed and built in Japan [122].

Now that it has been shown to be possible to regenerate a weak cation exchanger loaded with an aqueous solution of SO_2, the decision to use

these results for implementing a combined scheme, will depend on economic factors, combined with increasing pressure for minimizing air and water pollution.

The big advantage of the scheme proposed as a result of the work in this thesis is it leads to an integrated scheme of water treatment and the removal of SO_2 from waste gases.

There however remain several features which decrease the attractiveness of the process. The scrubbing of the SO_2 from stack gages with water alone means that large quantities of water are needed and the scrubbing tower must be large. This scrubbing solution,before it can be used as a regenerant, must have a pH below about 1,6 and it is doubtful if this figure can be achieved directly from scrubbing the stack gases.

On the other hand, as the final solid product is $Ca\ SO_3$, some of this could be thermally decomposed into lime and SO_2 and the latter recycled to increase the SO_2 concentration to the desired level while the lime can be used.

The big advantage of this integrated scheme is that the gaseous and water treatment effluents are combined into a single solid substance, the excess of that which is needed as previously mentioned can be also thermally decomposed into lime which can be sold for effluent treatment, and concentrated SO_2 suitable for use in a sulphuric acid manufacturing plant, thus effectively producing no effluent.

Whether at present the economics are favourable for such a scheme is not known. Nevertheless the economics of today might not be the economics of tomorrow and tighter regulations on air pollution and effluent disposal could transform the process into a desirable as well as an economical one.

APPENDIX A.

DETAILED DESCRIPTION OF THE EXPERIMENTS IN WHICH A WEAK ACID CATION EXCHANGE RESIN, LOADED WITH $[Cu(NH_3)_4]^{++}$, or Ca^{++}, Mg^{++} & Na^{+} WAS REGENERATED WITH A SOLUTION OF SO_2 IN WATER

1. Introduction

Since the experiments were carried out in groups of 7, 5 and 3, the details will be given in respect of each set of experiments. Nevertheless where it is possible, the details will be put together to avoid repetition.

2. Apparatus and Instruments

The loading and regeneration took place in a 'Sintered Glass (S.G.) column which had the internal diameter of 1.2 cm., in the first and fourth set and 5 cm. in the second, third and fifth set of experiments.

A pH meter radiometer, PHM-26 monitored the pH during the loading and regeneration.

All the solutions were analysed using an Atomic Absorbence Spectrophotometer (Varian 1200) equipped with special lamps for Ca^{++}, Mg^{++}, and Cu^{++}.

3. Materials and methods

3.1. SO_2 gas

SO_2 was dissolved in water by bubbling the gas stream through the water until the pH dropped to 1 and remained at that level.

The gaseous SO_2 used was an anhydrous type, having a minimum purity of 99.9% and supplied by Afrox - Germiston.

The impurities contained were: water 100 ppm by weight oil 100 ppm, residue - 10 ppm, H_2SO_4 - nil.

3.2 Ion exchange resins

Only one type of resin was used: the gel form of a weak cation exchanger - Zerolite 236. It is supplied in white beads, in H^+ form. A batch of 25 ml. of resin, was used in the first and fourth set of experiments, and a batch of 200 ml. was used in the second, third and fifth set of experiments respectively.

Back washing was carried out before any loading step.

3.3 Loading solutions

A solution of calcium formate and acetate was used for the loading of the resin into the Ca^{++} form, in the first and second sets of experiments. The pH of that solution was 7.4.

In the third set of experiments, a solution containing Ca^{++}, Mg^{++} and Na^+ in water was used for loading. The pH of this solution was 7. 8.

An ammoniacal solution (pH = 10) of $[Cu(NH_3)_4]^{+2}$ was used for loading in the last two sets of experiments.

3.4 Regeneration solutions

A solution of SO_2 in demineralized water was used for the regeneration in the first set of experiments. The pH of the regeneration solution was 1.00.

SO_2 was dissolved in three different types of water, and those solutions were used for the regenerations, in the second and fifth sets: The three different types of water used were:

Demineralised water (contained no Ca^{++})
Tap water (contained 35 ppm Ca^{++})
Hard water (contained 179 ppm Ca^{++})

The pH of those solutions was 1. 00

In the third set of experiments, SO_2 was dissolved in the solution used for loading. The pH of that regeneration solution was 1.00.

3.5 Loading

Before the regeneration tests, the resin was loaded and the loading solution washed away with demineralized water. The loading was carried out in the S.G. Column, using the loading solutions described previously.

3.6 Regeneration

When the resin was loaded with Ca^{++} ions, a short counter current regeneration was followed by a long co-current regeneration (first and second sets). (Co current regeneration is carried out in the same direction as the loading step).

In the third set of experiments, the regeneration was performed in two different ways : in a co-current stream (as in the first and second sets) and in a counter current stream.

In both methods, the gas (SO_2) was dissolved in water before reac ing the resin bed. After the regeneration, the regeneration solution was washed away with demineralized water.

When the resin was loaded with Cu^{++} ions, a long counter-current regeneration was followed by a shorter co-current one. The regeneration solutions were coloured red before the regeneration, with the indicator methyl red. After the regeneration, the solution was washed away with demineralized water.

3.7 P.R. Tests

These tests were carried out using solutions of 2N HCl in a downwards flow and a flow rate not exceeding 0.6 l/h

4. Results

The results of the experiments and P.R. Tests are listed in the tables 2.4 - 2.13.

5. Flow Sheets and Graphs (see Chapter 2).

Figure 2.8 represents the arrangement used for the loading and regeneration of the weak cation exchanger. Figures 2.9, 2.10 and 2.11 represent the variation of the pH before, during and after the regeneration of the weak cation exchangers loaded with Ca^{++}, Mg^{++} and Na^{+}, and $[Cu\ (NH_3)_4]^{2+}$.

6. The Experiments

6.1 First set (7 experiments)

During the loading with Ca^{++} ions, the resin shrunk by 16%. The beads became gelatinous and slightly transparent. They lost their round shape and were compressed into each other, forming an obstacle to the flow of the loading solution.

The regeneration procedure was as follows: Before the regeneration of the loaded resin, 1 - 2 bed volumes of demineralized water were passed upwards through the loaded resin. (1 B.V. - is the volume occupied by the resin in the original state.) After that, 1 - 2 bed volumes of the regeneration solution were passed upwards through the resin at a flow rate of 2 l/h. Thereafter the regeneration solution was continuously passed downwards through the resin, until the end of the regeneration, at a flow rate of 0.4 l/h. When the effluent from the regeneration had the same pH $\pm$ 0.5, as the regeneration solution, the regeneration was considered complete.

After the regeneration, the resin was rinsed with demineralized water in a downwards flow at a flow rate of 0.6 l/h. The washing was stopped when the effluent

reached pH. 3. At the end of the rinsing, the resin returned to its original volume colour and shape. Immediately after the first, second and seventh regeneration of the resins loaded with Ca^{++} ions, three "Proper Regeneration Tests - P.R.T. - were performed. In these "tests" the resin was regenerated with 100 ml. 2N HCl and washed. e remining Ca^{++} ions were then eluted.

6.2 Second set of experiments (5)

During the loading with Ca^{++} ions, the resin shrunk by 13%. The beads became gelatinous and slightly transparent. They lost their round shape and were compressed into each other, forming an obstacle to the flow of the loading solution. The loading flow rates were between 1,5 - 2,0 l/h.

The regeneration procedure was as follows:
When Ca^{++} was loaded on the resin, 1 - 2 bed volumes of demineralized water was passed upwards through the ion exchanger. (2 l/h).

Thereafter, the regeneration solution was continuously passed downwards through the resin, until the end of the regeneration. The flow rate was 0.4 l/h.

When the effluent from the regeneration had the same pH $\pm$ 0.5 as the regeneration solution, the regeneration was considered complete.

After the regeneration, the resin was rinsed with demineralized water in a downwards flow (0.6 l/h). The washing was stopped when the effluent reached pH 2.7.

The same flow rate (0.6 l/h) was used during the rinsing and P.R. Tests.

6.3 Third set (4 experiments)

Four experiments were performed: three loading - regeneration experiments were carried out and one experiment

was devoted to the treatment of the effluents from regeneration.

During the first three experiments the weak acid cation exchanger was loaded with Ca^{++}, Mg^{++} and Na^{+} cations. All these cations were eluted during the regeneration step.

During the loading, the resin shrunk by 13%. The flow rate during the loading was 10 BV/h in a downwards direction.

The regeneration step was performed in two ways during these experiments. In the first experiment, a co-current flow regeneration was employed, during which the regeneration solution was passed downwards through the resin at a flow rate of 3 BV/h. This kind of regeneration was employed in all the experiments described until now.

Thus,only one co current regeneration was performed during the experiments in this set.

In the other two experiments of this set, a counter current flow regeneration was employed to gain information on the efficiency of this method.

During the counter-current regeneration, the acid solution was passed through the resin in an upwards flow, without fluidizing it. The flow rate was 5 BV/h.

Rinsing. After loading and regeneration the respective solutions were washed away with demineralized water. The flow rate employed during rinsing was 4-5 BV/h. In the first experiment, the loading solution was not washed away after the loading step. The rinsing after loading was carried out with a constant amount of demineralized water (600 ml) while the rinsing after the regeneration was carried out until the pH of the effluent rose to 2.7.

The PR Test was carried out with a downwards flow with a solution of 5N HCl, and a flow rate of 4 BV/h.

A separate experiment (the fourth in order) in which the regeneration effluent was treated, was also carried out: To a sample of one of the regeneration effluents, having pH = 1 and a concentration of 2810 mg/l Ca^{++}, 49 mg/l. Na^{+} and 44 mg/l Mg^{++}, a slurry of 2% $Ca(OH)_2$ was added, until the pH rose to 9-10.

The precipitate was allowed to settle and the clear solution above the precipitate was analysed. It had pH = 9.5 and contained 90 mg/l Ca^{++}, 6 mg/l Mg^{++} and 40 mg/l Na^{+}

6.4 Fourth Set (7 experiments) - (Copper loaded resin)
During the loading with Cu^{++} ions, the resin swelled up by 70%. The beads loaded with Cu^{++} were dark blue in colour.

The loading step was always performed in the same manner using the same kind of solution. Before the regeneration of Cu^{++} loaded resin, 5-6 bed volumes of demineralized water were passed upwards through the loaded resin, in a flow rate of ∿ 10 B.V. This pre-fluidization served the purpose of breaking the "cakes" formed within the resin, during the loading step. Since the regeneration step had to be carried out quickly, this step was very important in preparing the resin for a fast and effective fluidization. After that, the regeneration solution was passed upwards through the resin which was fluidized. The flow rate was 20 l/h at the beginning and dropped to ∿ 10 l/h at the end of the regeneration.

The solution level, above the fluidized bed was maintained at 2 cm. by means of a syphon. The bed expansion was very high in the first two experiments (60%).

The upward flow of the regeneration solution was stopped when most of the resin had a pink colour. Then, the

regeneration solution was passed downwards through the bed of the resin. The regeneration was considered complete when the effluent from the regeneration had the same pH $\pm$ 0.5 as the regeneration solution. After the regeneration, the resin was rinsed with demineralized water in a downwards flow of 0.6 l/h until the pH became 2.7. At the end of the rinsing, the resin returned to its original volume, colour and shape. Immediately after the first, second and seventh regeneration of the resins loaded with Cu^{++}, three "Proper Regeneration Tests" - P.R.T. - were performed. In these tests the resin was regenerated with 100 ml 2N HCl and washed. The flow rates of both PRT and washing were 0.6 l/h. The remaining Cu^{++} ions were thus then eluted.

6.5 Fifth set of experiments

During the loading with Cu^{++} ions, the resin swelled up by $\sim$ 70%. The beads loaded with Cu^{++} were dark blue in colour. The regeneration procedure was exactly the same as described above.

In the second experiment in this set, a technical mistake slowed down the regeneration, causing precipitation in the resin. The precipitate could not be dissolved by using more regeneration solution and was eluted during the loading for the next experiment. The P.R. Test was performed only after the last experiment ended.

Flow rates

The loading flow rate was 2 l/h. The upflow rate of the demineralized water add the regeneration solution was $\sim$ 40 l/h at the beginning. It was decreased during the regeneration to 20 l/h and at the end to 12 l/h. The downflow rate of the regeneration solution was 0.6 - 0.8 l/h and the same flow rate was used during rinsing and P.R.T. A new flow meter was designed, constructed and used in these measurements (Appendix B).

7. Examples of Calculation

A step by step calculation of two of the listed experiments is now given. The data used in the following example are listed in Table 2.8. The experiment is the last one, No.3.

Loading

30.5 litres (30500 ml.) of the loading solution was used.

By multiplying this quantity of the respective concentrations of the cations, the amounts of these cations (in mg) are found:*

$$30.5 \text{ x } 1. \quad \begin{bmatrix} 39 \\ 12 \\ 625 \end{bmatrix} \text{ mg/l.} = \begin{matrix} \text{IN} \\ \begin{bmatrix} 1189 \\ 381 \\ 19062 \end{bmatrix} \end{matrix} \text{ mg.}$$

These amounts are listed in Table 2.9 under IN (LOADING). The cations which passed through the resin, come out in two steps, namely in the loading effluent and in the rinsing effluent after the loading. (Table 2.8). The amount of loading effluent solution is the same as that of the loading solution: 30.5 l.

The rinsing effluent solution (after loading) amounted to 0.6 litres (600 ml).

The cations in these two effluents (in mg.) are as follows:

$$30.5 \text{ x } 1. \quad \begin{bmatrix} 38 \\ 10 \\ 387 \end{bmatrix} \text{ mg/l.} = \begin{bmatrix} 1159 \\ 305 \\ 11803 \end{bmatrix} \text{ mg.} \quad \text{loading effluent}$$

---

*The amounts in the big brackets are for Na^+, Mg^{++} and Ca^{++} cations in this order.

Na^+
Mg^{++}
Ca^{++}

$$0.6 \times \begin{bmatrix} 23 \\ 5 \\ 287 \end{bmatrix} = \begin{bmatrix} 14 \\ 3 \\ 172 \end{bmatrix} \quad \begin{matrix} \text{rinsing} \\ \text{effluent} \end{matrix}$$

The amount of cations coming out in [mg] is the summation of these two quantities, and is listed in Table 4.6. OUT (LOADING):

$$\begin{bmatrix} 1159 \\ 305 \\ 11803 \end{bmatrix}_{\text{mg.}} + \begin{bmatrix} 14 \\ 3 \\ 172 \end{bmatrix}_{\text{mg.}} = \begin{bmatrix} \underline{\text{OUT}} \\ 1173 \\ 308 \\ 11975 \end{bmatrix}_{\text{mg.}}$$

The amount loaded is the difference between the amount IN and that OUT, for each cation and is listed under LOADED in Table 4.6.

$$\begin{bmatrix} \underline{\text{IN}} \\ 1189 \\ 381 \\ 19062 \end{bmatrix} - \begin{bmatrix} \underline{\text{OUT}} \\ 1173 \\ 308 \\ 11975 \end{bmatrix} = \begin{bmatrix} \underline{\text{LOADED}} \\ 16 \\ 73 \\ 7087 \end{bmatrix}$$

Regeneration (Elution)

For the regeneration, the same solution was used as for loading. Therefore, Na^{+}, Mg^{++} and Ca^{++} cations were introduced into the column during the regeneration: thus, the amount of these cations coming IN during the regeneration, must be known. The amount of each cation entering during the regeneration is calculated by multiplying the quantity of the regeneration solution used, by the concentration of each cation:

$$5 \text{ l.} \times \begin{bmatrix} 39 \\ 12 \\ 625 \end{bmatrix}_{\text{mg.}} = \begin{bmatrix} \underline{\text{IN}} \\ 195 \\ 60 \\ 3125 \end{bmatrix}_{\text{mg.}}$$

These amounts are listed under IN (REGENERATION) in Table 2.9.

As a result of regeneration, the loaded cations are eluted, and they came off the resin in two steps: during the regeneration and during rinsing after the regeneration. The amount of each cation in each effluent, is calculated by multiplying the quantity of each effluent solution by the concentration of each cations in that solution (Table 2.8).

$$5 \times \begin{bmatrix} 38 \\ 28 \\ 1864 \end{bmatrix}_{mg/l} = \begin{bmatrix} 190 \\ 140 \\ 9320 \end{bmatrix}_{mg.} \quad \text{regeneration effluent}$$

$$1.8 \times \begin{bmatrix} 11 \\ 5 \\ 112 \end{bmatrix}_{mg/l} = \begin{bmatrix} 20 \\ 9 \\ 202 \end{bmatrix}_{mg.} \quad \text{rinsing effluent}$$

The summation of these amounts give the total amounts of each cation eluted during the regeneration.

The results are listed under ELUTED in Table 2.9.

$$\begin{bmatrix} 190 \\ 140 \\ 9320 \end{bmatrix}_{mg} + \begin{bmatrix} 20 \\ 9 \\ 202 \end{bmatrix}_{mg.} = \underline{\text{ELUTED}} \begin{bmatrix} 210 \\ 149 \\ 9522 \end{bmatrix}_{mg.}$$

Since during the regeneration, Na^{+}, Mg^{++} and Ca^{++} cations were introduced, these amounts must be subtracted now, to give the real quantity eluted for each cation.

The result is ootained by subtracting the amount IN (REGENERATION) from the first ELUTED amount.

$$\begin{bmatrix} 210 \\ 149 \\ 9522 \end{bmatrix} - \begin{bmatrix} 195 \\ 60 \\ 3125 \end{bmatrix} = \begin{bmatrix} 15 \\ 89 \\ 6397 \end{bmatrix}$$

These results are listed in Table 2.9 under ELUTED. They are the lower results, under the higher ones

Now that the amount of each cation loaded and eluted is known it is possible to calculate the amount accumulated (not eluted) after the regeneration, and the efficiency of the regeneration.

The amount accumulated can be found by subtracting the amount eluted during the regeneration from that loaded during the loading step for each cation (Table 2.9).

$$\begin{bmatrix} 16 \\ 73 \\ 7087 \end{bmatrix}_{mg.} - \begin{bmatrix} 15 \\ 89 \\ 6397 \end{bmatrix}_{mg.} = \underline{\text{ACCUMULATED}} \begin{bmatrix} 1 \\ -16 \\ 690 \end{bmatrix}_{mg.}$$

These results are listed under ACCUMULATED in Table 2.9.

The efficiency of elution is calculated by dividing the amount eluted by that loaded for each cation:

$$15/16=0.93$$
$$6397/7087=0.92$$

The data used in the following example are listed in Table 2.12. The experiment is the last one, number 5:

Loading

11 litres of the loading solution with a concentration of 1350 mg/l Cu^{++} ions, brought in

$11 \times 1350 = 14850$ mg. Cu.

This amount appears in Table 2.13 under IN.

The amounts which appear under OUT, were obtained by multiplying the quantities of the loading effluents, by their concentration.

4 l x 123 mg/l = 492 mg

4 l x 23 mg/l = 92 mg

3 l x 113 mg/l = 339 mg

To these amounts must be added that obtained from the rinsing effluent (after loading) - table 2.13.

0 6 1 x 179 mg/l = 107 mg.

Therefore, the amount loaded on the resin was obtained by subtracting the amount OUT from that IN (= LOADED)

14850 mg - (492 + 92 + 339) = 13820 (Table 2.13).

Regeneration (Elution)

Since hard water was used to prepare the regeneration solution, Ca^{++} ions were introduced into the column during the regeneration, and were expected to come out in the same amount

Therefore, the amount of Ca^{++} cations is counted on the way in, and on the way out, when they are together with the eluted Cu^{++} ions:

(Table 2.12)

$$\left\{\begin{matrix}4\ l \\ 1.8\ l\end{matrix}\right\} \times 197\ mg/_l = 1143.6\ mg\ (Table\ 2.13)_{Ca}$$

This is the amount of Ca coming IN

Coming OUT, is the regeneration effluent which contains

4 l	x	2950 mg/$_l$	Cu	=	1180C	mg Cu
1.8	x	790 mg/$_l$	Cu	=	1422	mg Cu
4 l	x	175 mg/$_l$	Ca	=	700	mg Ca
1.8 l	x	203 mg/$_l$	Ca	=	365	mg Ca

To these amounts must be added that of the rinsing effluent after the regeneration·

1.5	l	x	123 mg/$_l$	Cu	=	184 mg Ca
1.5	l	x	51 mg/$_l$	Ca	=	76 mg Ca

Therefore, the amount of Cu which came out is

11800 mg + 1422 mg + 184 mg = 13406 mg Cu.

and the amount of Ca^{++} coming out was

700 + 365 + 76 = 1141 mg Ca.

The amount of Cu accumulated is the difference between the amount loaded and that eluted.

13820 - 13406 = 414 mg. Cu.

While the amount of Ca accumulated is the difference between the amount coming IN with the regeneration solution and that coming out during the elution and rinsing.

1143 - 1141 = 2 mg Ca

(Table 2.13)

During the P.R. Tests, the amounts eluted were:

$$2.690 \times (153 \text{ mg/l Cu}) = 413 \text{ mg Cu}$$
$$2.7\ 1 \quad (15 \text{ mg/l Ca}) = 41 \text{ mg Ca}$$

which agrees well with the calculated values above.

Therefore, the efficiency is:

$$(13406 / 13820) \times 100 = 97\% \text{ for Cu elution}$$

and

$$(1141 / 1143) \times 100 = 99.8\% \text{ for Ca}$$

APPENDIX B.

THE DESIGN AND CONSTRUCTION OF A NEW TYPE OF FLOW METER

1. Introduction

It was mentioned in Chapter 2 that during the regeneration of the Cu^{++} loaded weak cation resin, the bed was fluidized and heavy, bulky precipitates were removed from the column.

To be able to remove the precipitates and at the same time to measure the flow rate of the slurry, a new type of flow meter was designed, built and used.

2. Flow measurement instruments

Several types of flow meters are available for the measurement of slurry: Mechanical flowmeters (propeller and turbine types) differential pressure flowmeters (venturi tube and orifice plate) electromagnetic flowmeters, vortex-shedding flowmeters, ultrasonic flowmeters. Some of these devices contain moving parts which can be blocked or corroded and others are expensive and require care in installation. Generally the measurements are less accurate for lower values when the range is wide. Therefore the situation can become very complicated when low and high slurry flow rates have to be measured in a short period of time.

During the regeneration experiments of the Cu^{++} loaded resin, high flow rates were employed to fluidize the bed. Gradually they were reduced to low levels, as the regeneration went along. The regeneration solution, which was corrosive (since it contained SO_2 in water at pH 1) contained a precipitate after passing the loaded resin.

It was decided to build a simple flowmeter which would enable measurements of low and high flowrates of slurry.

3. The flow meter

The flow meter consists of two tubes, one inside the other (Fig. B.1). The inside tube contains three holes at different levels, the bottom one being the "Basic" hole. The liquid comes in from the bottom of the inside tube and flows upwards through it. The liquid is discharged through the holes. At slow flow rates, the discharge is through the bottom hole only, but as the flow increases, the level of the liquid (slurry) increases until, when the flow rate is high, the discharge occurs through the second or even third hole. The discharged slurry flows out at the bottom of the second tube.

The flow meter is simple, robust, has no moving parts and will not be corroded by most slurries; the reading of the flow rate on the flow meter is straightforward. The flow meter was built from two parts only, which could be disassembled easily. Therefore, it could be easily cleaned with a brush, and since it has no moving parts, its maintenance is simple

Since the column of liquid above the discharge hole is constant for a given flow rate, a density gradient can develop between the top of the liquid column and the discharge level, due to the settling of the particle If the slurry is dilute or not very different in density from the liquid, the resulting error will be small.

The calibration graph is given in Fig.B2 and it was constructed using the data in Table B1.

4. Dimensions

The flow meter designed, constructed and used in the experiments, has the following dimensions:-

D_{IN} = 0.7cm D_{OUT} = 2.5cm h_T = 47cm

d_x = 2mm n = 3 $h(d_1)$ = 20cm $h(d_2)$ = 32

Flow rate range : 7 - 75 $l/_h$

Where D_{IN} and D_{OUT} are the inside and the outside diameter of the tubes, h_T is the total height of the instrument, d_x is the diameter for the three (n) holes, while $h(d_i)$ is the height of the holes above the first one.

5. Variables

The newly designed flow meter can be made suitable to a wide range of flow rates by use of three variables:

(A) The diameter of the holes.
(B) The number of holes.
(C) The height of the flow meter inner column.

(A) The diameter of the hole influences the discharged quantity according to formula

$$q_i = Cd_i \frac{\pi D^2}{4} \sqrt{2g_c(h - h_i)}$$

q_i is the flow rate from the ith hole and D the diameter of the hole. It can be seen that the flow rate is directly proportional to the area of the hole or is proportional to the square of the diameter of the hole (D) when the hole is circular:

(B) The number of holes. From the calibration graph and from experience, it was felt that around the holes (just under and just above them), the measurement was not certain and therefore measurements at the level of the holes should be avoided. If the diameter of the hole is large, the height at which measurements should not be done, increases while on the calibration graph it becomes a "dead" area.

To avoid this, the total discharge area can be increased by having more holes, with the same diameter, at the same level. Then, the "dead" area will remain the same in the calibration graph, while the discharge rate will increase.

Attention must be drawn to the fact that more holes along the tube will increase the discharge rate too, but will increase the "dead" area on the calibration curve and will restrict the area over which measurements can be carried out.

(C) The liquid height in the inner tube is the actual parameter which varies and enables the measurement of the flow rate.

According to the formula mentioned above, the flow rate is proportional to the square root of the liquid head.

$$q_i = C_d A \sqrt{2g_c \Delta h} = C_d A \sqrt{2g_c} \sqrt{h - h_i}$$

Therefore, the maximum range of the newly designed flow meter is set by the height of the central column above the first hole from the bottom (the Basic hole) together with the diameters and the number of holes.

Since the flow rate is proportional only to the square root of the liquid height, it is clear that small and medium size flow meters are able to handle a large range of flow rates.

6. Minimum and maximum sizes

The tubes in the flow meter must not be made too small.

If the diameter is too small, forces such as the surface tension of the liquid start interfering with the gravitational forces on which the flow meter is based, leading to errors in measurements. This requirement must also hold for the annulus diameter: D_{ANN} ($D_{ANN} = D_{OUT} - D_{IN}$).

The annulus diameter must also be large enough so that the level of

the liquid flowing out does not rise above the first hole, at the maximum flow rate.

If flow rates of slurries are to be measured, the diameter of the inner tube should be large enough not to be blocked by the particles in suspension or conglomerates created during the flow.

The hole diameter should also not be too small; it should be larger than the largest particle in suspension or any size of conglomerate.

The number of holes should be kept to a minimum because of the regions around them at which the measurements are not certain. Since this problem can be partially solved by increasing the number of holes at the same level, the maximum number of holes at the same level should be used. On the other hand, it must be remembered that the inner tube becomes weaker with every hole at the same level and therefore it is recommended that not more than a third of the perimeter of the inside tube will be holes. This will ensure that the tube will not break easily.

7. Discharge rate of the flowmeter

The discharge rate of the flowmeter is given by

$$Q = q_1 + q_2 + \cdots + q_n = \Sigma\, q_i$$

where Q is the total volumetric flow rate and q_i is the volumetric flow rate through the i-th hole.

On the other hand, if we make the simple assumption that the flow through each hole can be described according to the formula in section 6.7, then

$$Q = \sum_i C_{d_i} A_i \sqrt{2g_c(h - h_i)}$$

$$= \sum_i C_{d_i} A_i \sqrt{2g_c}\sqrt{h - h_i}$$

$$= \sqrt{2g_c}\sqrt{h} \sum C_{d_i} A_i \sqrt{1 - \frac{hi}{h}}$$

For the first hole $h_1 = 0$

Thus Q versus $\sqrt{h}$ should be a straight line for discharge from the first hole. When the 2nd hole starts discharging slurry as well the effect of the term

$C_{d_2} A_2 \sqrt{1 - \frac{h_2}{h}}$ will not be a negligible function of height but as this is additive to the first term $C_{d_1} A_1$ its variation with height will not be so noticeable. This will be even more true as further holes are used, as each of the lower terms

$$\sqrt{1 - \frac{h_1}{h}} \rightarrow 1$$

The situation is complicated by the fact that there is a flow passing each hole except the upper utilized one, and so the formula given will not be strictly correct. However, a plot of Q versus h seems to be a way of correlating the results, as shown in Fig.B.2

8. Measurement errors

During the qualibration, there was an uncertainty in measuring the liquid level height. This was felt to be not more than 0.1 cm. The volumetric flow rate reading was dependent on the stop watch reading and the reading of the volume in the measurement cylinder. The stop watch was read to $\pm$ 1 sec., while the error in reading the exact volume was $\pm$ 5 ml. for each 200 ml. In view of these facts, the measurement error was estimated to be not more than $\pm$ 5% and is indicated by lines centred on the measurement points in Fig. B.2. Also the density of the slurry as pointed out in the text could introduce inaccuracies but these were negligible in this instance.

9. LIST OF SYMBOLS

D_{IN}	-	Diameter of the inside Column (cm)
D_{OUT}	-	Diameter of the outside tube (cm)
D_{ANN}	-	Diameter of the annulus (cm)
$D_1 d_x$	-	Diameter of the hole (cm), (mm)
n	-	The number of boles
h	-	The liquid height (cm)
$h(d_x)$	-	The level of the nole x above the first hole from the bottom (cm).
h_T	-	The height of the central tube (cm)
h_i	-	The height of the liquid above the hole i.
C_{di}	-	Discharge coefficient of hole i.
A_i	-	Area of the hole i (cm^2), (mm^2)
g_c	-	Gravity coefficient ($^{cm}/_{sec^2}$)
Q	-	Flow rate (total) (l/h) ($^{cm^3}/_{min}$)
q_i		Flow rate through the ith hole (l/h) ($^{cm^3}/_{min}$)

Table B.1. Water flow rates measured for the calibration curves.

H (cm)	Flow rate ($^{l}/_{h}$)
2	7.0
4	10.6
8	15
9	16
12	19
14	20
18	23
19	24
20	Hole
22	32
24	36
26	41
30	47
32	Hole
34	58
36	64
38	69
41	75

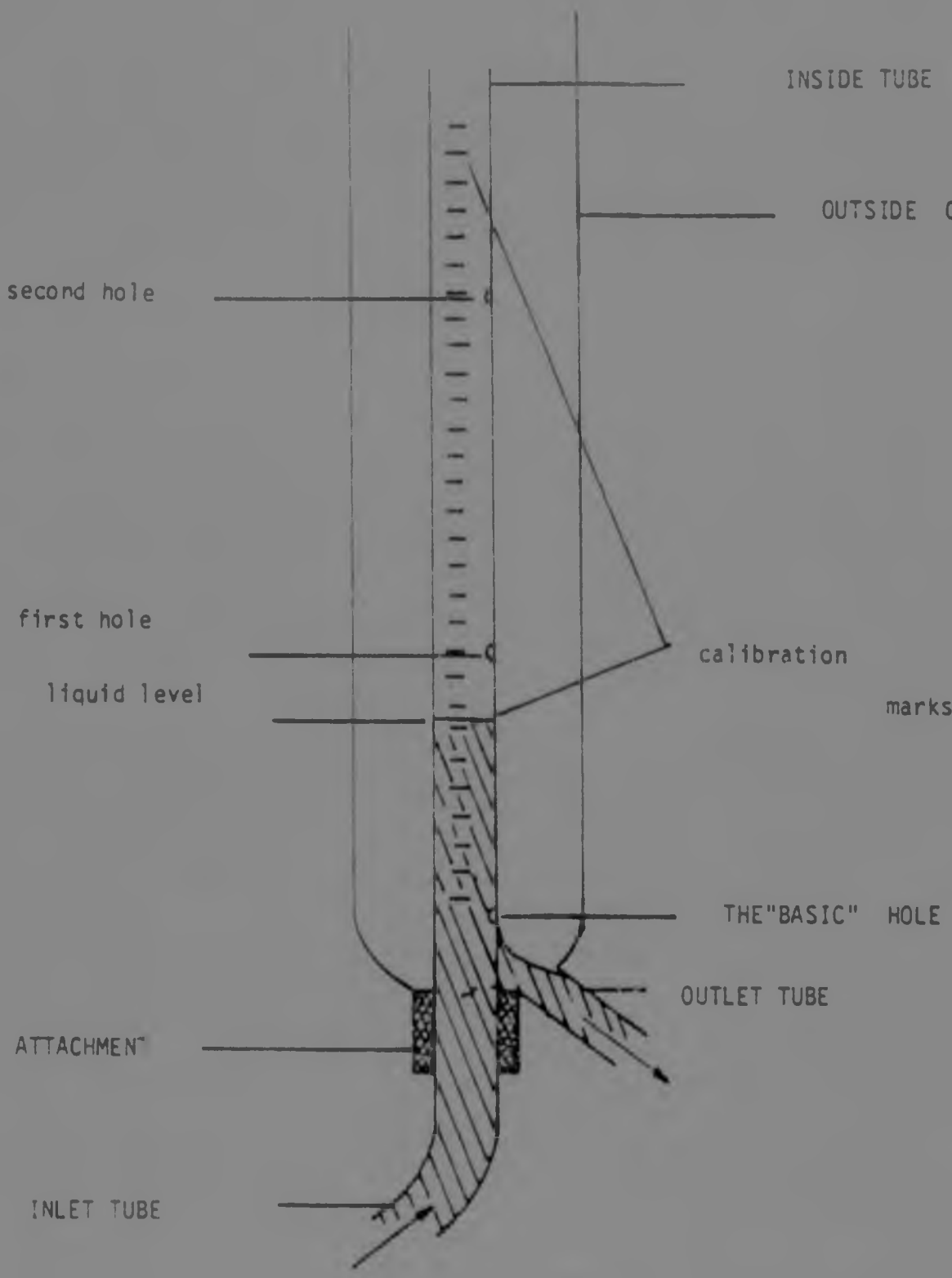

Fig. B.1. Flow meter:
designed, built and used
for the Cu^{++} experiments.

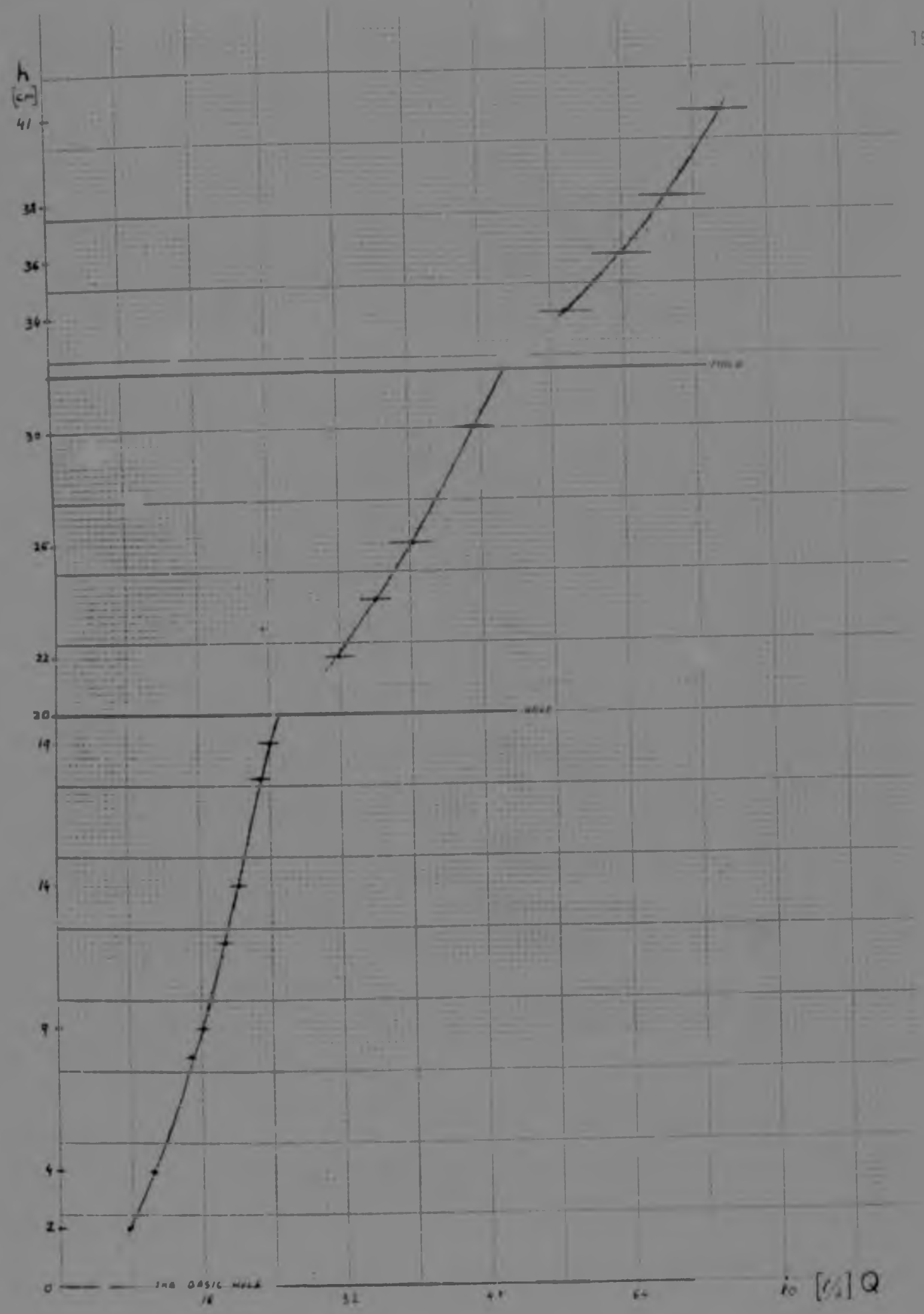

Fig. B.2. : Calibration curve for the flow meter (using water).

APPENDIX C.

DETAILED DESIGN OF AN ABSORPTION TOWER FOR SO_2 SCRUBBING(*)

1. Brief Theoretical Background

It is not an object of this thesis as a whole or of this appendix in particular to give or to discuss the thecries on which the absorption towers are designed, but just to size such columns. The theories on which the design is based, are given in detail in many sources [96, 146-156]. Therefore, only a few basic equations will be given below. These equations will be used for the design:

The wetting rate, L, is given by

$L = \frac{V_1}{S}$, V_1 being the liquid flow rate over the given cross section, and S being the surface area per unit volume of packing.

The height, l, of the tower, can be calculated by either

$$l = \frac{W}{S x a x (K_g x \Delta p)_m} \quad \text{or} \quad l = \frac{W}{K_{gm} x S x a x \Delta p_m}$$

In the first of these two equations, the height is calculated using the mean overall coefficient K_{gm} and the mean driving force, Δp_m.

In the second equation, l is calculated using the mean values of the product "overall coefficient X driving force." $(K_g x \Delta p)_m$.

In both equations, W is the absorption rate, S is the surface area per unit volume of packing, and a is the cross section area.

(*) All the formulas, data, tables, graphs and illustrations in this chapter are taken from [96] , except for Figs. C2, C3 and table C1 and C9.

The overall gas coefficient K_g is given by:

$$\frac{1}{K_g} = \frac{1}{k_g} + \frac{1}{Hk_l}$$

where k_g is the gas film coefficient and k_l is the liquid film coefficient.

k_g can be found from the equation.

$$k_g = \alpha R_g C\rho_{rs} V^{0.75} \frac{P}{(P-p)_{lm}} \frac{1}{p^{0.25}} \left(\frac{Tr}{T_f}\right)^{0.56}$$

where α is a constant, R_g is the gas film packing factor, C is the gas mixture constant v is the relative velocity ($v = v_g + v_l$), $\frac{P}{(P-p)_{lm}}$ is the drift factor in which P is the overall pressure and p is the partial pressure and the last two terms are correction factors for pressure and temperature respectively. They can be found in Fig. C.14.

$v_g = \frac{Vg}{3600\ E}$ where E is the voidage and V_g is the gas rate.

k_l - the liquid film coefficient can be calculated from the equation:

$$k_l = R_l \times K \times L^{0.7},$$

where R_l is the liquid film packing factor, K is a constant and L is the wetting rate.

Having all the coefficients calculated, a driving force diagram can be drawn (Fig.C.11) and the mean value of $(K_g \times \Delta p)_m$ can be calculated.

1.1. <u>Pressure drop</u> (ΔP) is given by the equation

$\Delta P = 0.005\ N_p\ V_p^2 l$ where V_o is

the gas velocity in the middle position, N is the number of velocity heads lost per foot of packing, and l is the lower height.

The tables and diagrams which were used during the design are attached to this chapter.

1.2. Economic gas rates

Ideally, a tower should be designed so that the total annual charges, which are made up of the annual capital charges and running costs, are minimum. [153, 157]. In practice, this may not always be possible.

Nevertheless, optimum values can often be assigned on economic grounds to many of the factors entering into the design of a tower, such as the efficiency of absorption or stripping to be aimed at the gas/liquid ratio and the area of cross section. These economic optimum values can be determined by means of the procedure known as the economic balance. When the use of analytical methods is possible, the total annual charges are expressed in terms of the factor concerned, the value for which these charges are minimum being then determined by differentiation. This method has been used in the determination of economic gas rates; these are directly related to the economic areas of cross section.

Therefore, when an absorption tower is to be designed for treating a given quantity of gas per hour, the cross sectional area is determined by the superficial gas velocity which is chosen. The larger the gas velocity which is selected, the smaller will be the tower diameter but the larger will be cost of pumping the gas against the tower pressure drop. The economic gas velocity is the value which minimizes the total annual cost, including the fixed charges as well as the cost of power for operating. Figure C.1.

The economic gas rate is given by

$$V_E = Z_E \left[\frac{E_F}{N_H(1+X)}\right]^{0.33} \left(\frac{C_T}{NCp}\right)^{0.33} \left(\frac{\rho_{ar}}{P}\right)^{0.33}$$

Z_E = 115500 and is a constant
E_F = overall efficiency of fans and motors
N_H = time of operation
C_T = capital cost per unit volume of packing.
C_p = cost of electrical power
ρ_{ar} = density of air
ρ = density of gas
x = fraction of annual power costs added to allow for other charges.

2. Equilibrium data

Equilibrium data for SO_2 in water at different temperatures (partial pressure/concentration) are given in Fig.C2 and Table C3.

The mole fraction of SO_2 in water and vapors (X_e and Y_e) in equilibrium, at 30° is given in Table C1 and Fig. C3.

3. Introduction

To simplify the whole problem, some assumptions and approximations were made on the way to a complete design. Three of them are given below, before the beginning of the calculations, and others will be mentioned in the course of the calculations:

The flue gases were assumed to be cooled down to 25°C before their treatment in the absorption tower. This is not an entirely realistic figure but was taken for this exercise.

The figures used in the calculation of the economic gas rate, Table C7 are based on prices ruling in mid 1947(!) and can therefore be used for purposes of comparison only; they should not be used in

the preparation of detailed estimates unless an allowance is made for the change in prices since that date. They can, however, be used in calculations based on the economic balance, since costs appear in these calculations in the form of ratios.

It was assumed for the purposes of this design, that the liquid film coefficient for the standard disc tower, has been found to be 0.016g/sec cm^2 (g/cm^3) at 20°C and a wetting rate of 1 cm^3/sec. cm.

4. Detailed Design

The process is one in which both the gas and liquid films are of importance. The flow rate of flue gas is taken from a Japanese plant [122]

4.1. Choice of Packing

Before a suitable packing can be chosen, it is necessary to calculate the gas/liquid ratio, for which purpose the rate of absorption of sulphur dioxide is required.

4.1.1. Rate of absorption

The density of sulphur dioxide, ρ_{rs} is found in Table 5 to be 2.67 Kg/m^3. The mass flow of SO_2 at the tower inlet is therefore

$$467000 \times 0.02832 \times 0.003 \times 2.67 = 105.94 \text{ Kg/min.}$$
$$= 6356.7 \text{ Kg/h.}$$

The gas leaving the tower is to contain 0.01% by volume of SO_2. The volume flow of the insoluble gas (including the water vapour) at the tower inlet is given by

$$467000 \times 0.02832 \times 0.9999 = 13227.085 \text{ m}^3 / \text{min.}$$

Neglecting the change in water vapour content brought about by the cooling of the gases to 20°C in the tower, the sulphur dioxide content of the exit gas expressed as a mass flow is therefore

13227.085 x 0.0001 x 2.67 = 3.53 Kg/min.

The rate of absorption of sulphur dioxide in the tower is therefore

W = 105.94 - 3.53 = 102.41 Kg/min.

4.1.2. Gas/liquid Ratio

The absorbed SO_2 is to leave the tower in the form of a 0.1% solution by weight. i.e. a solution containing 1 Kg/m^3.

The water flow is therefor

$$V_l = \frac{102.41}{1} = 102.41\ m^3/min.$$

The gas consists mainly of air at the temperatures between 20°C and 25°C so that the factor ϕ can be taken as 1.0 and the effect of temperature on the gas volume can be neglected. Thus, the value of $\phi\ V_g/V_l$ is given by

$$1.0 \times \frac{13225.44}{102.41} = 129.14$$

Reference to fig.C4 shows that stacked stoneware rings of 2in.in diameter random metal rings and random stoneware rings of 1in.and 2in. in diameter can be used.

A design is worked out here for random rings (2in. x 2in. x 3/16in)although in practice complete designs for all the

possible packings would have to be worked out and the resulting total annual charges compared.

4.1.3. Area of cross section

From Fig.C4 the wetting rate, L, for 2in.random rings at the loading point when $\phi\ V_g/V_l$ is 129.14, is approximately $0.3\ m^3/hr\ m$.

Since from Table C6 the value of S is $95 m^2/m^3$, the liquid rate is given by

$$V_l = L \times S = 0.3 \times 95 = 28.5 m^3/hr\ m^2$$

The liq. flow is $102.41 m^3/min$ and therefore the min cross section is

$$\frac{102.41 \times 60}{28.5} = 215.6\ m^2$$

which correspond to a gas rate of

$$V_g = \frac{13225.44 \times 60}{215.6} = 3680.55\ m^3/h \cdot m^2$$

A gas rate 85% of this value, i.e. $3128.47 m^3/h \cdot m^2$

Corresponding to a cross section of $253.67 m^2$ is chosen so as to provide an adequate margin of safety in the operation of the tower. It must now be shown that this is a reasonable value from the economic standpoint.

The tower is of large size and requires an acid-resistant lining; the cost of the shell is therefore taken to be 50 £/$_m$3.

(For mild steel towers, the cost of the tower shell is

in the range of 18-120 £/$_m$3, the lower limit applying to very large towers and the upper to small towers. To allow for the possibility that expensive additions such as lagging or linings of brick, may be required, it is suggested that the range of costs for tower shells should be taken as 18-140 £/$_m$3)

50 £/$_m$3 is somewhat above the low limit applied for very large towers and the cost of the packing is in the range £27/m^3- £39/m^3 (table C7)

Thus, C_T is in the range 77-89 £/$_m$3.

For a gas rate of 3128.47 $m^3/h \cdot m^2$ and a gas liquid ratio of 129.14, the liquid rate is

$$V_1 = \frac{3128.47}{129.14} = 24.22 \ m^3/h \cdot m^2$$

and the wetting rate is

$$L = \frac{V_1}{S} = \frac{24.22}{95} = 0.25 \ m^3/h \cdot m^2$$

Hence, from Fig.C8 the pressure drop (expressed as the number of velocity heads lost per metre of packing) is

$$N = 3.28 \times 175 = 579$$

The economic gas rate is given by

$$V_E = 115500 \left[\frac{E_F}{N_H (1+X)}\right]^{0.33} \left(\frac{C_T}{NCp}\right)^{0.33} \left(\frac{\rho ar}{p}\right)^{0.33}$$

As in the calculation of the economic gas rates given in Table C8 the overall efficiency of the fans and motors E_F will be taken as 80%, the number of hours operation per year as 8400 (350 days x 24 hours/day) and the

fraction of the power costs (X) added to allow for other charges will be taken as 0.1.

Since the gas consists mainly of air (about 93% by volume) the correction factor $(\rho_{ar}/\rho)^{0.33}$ for the difference in gas density from that of air will be taken as unity.

As the cost figures for the shell and packing are chosen already, the value C_p is 0.7 pence/KWh. Inserting these figures together with the lower value of C_T of $77£/m^3$ in

$$V_E = 115500 \left[\frac{0.5}{8400 \times 1.1}\right]^{0.33} \left(\frac{77}{574.07}\right)^{0.33} (1)^{0.37}$$

$$= 115500 \cdot 0.0\ 3908 \cdot 0.58 = 2616.7\ m^3/hm^2$$

Similarly, for a higher value of C_T ($89£/m^3$) or a higher overall efficiency of the fans and motors, E = 80% (E_F = 0.8) the value of V_E is found to be V_E = 3204.57. Thus, the chosen gas rate of 3350 approximates closely to the higher extreme of the range of economic gas rate - Table C8 ($2250 - 3350\ m^3/hm^2$)

4.1.4. Height of packing

The height of packing required is given by the formula:

$$1 = \frac{W}{S \times a \times (K_g \times \Delta p)_m}$$

The overall coefficient K_g is given by the equation

$$\frac{1}{K_g} = \frac{1}{k_g} + \frac{1}{Hk_l}$$

Therefore, the gas film coefficient, k_g, the liquid film coefficient k_l and the solubility factor H must be known before the height of the tower can be calculated.

(The rate of absorption has been found to be 102.41 x 60 = 6144.6Kg/h = W.)

The value of S for random rungs (2 x 2 x 3/16in.)is found in Table C6 : S = 95m^2/m^3 and the area of cross section a, is 253.64m^2.)

The inlet gas contains 3% by volume of water vapour (p_v = 0.75Kg/m). At the top of the tower, if the gas is assumed to be saturated with water at 20°C, it contains 2.3% by volume of water vapour and 0.01% SO_2. The flow of the insoluble gas (excluding water vapour) is

$$793526 \times 0.967 = 767340.02 \ m^3/h$$

(96.7% = 100% - 0.3% - 3%)

The total flow of gas leaving the tower is

$$767340.02/0.9769 = 785484.71$$

(97.69% = 100% - 0.01% - 2.3%)

By assuming that the temperature of the liquid (aquous solution of 0.1% SO_2) leaving the tower rose by only 1°C because of the absorption process, it is possible to calculate the conditions in three different points of the adsorption tower (Table C9)

These conditions are necessary to calculate the mean value of the product "overall coefficient driving force" : $(K_g \times \Delta p)_m$.

4.2. Gas film Coefficient

There is a volume change less than 5% and corrections for temperature and pressure are negligible.

$$k_g = 36.1\ R_g\ C\rho_{rs}\ V^{0.75}$$

No correction are made for the reduction of voidage owing to liquid hold-up.

$$v = v_g + v_l$$

The voidage for random rungs (2 x 2 x ^{3}/16in.) is 0.79 from Table C.6 and the gas rate V_g is 3128.47m^3/$_{hm^2}$. Thus, the gas velocity is

$$v_g = \frac{V_g}{3600E} = \frac{3128.47}{3600 \times 0.79} = 1.1 \text{ m/sec}$$

From Fig.C.10 the liquid surface velocity v_l for the wetting rate of 0.25in.^{3}/h.in. is 0.125 in/sec. so that the relative velocity is
$V = 1.1 + 0.125 = 1.255$ in/sec.
The packing factor R_g is found in Table C6 to be 2.8, while ρ_{rs} for sulphuric dioxide Table C5 is 2.67Kg/$_{m^3}$. The gas mixture constant C is found in Table C7 to be 0.54. Therefore

$$k_g = 36.1 \times 2.8 \times 0.54 \times 2.67 \times (1.225)^{0.75}$$

$$169.7\ K_g/h\ m^2\ atm.$$

4.3. Liquid film coefficient $k_l = kR_l L^{0.7}$

Since the liquid rate is constant and the temperature varies only by 1°C, a constant value of k_l calculated for 20°C can be satisfactorily used. The liquid-film coefficient for the disc tower is 0.016 at a wetting rate of 1cm^3/sec cm and 20°C. The corresponding values are 0.58 Kg/h m^2 and 0.36 m^3/hm for the coefficient and the wetting rate respectively.

The actual wetting rate to be used is 0.078 m^3/hm and the liquid film packing factor R_l is found in Table C.6 to be 0.67.

Thus, the liquid film coefficient is given by

$$k_l = 0.67 \times 0.58 \times \left(\frac{0.25}{0.36}\right)^{0.7} = 0.30\ K_g/h\ m^2\ (Kg/m^3)$$

4.4. Overall Coefficient

$\frac{1}{K_g} = \frac{1}{k_g} + \frac{1}{Hk_l}$ Using the values of H (the solubility coefficient, given in Table C.9 three different values for Kg can be obtained.

Bottom of the tower

$$\frac{1}{K_g} = \frac{1}{169.7} + \frac{1}{508 \times 0.3}$$

(K_g) bottom = 80.34

Middle position : $\frac{1}{K_g} = \frac{1}{169.7} + \frac{1}{454.88 \times 0.3}$

$(K_g) = 75.64$

Top position : $\frac{1}{K_g} = \frac{1}{169.7} + \frac{1}{355 \times 0.3}$

$(K_g)_{top} = 65.44$

4.5. Mean value of coefficient x driving force

$(K_g \Delta p)$ for the top, middle or bottom positions are obtained by multiplying the above Kg's with the values of Δp from the Table C.12 $(K_g \Delta p)$ average = $\frac{1}{2}(K_g \Delta p_{top} + K_g \Delta p_{bottom})$

Therefore

$(K_g \Delta p)_{bottom} = 0.084$, $(K_g \Delta p)_M = 0.047$

$(K_g \Delta p)_{top} = 0.0065$ $(\Delta K_g \Delta p)av = 0.045$

$(K_g \Delta p)_M / (K_g \Delta p)_{av} = 1.044$ $(K_g \Delta p)_{bottom} / K_g \Delta p)_{top} = 12.92$

From Fig. C.6 the ratio of mean to the arithmetic mean is then found to be 0.7, so that $(K_g \Delta p)_m = 0.7 \times (K_g \Delta p)_{av} = 0.7 \times (0.045)$

$= 0.0315$

Now it is possible to calculate the height of the packing:

$$l = \frac{W}{S \times a \times (K_g \Delta p)m}$$

W is the rate of absorption which has been found to be $102.41 \times 60 = 6144.6$ Kg/h

The value of random rings ($2 \times 2 \times \frac{3}{16}$ in) from table (6) is 95 m^2/m^3 and the area of cross section a is 253.64 m^2

$$l = \frac{6144.6}{95 \times 253.64 \times 0.0315} = 8.095 \text{ m.}$$

The height of packing would normally be increased by as much as 15% to avoid any effect of maldistribution.

As a result of approximations introduced in the calculations, the overall coefficient has been underestimated and the height of packing calculated is already in excess of that required to give the specified performance (96.5%).

4.6. Liquid distributor

A splash type liquid distributor is suggested. Since the packing consists of random rings, the secondary distribution could be omitted and the packed height increased to 8.5 m., the extra packing serving as a secondary distributor, providing that the additional pressure-drop could be tolerated.

4.7. Pressure drop

The pressure drop is calculated for the packing alone while the pressure losses at inlet and exit are neglected:

$$\Delta P = 0.005 \rho V_o^2 l.$$

V_o is the gas velocity in the middle position (785505.55/3600 x 253.64) = 0.86m/sec. ρ = 1.23 Kg/m^3 and l = 8.095.

From Fig C.8. the number of velocity heads lost per metre of packing is found to be 280 for random rings (2 x 2 x $\frac{3}{16}$)at a wetting rate of 0.47 m^3/m^{2}h, is

$$\Delta P = 0.005 \times 280 \times 1.23 \times (0.86)^2 \times 8.095 = 10.309 \text{ m atm.}$$

This will be increased to 10.82 m atm. if the additional 49 cm of packing is used as a secondary liquid distributor as suggested.

4.8. Materials of construction [122, 158, 159]

The conditions under which the Toyamo-Shinka [122] F.G.D. Plant (Japan) runs, are much more drastic than those which could be encountered at the present designed scrubbing tower:

There, 2.3% sulphuric acid solution is used for the SO_2 absorption and the experience accumulated running that plant, proved to be very useful for the present design.

Therefore, the most recommended materials for construction are the 316L stainless steel and Incoloy 825.

304L stainless steel is not suitable as it can be badly corroded.

5. Summary of design

The adsorption tower, having a height of approximately 9m. and an area of cross section of 253.54 m^2 is required for lowering the concentration of SO_2 from 0.3% to 0.01%. The tower will be parked with random rings (2 x 2 x 3/16 in.) and will be built of 316 stainless steel.

6. LIST OF SYMBOLS

Symbol	Significance	Units
a	Area of cross-section of tower	$m.^2$
C_p	Cost of electric power	pence/kWh.
C_T	Capital cost of shell and packing per unit volume of packing	£/$m.^3$
c_a	Equilibrium concentration of free dissolved gas	kg./$m.^3$
c_g	Concentration of soluble gas in equilibrium with gas of partial pressure p_g	kg./$m/^3$
E_T	Overall efficiency of fans and motors	-
H	Solubility co-efficient	kg./$m.^3$ atm.
K_G	Overall coefficient on gas-phase basis	kg./hr.$m.^2$ atm.
K_{Gm}	Mean overall coefficient on gas-phase basis	kg./hr.$m.^2$ atm.
K_L	Overall coefficient on liquid-phase basis	kg./hr.$m.^2$ (kg./$m.^3$)
K_{Lm}	Mean overall coefficient on liquid phase basis	kg./hr.$m.^2$ (kg./$m.^3$)
k_G	Gas-film coefficient	kg./hr.$m.^2$ atm.

Symbol	Significance	Units
k_1	Liquid-film co-efficient	kg./hr.m.^{2}(kg./m.^{3})
L	Wetting rate (liquid volume rate per unit periphery)	m.^{3}/hr.m.
N	Number of velocity heads lost per unit height of packing	-
N_H	Time of operation	hr./yr.
P	Total gas pressure	atm.
p	Partial pressure of soluble gas	atm.
pg	Actual partial pressure of soluble gas	atm.
pi	Partial pressure of soluble gas interface	atm.
pl	Partial pressure of soluble gas in equilibrium with liquid of concentration c_1	atm.
$(P-p)_{lm}$	Log mean partial pressure of insoluble gas in the gas film	atm.
R_g	Gas-film packing factor	-
R_l	Liquid-film packing factor	-
S	Surface area per unit volume of packing	m.^{2}/m.^{2}
T_f	Absolute temperature of gas film	$^\circ$K

Symbol	Significance	Units
T_r	Reference temperature (absolute)	^{o}K
V_E	Economic gas rate per unit area of cross section	$m.^3/hr.m.^2$
V_l	Liquid rate per unit area of cross-section	$m.^3/hr.m^2$
V_o	Mean equivalent empt. tower velocity	m./sec.
v, v_g	Gas velocity relative to liquid surface and through packing respectively.	m./sec.
v_l	Liquid surface velocity	m./sec.
W	Rate of absorption	kg./hr.
x	Fraction of annual power costs added to allow for other charges, e.g. maintenance of fans and motors	-
z_E	Constant in equation for economic gas rate	-
α	Constant in equation for gas-film coefficient	-
Δc	Driving force on liquid-phase basis	$kg./m.^3$
Δc_{ae}	Arithmetic mean driving force on liquid-phase basis	$kg./m.^3$
Δc_{lm}	Log mean driving force on liquid-phase basis	$kg./m.^3$

Symbol	Significance	Units
ΔP_{M}	Driving force at middle position on gas-phase basis	
Δp_m	Mean driving force on gas-phase basis	atm.
E	Voidage	-
K	Experimentally determined constant used in calculating liquid-film coefficients	-
p	Density of gas mixture	kg./m.^{3}
pa	Density of air	kg./m.^{3}
pi	Density of insoluble gas	--
pl	Density of liquid	--
ps	Density of soluble gas	kg./m.^{3}
ϕ	Dimensionless factor used to allow for the effect of gas density on the loading rate	--

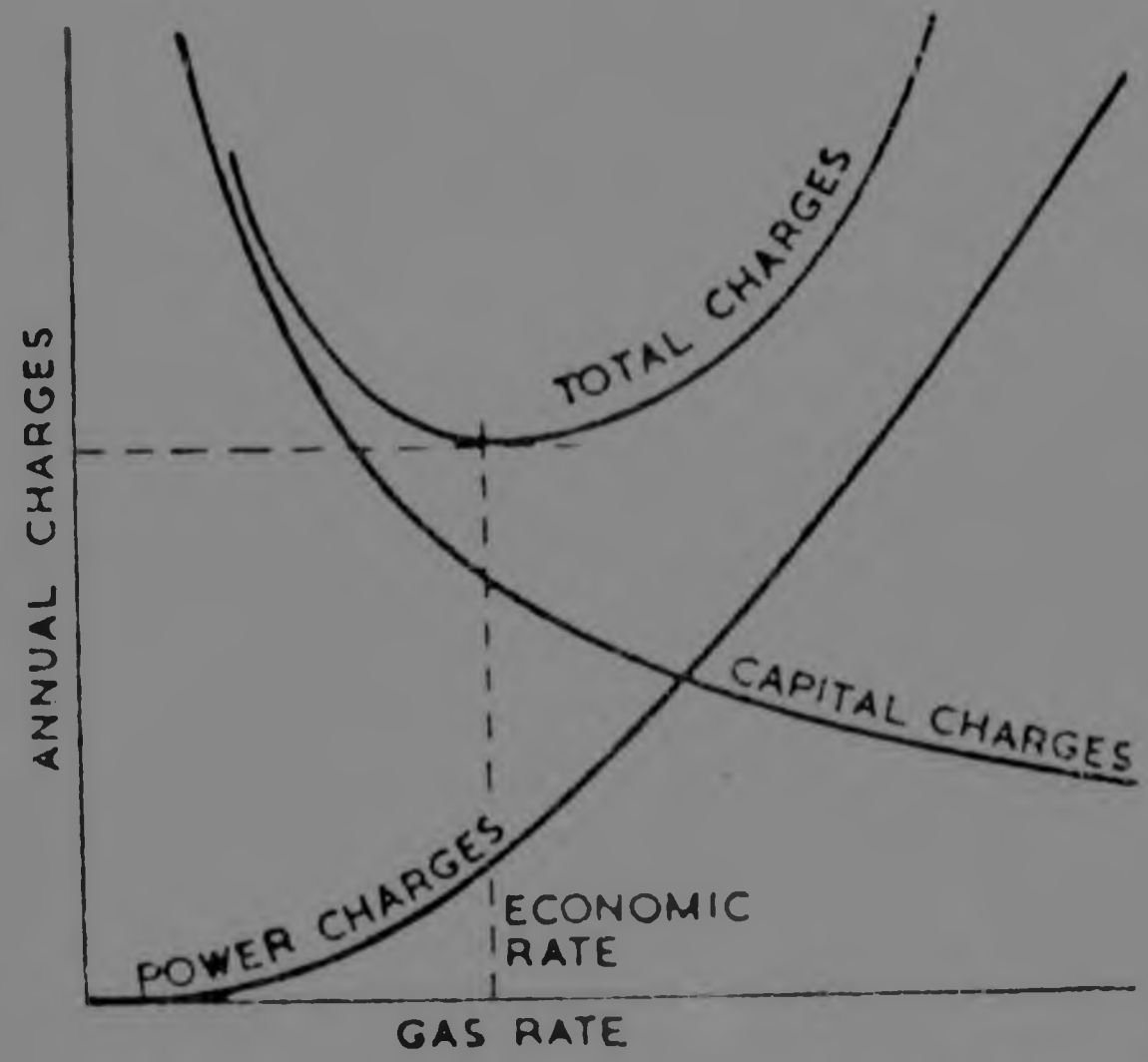

Figure c.1. *Variation of annual charges with gas rate*

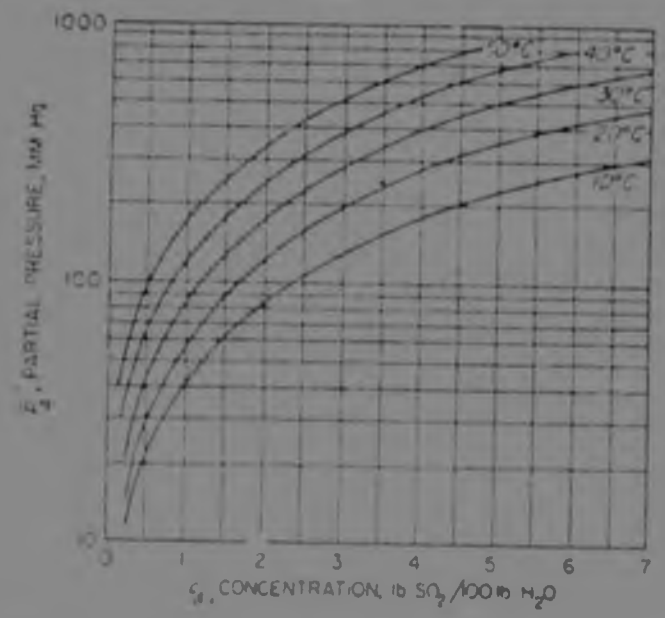

Figure C2 *Partial pressure of sulfur dioxide over aqueous solution.*

Source [146]

c_A, lb SO_2/ 100 lb H_2O	p_A, mm Hg	$y_* = \frac{p_A}{760}$	$x_* = \frac{c_A/64}{c_A/64 + 5.56}$
1.0	55	0.112	0.0023
2.0	178	0.232	0.0056
3.0	273	0.359	0.0084
4.0	376	0.495	0.0111
5.0	482	0.634	0.0139
6.0	588	0.774	0.0166

Table C1 *Equilibrium concentration of SO_2 in water at 30°C.*

Source (146)

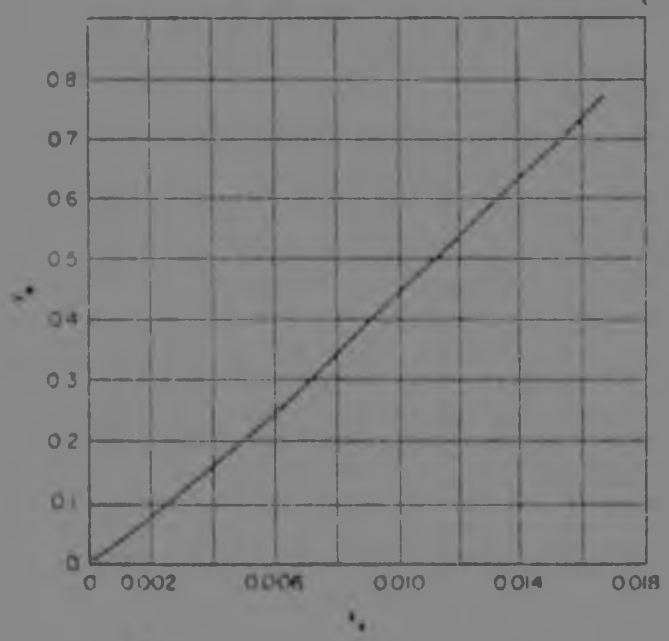

Figure C3 *Equilibrium curve, sulfur dioxide in water at 30°C, 1 atm*

Source [146]

Table C2 Properties of Gases

Gas	Viscosity at R.t.p. (g./cm.sec. × 10^{-4})	Diffusion Coefficient for Air at R.t.p. (cm.²/sec.) 100% Air	100% Gas	Diffusion Coefficient for Water at 20°C. (cm.²/sec. × 10^{-5})
Acetylene	1·00	0·158	0·155	1·80
Air	1·81	—	—	—
Ammonia	1·00	0·203	0·100	2·04
Bromine	1·54	0·086	0·104	1·29
Carbon dioxide	1·47	0·144	0·152	1·74
Carbon disulphide	0·98	0·091	0·103	—
Carbon monoxide	1·75	0·202	0·201	1·90
Chlorine	1·33	0·108	0·121	1·41
Ethylene	1·01	0·152	0·151	1·59
Hydrogen	0·88	0·883	0·690	5·04
Hydrogen chloride	1·43	0·156	0·161	2·80
Hydrogen cyanide	0·74	0·133	0·132	1·66
Hydrogen sulphide	1·25	0·151	0·154	1·63
Methane	1·09	0·223	0·206	2·00
Nitrogen	1·76	0·202	0·201	1·90
Oxygen	2·02	0·200	0·204	2·08
Sulphur dioxide	1·28	0·109	0·121	1·47
Sulphur trioxide	1·27	0·102	0·116	—
Water vapour	0·95	0·194	0·182	—

Table C3 Solubility in Water of Gases which deviate from Henry's Law

Gas	Partial Pressure (atm.)	Solubility* (kg./m.³ of water) 10°C.	20°C.	30°C.	40°C.	50°C.
Ammonia	0·01	20	12·5	7·7	5·1	3·4
	0·05	94	58	38	25·3	17
	0·10	160	108	72	50	34
	0·30	337	250	180	130	94
	0·50	460	340	265	195	140
	1·00	690	520	410	315	240
	3·0	—	1,120	855	670	530
	5·0	—	—	—	985	775
Carbon dioxide	0·01	0·024	0·0175	0·013	—	—
	0·05	0·120	0·0875	0·065	—	—
	0·10	0·240	0·175	0·130	—	—
	0·30	0·72	0·52	0·39	—	—
	0·50	1·20	0·87	0·65	—	—
	1·00	2·36	1·73	1·28	—	—
	3·00	6·92	5·05	3·75	—	—
	5·0	11·2	8·15	6·07	—	—
	10·0	21·0	15·3	11·4	—	—
Chlorine	0·01	0·54	0·52	0·50	0·48	0·46
	0·05	1·17	1·05	0·97	0·92	0·89
	0·10	1·73	1·52	1·38	1·23	1·14
	0·30	3·70	2·95	2·52	2·20	2·00
	0·50	5·50	4·26	3·54	3·00	2·65
	1·00	9·65	7·40	5·80	4·78	4·07
	3·00	—	19·2	14·6	11·4	9·3
Hydrogen chloride	0·01	440	415	380	340	310
	0·05	435	500	460	425	395
	0·10	585	540	500	465	430
	0·30	660	620	575	540	500
	0·50	710	660	615	575	540
	1·00	780	730	685	640	595
Hydrogen sulphide	0·01	0·0525	0·0397	0·0312	0·0254	0·0214
	0·05	0·2625	0·198	0·1555	0·127	0·107
	0·10	0·524	0·396	0·311	0·254	0·214
	0·30	1·57	1·185	0·933	0·76	0·64
	0·50	2·62	1·97	1·555	1·27	1·07
	1·00	5·18	3·93	3·10	2·5	2·1
Sulphur dioxide	0·01	2·9	1·8	1·4	1·0	0·7
	0·05	10·2	6·9	5·3	3·5	2·6
	0·10	18·6	12·6	9·7	6·4	4·6
	0·30	51	35	26	18	14
	0·50	81	55	41	29	22
	1·00	154	106	79	56	43

* [illegible]

Table C4 Values of Gas-mixture Constant

Soluble Gas	Gas-mixture Constant C*					
	Hydrogen		Oxygen, Nitrogen, Air, Water vapour, Carbon monoxide or Ammonia†		Carbon dioxide	
	0%	100%	0%	100%	0%	100%
Acetylene	1·49	0·72	0·72	0·64	0·61	0·65
Ammonia	1·42	0·76	0·71	0·72	—	—
Bromine	1·87	0·62	0·86	0·48	0·67	0·46
Carbon dioxide	1·59	0·73	0·73	0·61	—	—
Carbon disulphide	1·70	0·61	0·77	0·49	0·63	0·48
Carbon monoxide	1·50	0·82	0·71	0·71	0·61	0·73
Chlorine	1·69	0·67	0·77	0·54	0·63	0·53
Ethylene	1·50	0·71	0·72	0·63	0·61	0·64
Hydrogen	—	—	0·79	1·46	0·73	1·59
Hydrogen chloride	1·55	0·75	0·73	0·64	0·61	0·64
Hydrogen cyanide	1·49	0·66	0·71	0·59	0·61	0·60
Hydrogen sulphide	1·54	0·73	0·72	0·63	0·61	0·64
Methane	1·40	0·79	0·71	0·75	0·61	0·78
Nitrogen	1·51	0·82	0·72	0·72	0·61	0·73
Oxygen	1·51	0·82	0·72	0·72	0·61	0·73
Sulphur dioxide	1·67	0·67	0·75	0·54	0·63	0·53
Sulphur trioxide‡	—	—	0·77	0·51	0·63	0·51
Water vapour	1·42	0·75	0·71	0·70	0·61	0·73

* Values of C are shown corresponding to [illegible]

† Average values.

‡ Figures based on [illegible]

Table C5 Densities of Gases at R.t.p.

Gas	Density at R.t.p.* ρ_w		Gas	Density at R.t.p.* ρ_w	
	lb/ft³	kg/m³		lb/ft³	kg/m³
Acetylene	0·068	1·09	Hydrogen chloride	0·095	1·52
Ammonia	0·044	0·709	Hydrogen cyanide	0·070	1·13
Bromine	0·416	6·66	Hydrogen sulphide	0·089	1·42
Carbon dioxide	0·114	1·83	Methane	0·042	0·668
Carbon disulphide	0·197	3·17	Nitrogen	0·073	1·17
Carbon monoxide	0·073	1·16	Oxygen	[illegible]	1·33
Chlorine	0·185	2·98	Sulphur dioxide	0·167	[illegible]
Ethylene	0·073	1·17	Sulphur trioxide	0·208	3·34
Hydrogen	0·0052	0·084	Water vapour	0·047	0·75

* Values are calculated on the assumption that the ideal gas laws are obeyed.

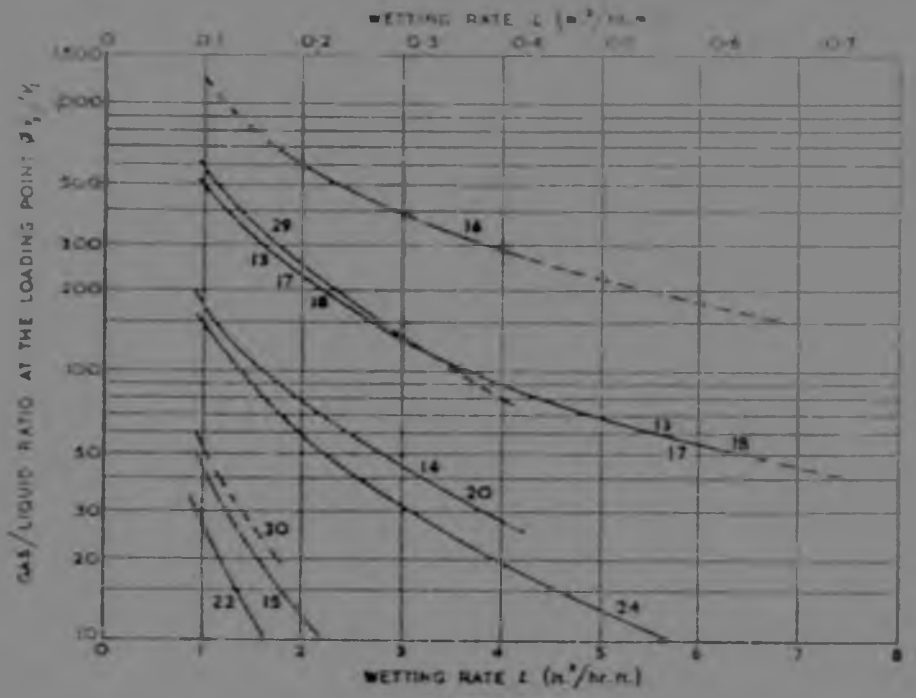

Figure C4 *Relation between gas/liquid ratio and wetting rate at the loading point for random rings and solids*

Curves shown in broken lines are based on estimated figures.

Random metal rings:

13 2 in. × 2 in. × $^{1}/_{16}$ in.
14 1 in. × 1 in. × $^{1}/_{16}$ in.
15 $^{1}/_{2}$ in. × $^{1}/_{2}$ in. × $^{1}/_{32}$ in.

Random stoneware rings:

16 3 in. × 3 in. × $^{3}/_{8}$ in.
17 2 in. × 2 in. × $^{1}/_{4}$ in.
18 2 in. × 2 in. × $^{1}/_{16}$ in.
19 $1^{1}/_{2}$ in. × $1^{1}/_{2}$ in. × $^{3}/_{16}$ in.*
20 1 in. × 1 in. × $^{3}/_{32}$ in.
21 $^{3}/_{4}$ in. × $^{3}/_{4}$ in. × $^{3}/_{32}$ in.*
22 $^{1}/_{2}$ in. × $^{1}/_{2}$ in. × $^{1}/_{16}$ in.

Random carbon rings:

23 2 in. × 2 in. × $^{1}/_{4}$ in.†
24 1 in. × 1 in. × $^{3}/_{16}$ in.
25 $^{1}/_{2}$ in. × $^{1}/_{2}$ in. × $^{1}/_{16}$ in.‡

Coke:

26 3 in.*
27 1–2 in.*
28 1 in.*

Quartz:

29 2 in.
30 $^{1}/_{2}$–$1^{1}/_{2}$ in.

* No information available
† Probably same as 17
‡ Probably same as 22

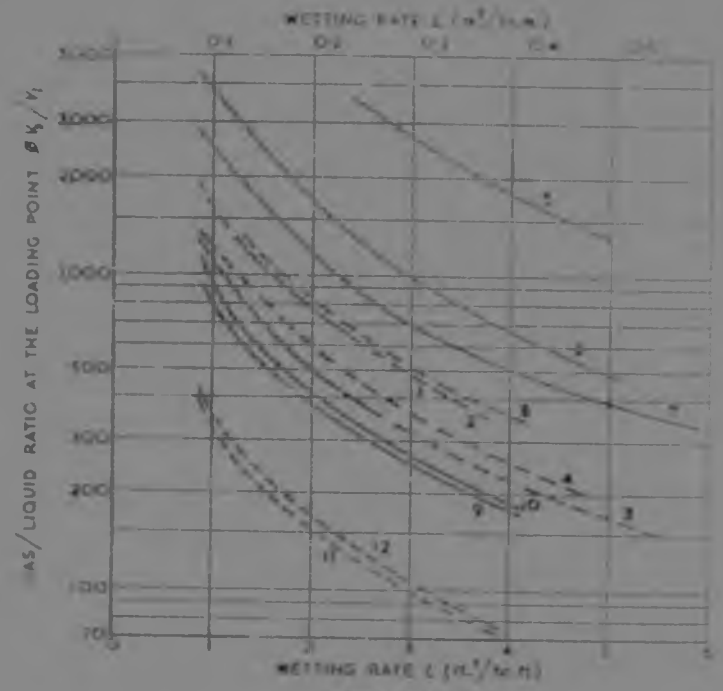

Figure C5 *Relation between gas/liquid ratio and wetting rate at the loading point for grids and stacked rings*

Curves shown in broken lines are based on estimated figures.

Plain grids:

1 1 in. × 1 in. × $^{1}/_{16}$ in.
2 1 in. × 2 in. × $^{1}/_{16}$ in.
3 1 in. × 1 in. × $^{1}/_{8}$ in.
4 1 in. × 2 in. × $^{1}/_{8}$ in.

Serrated grids:

5 4 in. × 4 in. × $^{1}/_{8}$ in.
6 2 in. × 2 in. × $^{3}/_{16}$ in.
7 $1^{1}/_{2}$ in. × $1^{1}/_{2}$ in. × $^{3}/_{16}$ in.

Stacked stoneware rings:

8 4 in. × 4 in. × $^{3}/_{8}$ in.
9 3 in. × 3 in. × $^{3}/_{8}$ in.
10 3 in. × 3 in. × $^{1}/_{4}$ in.
11 2 in. × 2 in. × $^{1}/_{4}$ in.
12 2 in. × 2 in. × $^{3}/_{16}$ in.

Table C6 Properties of Packings

Type	Material	Serial No.	Dimensions (in.) Pitch or dia.	Height	Thickness	Serial No.	Number per cubic foot*	Number per cubic metre*	Voidage ε	Surface Area per unit Volume† S (ft²/ft³)	(m²/m³)	Gas-film packing factor R_g	Liquid-film packing factor†† R_l
Plain Grids	Metal	1	1	1	$^1/_{16}$	1	—	—	0·93	[illegible]	63·5	2·5	0·9‡
		2	1	2	$^1/_{16}$	2	—	—	0·93	[illegible]	61·5	2·0‡	0·72‡
	Wood	3	1	1	$^1/_4$	3	—	—	0·75	30·0	98·5	1·6	0·88
		4	1	2	$^1/_4$	4	—	—	0·75	27·0	88·5	1·5	0·70‡
Serrated Grids	Wood	5	4	4§	$^3/_8$	5	—	—	0·69	6·0	19·5	1·5	0·69‡
		6	2	2§	$^3/_8$	6	—	—	0·83	13·0	42·6	2·4	0·72‡
		7	$1^1/_2$	$1^1/_2$§	$^5/_{16}$	7	—	—	0·83	16·5	54·0	2·3‡	0·77
Stacked Rings	Stoneware	8	4	4	$^5/_8$	8	27	950	0·73	19·0	62·5	1·4‡	0·60‡
		9	3	3	$^5/_8$	9	65	2,300	0·66	25·0	82·0	1·4	0·65‡
		10	3	3	$^3/_8$	10	65	2,300	0·78	25·0	82·0	1·4‡	0·68
		11	2	2	$^3/_8$	11	210	7,400	0·67	36·0	118	1·4‡	0·70‡
		12	2	2	$^5/_{16}$	12	210	7,400	0·73	36·0	118	1·4‡	0·70‡
Random Rings	Metal	13	2	2	$^1/_{16}$	13	175	6,100	0·92	30·0	98·5	3·3	0·67
		14	1	1	$^1/_{16}$	14	1,350	47,600	0·86	59·0	194	3·0‡	0·80‡
		15	$^1/_2$	$^1/_2$	$^1/_{32}$	15	10,500	370,000	0·87	115	377	3·1	0·88
	Stoneware	16	3	3	$^3/_8$	16	52	1,840	0·72	20·0	65·5	2·5	0·80‡
		17	2	2	$^1/_4$	17	165	5,820	0·74	28·0	92·0	2·7‡	0·65‡
		18	2	2	$^5/_{16}$	18	170	6,000	0·79	29·0	95·0	2·8	0·87
		19	$1^1/_2$	$1^1/_2$	$^3/_{16}$	19	400	14,100	0·73	[illegible]	153	2·7‡	0·75‡
		20	1	1	$^3/_{32}$	20	1,300	46,000	0·69	56·0	184	2·7	0·82
		21	$^3/_4$	$^3/_4$	$^3/_{32}$	21	3,000	106,000	0·71	72·0	236	2·7‡	0·88‡
		22	$^1/_2$	$^1/_2$	$^1/_{16}$	22	10,500	370,000	0·73	115	377	2·7‡	0·88‡
	Carbon	23	2	2	$^1/_4$	23	165	5,820	0·74	28	92·0	2·7‡	0·65‡
		24	1	1	$^3/_{16}$	24	1,250	44,000	0·68	37	120	2·7‡	0·88
		25	$^1/_2$	$^1/_2$	$^1/_{16}$	25	10,500	370,000	0·73	115	377	2·7‡	0·88‡
Solids	Coke	26	3			26	—	—	0·50**	15	49·0	2·3‡	0·45‡
		27	1—2			27	—	—	0·40**	35	115	2·1	0·55‡
		28	1			28	—	—	0·43**	40	131	2·5‡	0·58
	Quartz	29	2			29	—	—	0·46	19	62·5	2·7‡	0·50‡
		30	$^1/_2$—$1^1/_2$			30	—	—	0·40	34	114	[illegible]	0·55‡

* Values given apply when the diameter of the tower is about [illegible] times the nominal diameter of the rings. For small towers, the numbers may be approximately 10% less, and for large towers approximately 10% greater, than those shown.

‡ Estimated value.

** Does not include the pore space.

†† At the standard wetting rate.

† The surface area includes that of the edges. No allowance has been made for surface [illegible] points of contact between packing elements. The surface area of [illegible] has been [illegible] values of S for grid packings. The figures given can be used to calculate the equivalent diameter of the packing which is given by 4ε/S [illegible] number.

§ From top of grid bar to tip of serration.

Figure C6 Chart for determining ratio of proper mean to arithmetic mean driving force

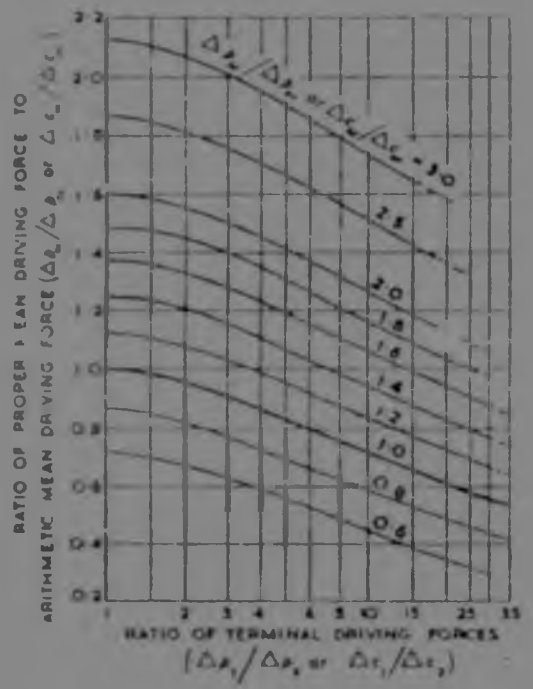

Table C7

Type	Material	Serial No.	Dimensions (in.)			Installed Cost	
			Pitch or dia.	Height	Thickness	Shillings/ft.²	£/m.²
Plain Grids	Mild steel	1	1	1	3/16	60	100
		2	1	2	5/16	50*	85*
	Wood	3	1	1	1/4	10†	18†
		4	1	2	1/4	8*†	14*†
Serrated Grids	Wood	5	4	4	1/4	6*†	10·6*†
		6	2	2	3/8	10†	18†
		7	1 1/8	1 1/8	3/16	17*†	30*†
Stacked Rings	Stoneware	8	4	4	3/4	4–15	7–27
		9	3	3	3/4	6	10·6
		10	3	3	1/2	13–21‡	23–37‡
		11	2	2	1/2	13	23
		12	2	2	3/16	20–29‡	35–51‡
Random Rings	Mild steel	13	2	2	3/16	16·5	29
		14	1	1	3/16	70	123
		15	1/2	1/2	1/32	340	600
	Stoneware	16	3	3	3/4	4·5–10	8–28
		17	2	2	1/4	9	16
		18	2	2	3/16	15–22‡	26·5–39‡
		19	1 1/2	1 1/2	3/16	15–20	26·5–51
		20	1	1	3/32	23–36	46–62·5
		21	3/4	3/4	3/32	—	—
		22	1/2	1/2	1/16	170‡	300‡
	Carboo	23	2	2	1/4	—	—
		24	1	1	3/16	130	230
		25	1/2	1/2	1/16	650	1,150
Solids	Coke	26	3			2·5§	4·4§
		27	1·5			3·0§	5·3§
		28	1			3·5§	6·2§
	Quartz	29	2			15**	26·5**
		30	1 1/2–1 1/2			18**	32**

* Estimated figure.
† Figures apply to standardized sizes. Assumed from makers of water cooling towers.
‡ Wide assortment and alternative sizes.
§ Figures apply to metallurgical [illegible] referred since 91 millimetres and bulk density 50 lb. ft.³); an allowance has been made for screening.
** Figures based on price of a [illegible] supplier with an allowance for screening.

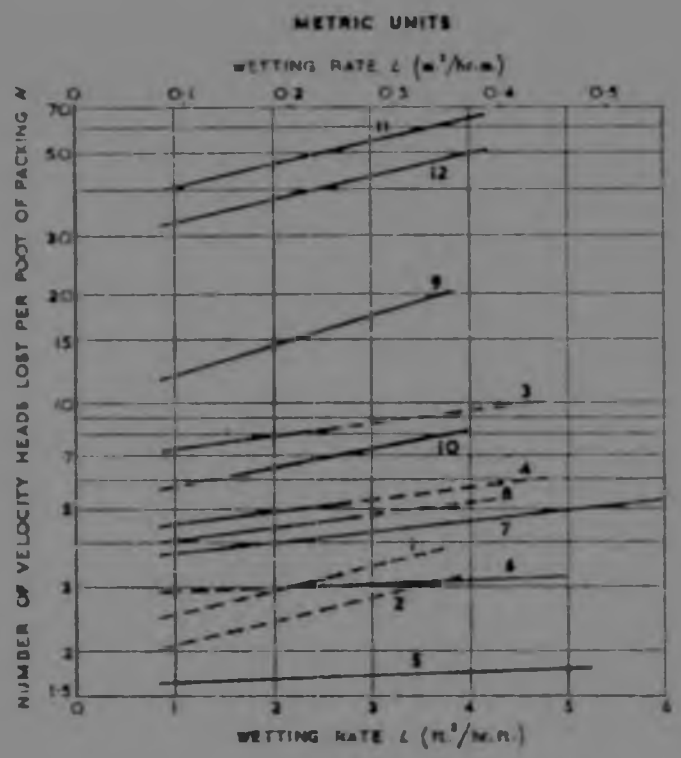

Figure C7 *Pressure-drop through grids and stacked rings*

The number of velocity heads lost per metre of packing is found by multiplying the values obtained from the curves by 3·28. Curves shown in broken lines are based on estimated figures.

Plain grids:
- 1 1 in. × 1 in. × $^1/_{16}$ in.
- 2 1 in. × 2 in. × $^1/_{16}$ in.
- 3 1 in. × 1 in. × $^1/_8$ in.
- 4 1 in. × 2 in. × $^1/_8$ in.

Serrated grids:
- 5 4 in. × 4 in. × $^1/_8$ in.
- 6 2 in. × 2 in. × $^1/_8$ in.
- 7 $1^1/_2$ in. × $1^1/_2$ in. × $^1/_{16}$ in.

Stacked stoneware rings:
- 8 4 in. × 4 in. × $^1/_8$ in.
- 9 3 in. × 3 in. × $^1/_8$ in.
- 10 3 in. × 3 in. × $^1/_4$ in.
- 11 2 in. × 2 in. × $^1/_4$ in.
- 12 2 in. × 2 in. × $^1/_{16}$ in.

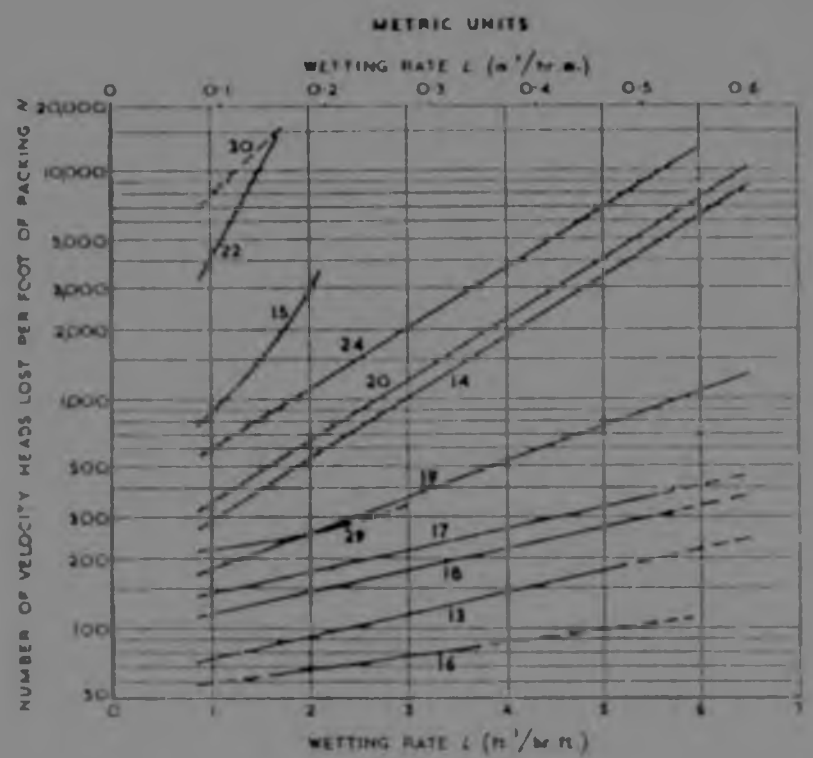

Figure C8 *Pressure-drop through random rings and coke*

The number of velocity heads lost per metre of packing is found by multiplying the values obtained from the curves by 3·28. Curves shown in broken lines are based on estimated figures.

Random metal rings:
- 13 2 in. × 2 in. × $^1/_{16}$ in.
- 14 1 in. × 1 in. × $^1/_{16}$ in.
- 15 $^1/_2$ in. × $^1/_2$ in. × $^1/_{24}$ in.

Random stoneware rings:
- 16 3 in. × 3 in. × $^1/_8$ in.
- 17 2 in. × 2 in. × $^1/_8$ in.
- 18 2 in. × 2 in. × $^1/_{16}$ in.
- 19 $1^1/_2$ in. × $1^1/_2$ in. × $^1/_{16}$ in.
- 20 1 in. × 1 in. × $^1/_{32}$ in.
- 21 $^3/_4$ in. × $^3/_4$ in. × $^1/_{32}$ in.*
- 22 $^1/_2$ in. × $^1/_2$ in. × $^1/_{24}$ in.

Random carbon rings:
- 23 2 in. × 2 in. × $^1/_8$ in.†
- 24 1 in. × 1 in. × $^1/_{16}$ in.
- 25 $^1/_2$ in. × $^1/_2$ in. × $^1/_{16}$ in.‡

Coke:
- 26 3 in.*
- 27 1–2 in.*
- 28 1 in.*

Quartz:
- 29 2 in.
- 30 $^1/_2$ – $1^1/_2$ in.

* No information available
† Probably same as 17
‡ Probably same as 22

Table C8 Economic Gas Rates for Various Packings

Packing						Economic Gas Rates*		Equivalent Empty-tower Velocities*	
Type	Material	Serial No.	Dimensions (in.) Pitch or dia.	Height	Thickness	(ft.³/hr.ft.²)	(m.³/hr.m.²)	(ft./sec.)	(m./sec.)
Plain Grids	Metal	1	1	1	1/16	28,200—35,300†	8,600—11,000†	7·8—9·8†	2·4—3·1†
		2	1	2	1/16	28,200—35,300†	8,600—11,000†	7·8—9·8†	2·4—3·1†
	Wood	3	1	1	1/4	17,700—28,200‡	5,400—8,600‡	4·9—7·8‡	1·5—2·4‡
		4	1	2	1/4	20,300—29,700‡	6,200—9,000‡	5·6—8·2‡	1·7—2·5†
Serrated Grids	Wood	5	4	4	1/2	28,200—42,400†‡	8,600—13,000†‡	7·9—11·8†‡	2·4—3·6†‡
		6	2	2	3/8	24,700—38,800†	7,500—11,800†	6·9—10·8†	2·1—3·3†
		7	1½	1½	5/16	24,700—35,300†‡	7,500—10,500†‡	6·9—9·8†‡	2·1—3·0†‡
Stacked Rings	Stoneware	8	4	4	1/2	19,400—28,900	5,900—8,800	6·3—8·0	1·6—2·4
		9	3	3	3/8	13,400—17,300§	4,100—5,300§	3·7—4·8§	1·1—1·5§
		10	3	3	1/4	19,800§	6,000§	5·5§	1·7§
		11	2	2	1/4	10,300§	3,100§	2·9§	0·88§
		12	2	2	5/16	10,600§	3,200§	2·9§	0·89§
Random Rings	Metal	13	2	2	1/16	8,470—10,660§	2,600—3,250§	2·4—3·0§	0·72—0·90§
		14	1	1	1/16	6,710—8,120	2,050—2,500	1·9—2·3	0·57—0·69
		15	1/2	1/2	1/32	3,530§	1,080§	0·98§	0·3§
	Stoneware	16	3	3	3/8	7,770—14,800	2,400—4,500	2·2—4·1	0·67—1·2
		17	2	3	1/4	6,330—10,200§	1,950—3,100§	1·8—2·8§	0·54—0·86§
		18	2	2	5/16	7,410—10,900§	2,250—3,350§	2·4—3·0§	0·63—0·93§
		19	1½	1½	3/16	6,000—9,250	1,850—2,800	1·7—2·6	0·51—0·81
		20	1	1	3/32	4,940—7,060	1,500—2,150	1·4—2·0	0·42—0·60
		21	3/4	3/4	3/32	—	—	—	—
		22	1/2	1/2	1/16	2,290§	700§	0·64§	0·19§
	Carbon	23	2	2	1/4	10,200‡§	3,100‡§	2·8‡§	0·86‡§
		24	1	1	3/16	5,300§	1,600§	1·5§	0·44§
		25	1/2	1/2	3/16	2,290§	700§	0·64§	0·19§
Solids	Coke	26	3			6,360—11,300‡	1,950—3,450‡	1·8—3·1‡	0·54—0·96‡
		27	1—2			3,180‡	950‡	0·88‡	0·28‡
		28	1			1,770—3,180‡	550—950‡	0·49—0·88‡	0·15—0·28‡
	Quartz	29	2			6,060—7,050§	1,850—2,150§	1·7—2·0§	0·51—0·60§
		30	1/2—1½			1,580§	480§	0·44§	0·13§

* Values given have been calculated on the assumption of gas-film limitation and apply to air at N.t.p. For other gases multiply by the factor—(Density of air at [illegible]/Actual density of gas)$^{0.5}$

‡ Estimated values.

† Higher gas rates are indicated on economic grounds alone, but there is no practical experience with such rates. Excessive [illegible] would be expected.

§ Higher gas rates are indicated on economic grounds, but the loading rate would then be exceeded.

	Gas Inlet	Middle Position	Gas Outlet
Gas flow ($m^3/_{hr}$)	793526.4	789505.55	785484.71
Partial pressure of SO_2 (atm) in gas	0.003	0.0016	0.0001
Gas temperature (°C)	25	22.5	20
Liquid temperature (°C)	21	20.5	20
Concentration of (Kg/m^3) dissolved SO_2	0.0355	0.0177	0
Equilibrium partial (atm) pressure of SO_2	00195	0.000975	0
Equilibrium concentration of dissolved SO_2 (Kg/m^3)	0.57	0.302	0.0355
Driving force (Δp) (atm)	0.00105	0.000625	0.0001
(Δc) (Kg/m^3)	0.534	0.2843	0.0355
H, Solubility coefficient (Kg/m^3 atm)	508.57	454.88	355
	bottom position		Top position

Table C9 Conditions for absorption of sulphur dioxide in the designed packed tower.

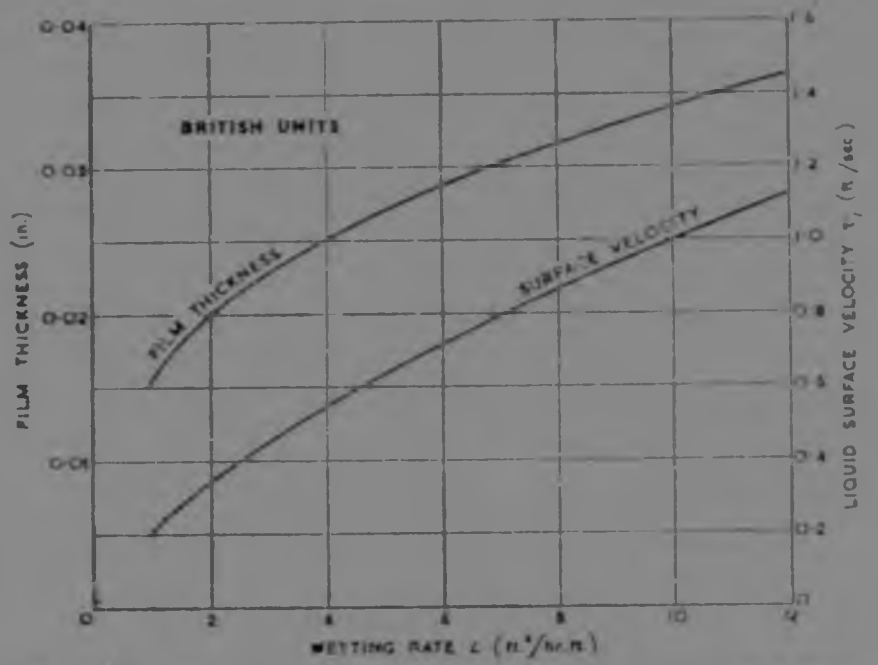

Figure C9 *Film thickness and liquid surface velocity for packings (British units)*
The values obtained from the curves given here apply only to water at 68°F. For other liquids and at other temperatures these values should be divided by the factor $0.215\ (\rho_l/\eta_l)^{0.33}$ in the case of the film thickness, and multiplied by the same factor in the case of the liquid surface velocity, where ρ_l and η_l are the density and viscosity of the liquid respectively in C.G.S. units. The wetting rate is the liquid rate per unit periphery and is given by $L = V_s/S$.

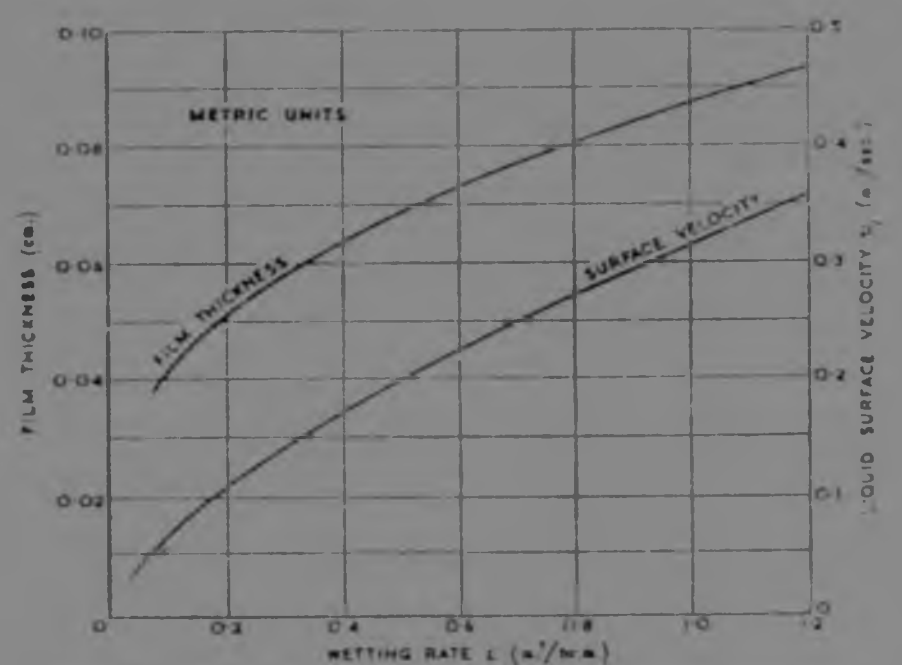

Figure C10 *Film thickness and liquid surface velocity for packings (metric units)*
The values obtained from the curves given here apply only to water at 20°C. For other liquids and at other temperatures these values should be divided by the factor $0.215(\rho_l/\eta_l)^{0.33}$ in the case of the film thickness, and multiplied by the same factor in the case of the liquid surface velocity, where ρ_l and η_l are the density and viscosity of the liquid respectively, in C.G.S. units. The wetting rate is the liquid rate per unit periphery and is given by $L = V_s/S$.

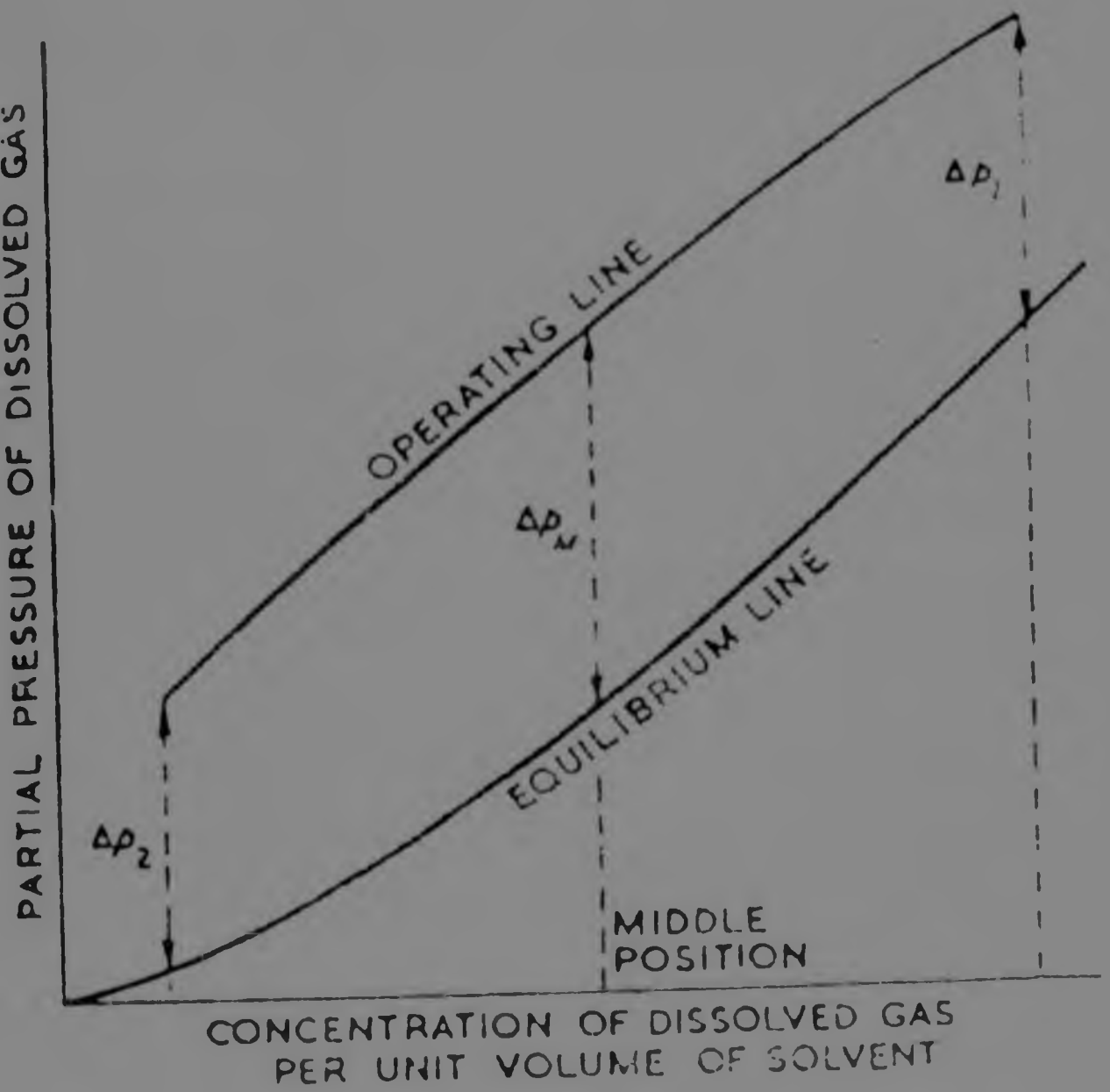

Figure on *Driving-force diagram to illustrate significance of middle position*

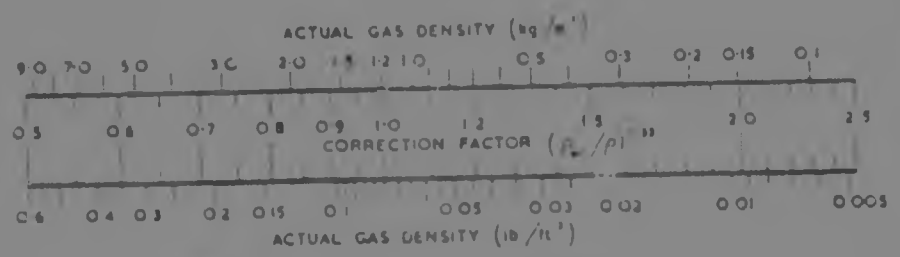

Figure C12 *Gas-density correction to economic gas rate*

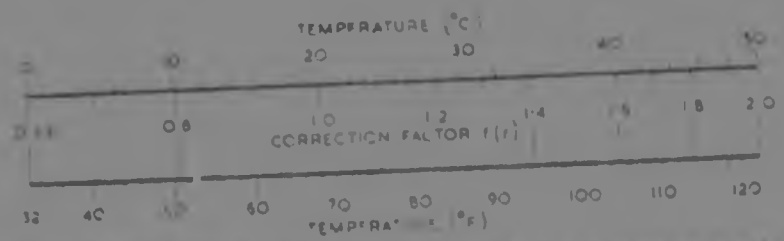

Figure C13 *Temperature correction factor for absorption in water*

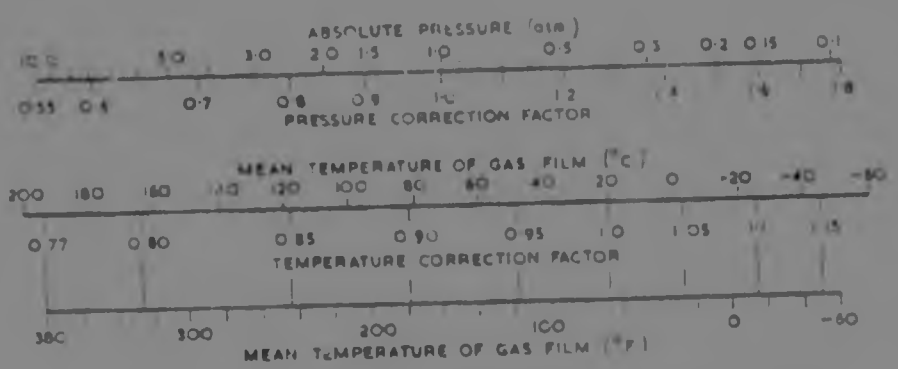

Figure C14 *Pressure and temperature correction factors for gas-film coefficients*

APPENDIX D.

DETAILED DESIGN OF THE ION EXCHANGE UNIT

1. Theoretical Approach to the Design

The equations given below are the ones used in the process of parameters calculations for the ion exchange unit.

1.1. Brackish water, passing through the weak cation exchange resin, exchanges an amount of divalent cations equivalent to its alkalinity content according to the reaction:

$$2\ RCOOH + Ca^{++}\ (\text{or } Mg^{++}) + 2HCO_3^- \rightleftarrows (RCOO)_2\ Ca + 2H_2O + 2CO_2$$

1.2. The volume occupied by the resin is given by

$V = \frac{\pi d^2}{4} L$ where d is the diameter of the unit, as well as of the resin bed, and L is the height of the bed.

1.3. The pressure drop, Δp, is given by the equation

$$\Delta p = \frac{200\ G\mu L(1-E)^{3-n}}{Dp^2\ \phi s^{3-n}\ \rho\ Fg_c G^3}$$

D_p is the particle diameter, G is the fluid where mass velocity, E - the voidage of the bed, L is the resin height, μ - the fluid viscosity, ϕ_s is the bed shape (spherical in our case), ρ_F is the density of the fluid and g_c is a conversion factor. n is a factor which depends on Reynolds number - Re. [150]

1.4. The Reynolds number for fluid flowing through a packed bed is given by the equation

$Re = \frac{Dp\ G}{\mu}$ and the dependence of n on Re is given below.

Re	n
up to 10	1
" " 30	1.3
up to 50	1.5
" " 70	1.6
up to 90	1.7

1.5. The optimum cycle

The design of the optimum cycle for a particular ion exchange installation involves an interesting interplay of variables. An economic balance can lead to a figure like Fig.D1 [160] in which the minimum total cost correspondence to a certain number of cycles per day. In our case, no attempt was made to calculate the optimum cycle, because of the special arrangement in which the ion exchange unit is fixed.

It must be remembered that the ion exchange does not work as an independent unit, and as suggested in this thesis, it is linked to the SO_2 scrubbing unit on the one side, and to the effluent treatment unit on the other side.

On the other hand, the longer the service cycle the more resin is required and proportionally, more regeneration solution is required. On the same principle, the shorter the cycle, more significant loss of resin is encountered due to the attrition.

For the purpose of this thesis, the calculations of the size and the pressure drop within the resin bed will be shown.

2. Detailed Calculations [162-168]

For the purpose of this thesis the water to be treated in the ion exchange unit has the composition as shown in Table 1. [10].

Table D1

Water Composition

Cations	meg/l	Anions	meq/l
Na^+	33.8	Cl^-	36.3
Ca^{++}	7.2	HCO_3^-	9
Mg^{++}	10	SO_4^-	5.2
Total	51 meq/l	Total	50.5 meg/l

Hardness = 7.2 + 10 = 17.2 meg/l
Alkalinity = 9 meq/l

Table 1 shows that 33.7% of the total cations are hard cations, Ca^{++} and Mg^{++}. More than half (9/17.2) of the total hardness can be loaded on the weak cation exchange resin. Therefore, the strong cation exchange resin (which usually follows the weak one) can work for a longer period by loading on it only the remaining 82.3% cations.

2.1 The capacity of the weak cation resin was taken as 3 eq/l_r resin, a value slightly lower than that commonly quoted (3.5 eq/l_r). [161].

2.2 The flow rate of the brackish water is 90 gal/min, [122], or 20.44 m^3/h.

At a flow rate of 20 Bed volumes per hour (20 B.V./h = 20 $m^3/h\ m_r^3$), an amount of

$$\frac{20.44\ m^3/h}{20\ m^3/m_r^3 h} = 1.022\ m^3$$ of resin is needed

A safety margin of 25% is taken in case the flow rate of the brackish

water must be increased or the capacity of the resin drops suddenly.

Therefore 1.277 m of rc is required.

As explained above, 9 meq/l of Ca^{++} and Mg^{++} (together) can be removed from the brackish water by the weak cation resin.

The total amount of Ca^{++} and Mg^{++} removed by the 1022 litres of resin, is

$$1022 \times 3 = 3066 \text{ eq } (Ca^{++} \text{ and } Mg^{++})$$

The flow rate, in eq/h units of the brackish water is

$$20.4 \times 0.009 \times 1000 = 183 \text{ eq/h}$$

Therefore, 3066/183 = 16.75 hours will pass before the weak cation resin will be fully loaded which is the minimum period between two regenerations.

The flow rate of the regeneration solution as it comes out of the scrubbing tower, is 6144,6 l/h (Appendix C)

From the newly developed regeneration process, between 10 and 15 Bed Volumes of regeneration solution (SO_2 in water) are necessary for the regeneration of the weak cation exchanger.

If the higher figure (15 B.V.) is considered, the solution needed for regeneration is

$$1.2775 \times 15 = 19.16 \text{ m}^3 \text{ or } 19160 \text{ litres.}$$

19160 litres is the amount of scrubbing effluent coming out during

$$19160/6144.6 = 3.118 \text{ hours}$$

Thus most of the scrubbing effluent will be passed directly to the treatment and only 19160 litres will be stored for the regeneration.

At least 3.12 hours before the regeneration, the accumulation of the scrubbing effluent should be started.

It is advisable to use two units, each containing 1,277 m^3 weak cation resin, so that while one is regenerated, the other one is in service.

In this way, at least 16.75 hours will pass between the regenerations, each unit being regenerated once in

$$16.75 \times 2 = 33.5 \text{ hours.}$$

This arrangement is suitable for the men who service the water treatment unit, and enables some analysis and maintenance work to be conducted.

The effluent treatment unit can be set to process the effluents continuously or in batches.

If it is set for continuous process, an accumulation pond or tank for the effluent must still be provided, in case of emergency situations. Therefore, it is advisable to set the effluent treatment plant for batch processing.

In this case, the effluent treatment unit can be shut down for the interval when the scrubbing effluent is accumulated for regeneration.

During that period, (more than three hours) maintenance work can be conducted.

2.3. <u>The size of the unit for the weak cation exchange resin :</u>

The volume of the resin is 1.277 m^3.

$V = \frac{\Pi \times d^2}{4} \times L$ In industrial units, the head of the resin bed is 1.5 times the diameter

Therefore it can be written:

$$V = \frac{\Pi \times d^2}{4} \times 1.5d = \frac{\Pi \quad 1.5}{}$$

$$\rightarrow d = \sqrt[3]{\frac{4 \times V}{1.5 \times \Pi}} = 1.027 \text{ m}$$

$$L = 1.027 \times 1.5 = 1.54 \text{ m.}$$

The height of the unit, should be chosen in such a way as to give enough room for the expansion of the resin during the backwash and for all the accessories inside the tank (delivery pipes, distributors, trays, etc.)

In this case, 50% expansion of the resin is necessary plus another 20% free space for accessories:

1.54 + 1.078 = 2.618 m will be the height of the ion exchange unit.

2.4. Pressure drop. Before the pressure drop is calculated, the flow regime through the bed is needed for the substitution of the right value for "n" in the pressure drop equations.

$$Re = \frac{Dp\ G}{\mu} \qquad Dp = 0.07 \text{ cm}$$

$$G = \frac{20.44 \times 10^6}{3600} / \Pi \times 102.7^2 = 0.68 \text{g/sec.}$$

μ = 0.01g/sec cm

$$Re = \frac{0.07 \times 0.68}{0.01} = 4.76$$

n = 1

$$\Delta p = \frac{200\ G_u\ L\ (1 - E)^2}{D_p^2 \phi_s^2 \rho F g_c G^3}$$

$g_c = 1$
$\mu = 0.01$
$L_1 = 154$
$G = 0.35$
$\phi_s = 0.58$
$Dp_1 = 0.08$

$$\Delta p_1 = \frac{200 \times 0.68 \times 0.01 \times 154 \times (1-0.35)^2}{0.08^2 \times 0.58 \times 1 \times 1 \times 0.35^3}$$

$$= 0.96 \times 10^5 \text{ Kg/sec}^2\text{m} = 0.96 \text{ bar}$$

During loading, the resin shrinks by 13% (Zerolite 236) and therefore the Dp_1 changes to 0.07 cm and the height of the bed drops to 134 cm

$$L_2 = 134 \qquad Dp_2 = 0.07$$

$$\Delta p = 1.1 \times 10^5 \text{ Kg/Sec}^2\text{m} = 1.1 \text{ bar.}$$

Usually the company which supplies the ion exchange resins, also provides the unit in which the ion exchanger is contained and all the accessories Fig.D2 and D3. Therefore only the amount of the ion exchange must be known in making economic evaluations, the cost of the unit being dependent upon the amount of the resin required.[162-168]

3. Materials of construction. The unit will be preferably made of 316L stainless steel lined with a non corrosive material.

4. The pH of the regeneration solution must be 1 or < 1.6
If it is too high, it must be lowered to the limits.

This can be done by bubbling pure SO_2 through the regeneration solution until the pH drops to the required level.

The pure SO_2 originates in the effluent treatment plant and it can be returned after bubbling, to the same place (stream 19, Fig. 4.15 Chapter 4).

5. Summary of Design

Two ion exchange units, having 1.027m diameter and 2 62 m in height each, are required for the treatment of brackish water. Each unit will contain 1.2775 m weak and cation exchange resin (Zerolite 236)

The water flow is 90 gal/min or 20.44 m^3/h and the pressure drop through the resin is between 0.96 to 1.1. bar.

The brackish water contains 51 meq/l T.D.S. of which 9 meq/l are HCO_3^- anions.

Weak cation resins are more and more used in the water treatment these days.

A typical example is the SIRA Process,[10] developed in Italy, which has weak cation and anion resins and is a further development of the well known Dessal Process (Fig.D.4).[6]

6. Nomenclature

Symbol	Meaning	Units
D_p	Particle diameter	cm
G	Fluid mass velocity	g/cm^2 sec
L	Packed height	cm
Δp	Pressure drop	bar
G	Bed voidage	-
μ	Fluid viscosity	g/sec cm
ρ_F	Fluid density	g/cm^3
ϕ_s	Bed shape factor	-
Re	Reynolds number	
d	Unit Diameter	cm
C	resin capacity	eq/l
T.D.S.	Total dissolved solids	eq/l
B.V.	Bed Volume = the original volume of the resin	m^3 or l
r	Resin	

Economic Balance Finds Optimum Cycle

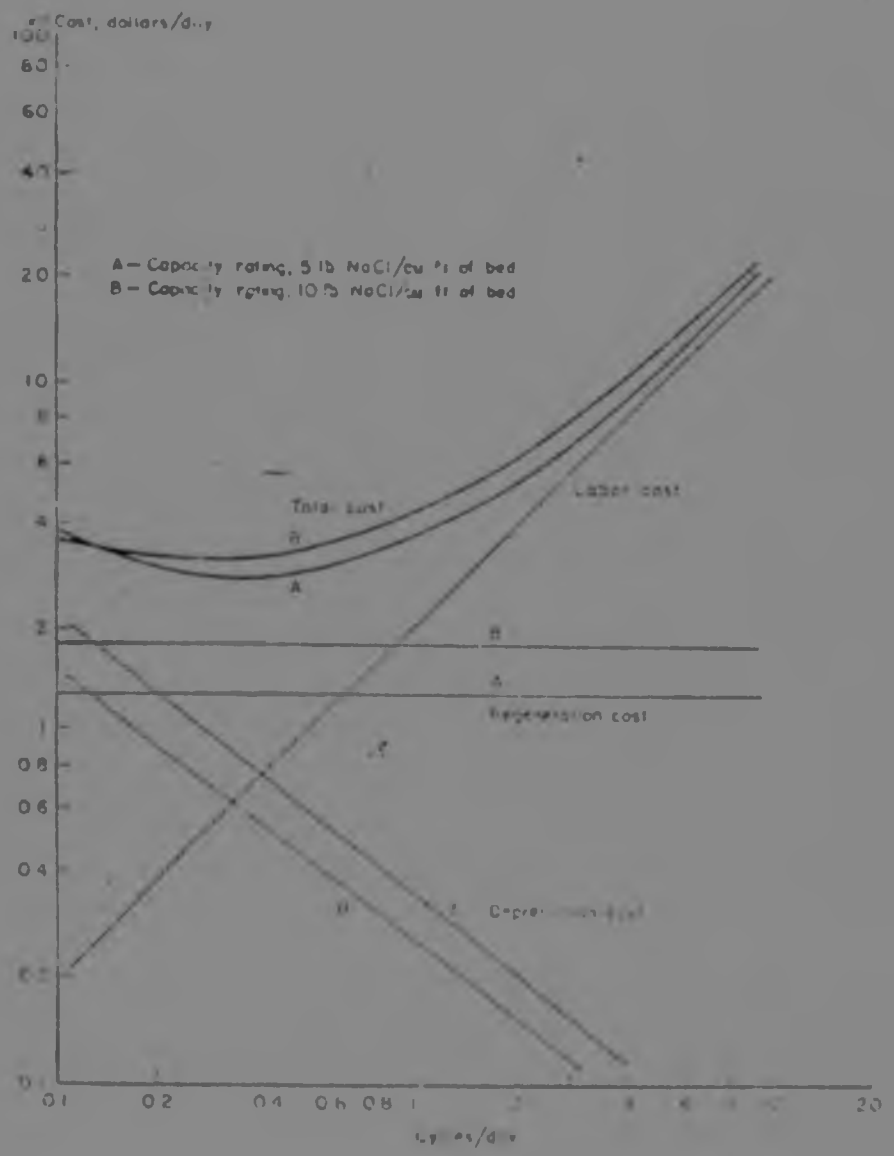

Figure D.1

Source [160]

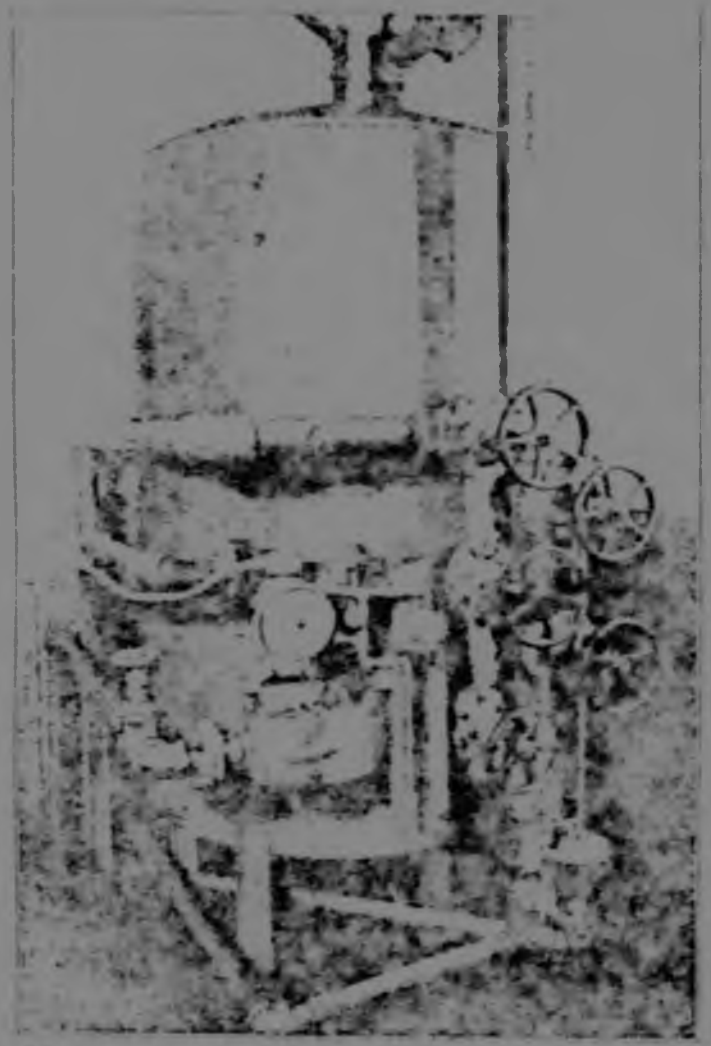

FIGURE D2 A typical industrial ion exchange water softening unit. Courtesy of Worthington Pump and Machinery Corporation.

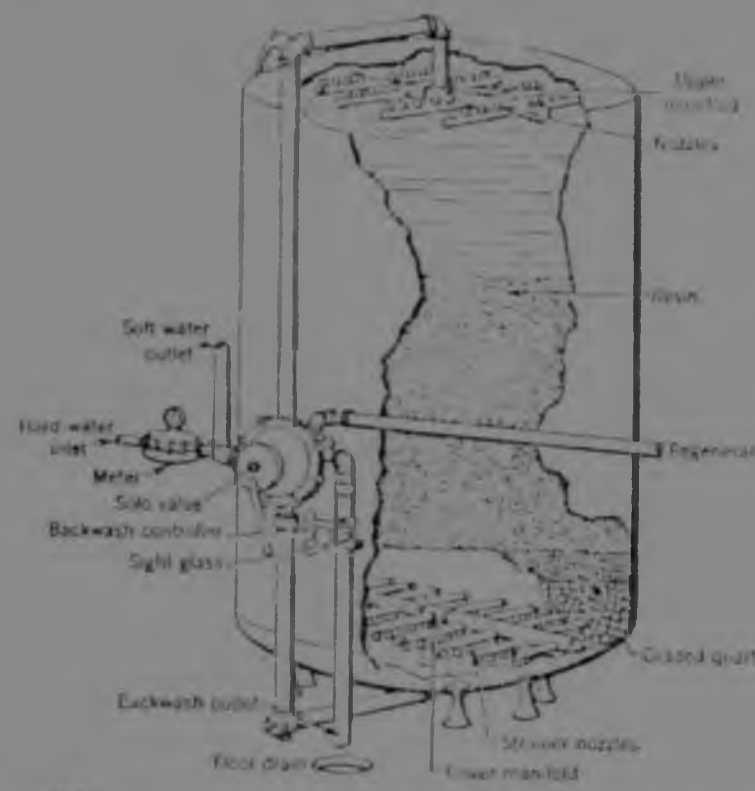

FIGURE D3 Cross-section of typical industrial ion exchanging unit with its regenerant

Source [12]

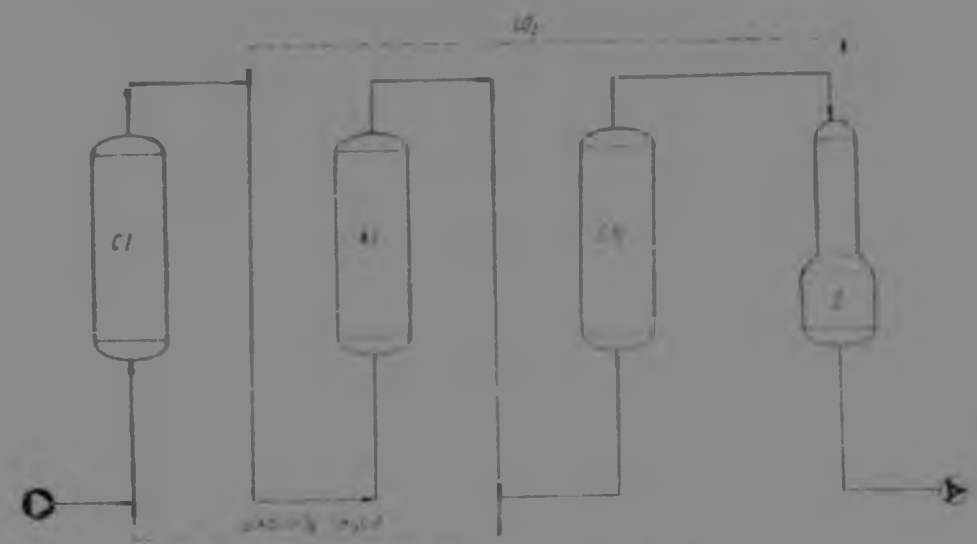

Fig. D.4. Basic version of the SIR V process

(C$_I$ – weak cation resin, A$_I$ – weak anion resin, C$_{II}$ – weak or strong cation resin, P – degasifier)

Rys. 4. Podstawowy wariant procesu SIR V

(C$_I$ – kationit słabokwasowy, A$_I$ – anionit słabo zasadowy, C$_{II}$ – kationit słabo lub silnie kwasowy, D – odgazowywacz)

Source [10]

REFERENCES

[1] R. Kunin, Ion exchange resins, Robert E. Krieger, Huntington, N.Y. USA, 1972.

[2] D 'Alelio, G.F., U.S. Patent 2 366 007 (Dec. 26, 1945)

[3] D 'Alelio, G.F., U.S. Patent 2593417 (April 22, 1952)

[4] McBurney, R., U.S. Patent 2591573 (April 1, 1952)

[5] Kunin, R., U.S. Patent 3.156.644 (1964)

[6] R. Kunin and B. Vassilion New deionization techniques based upon weak electrolyte ion exchange resins, I & E.C. Process Design and Development Vol.3, No.4, Oct. 1964, 704 - 709.

[7] R. Kunin, A new ion exchange desalination technique, Brit. Chem. Eng. 11, 1966, 1222 - 1225 - 1235.

[8] R. Kunin, A progress Report on Water Desalination and Water Renovation, Amber-Hi-lites, No.99 and No.100, May and July, 1967.

[9] Boari, G., Liberti, L., Merli, C. and Passino R., U.S. Patent 3679580 (1972).

[10] Boari, G. Liberti, L, Passino, R. The SIRA Process for brackish water demineralization by ion exchange. Environmental Protection Engineering, Vol.1, No.2, 1975, 165-176.

[11] D.E. Weiss, B.A. Bolto, R. McNeill An ion exchange process with thermal regeneration. Australian J. of chemistry, Vol. 19, 1966, 589-608.

[12] B.A. Bolto, Weiss, D.E. Australian Patent 274029.

[13] Stepanova Z.S, Kupinskayo, G.V., Kuz'micheva, L.V., Shchaleleva, G.A. : Use of a carboxylic cation exchanger for neutralization of regeneration waters at the Kostroma State Regional Power Plant. Izv. Vyssh. Ucheb. Zaved. Energ. 1977, 20(7) 57-61.

[14] A.J. Gilmore, Ion exchange recovery of copper, zinc, and nickel from acid-sulphate an and alkaline-cyanide waste water. Canadian Mines Br, Inform. Arc. 1970, IC 252.

[15] Hashimoto, Yasuhito; NaKamuro H, Shiraishi, M. Recovery of metal values and purified water from heavy metal-contaminated waste waters. Japan Kokai 78/55481, and Japan Kokai 78/55482, both 29 Oct, 1976.

[16] Tsuzuka, K, Howada M. Kasai M.: Neutralization of ion exchanged water, Japan Kokai 78/51180.

[17] G. Boari and R. Pass·no : Ion exchange pretreatment of feed waters to desalination plants. Ch. E. Progress Symp. Ser. Water 1970, 41-249.

[18] Ringel, Helmut; Zimmer E, Abdelmonem N,: Method and apparatus for loading weak acid cation exchange resins with uranyl ions German Patent 2733396 (Sep. 1978)

[19] G.W. Weber, R.L. Beatty, V.J. Tennery : Properties of carbonized and converted uranium-loaded weak acid resins. Oak Ridge Nat. Laboratory, ORNL-5201, February 1977.

[20] J.J. Wolff. Use of ion exchange resins in uranium extraction processes. Dia Prosim Technical report.

[21] I.S. Ganapathy, P.K. Padmanabhan, Ch. Ven Kateswarlu, Exchange of metal ions against hydrogen ion of a carboxylic acid exchanger, A.E.C. Bhabha At. Res. Cent , Bombay, India, Rep. 1973, B.A.R. C 720

[22] A. Biyabora, H. Shimizu, O. Nasu and A. Obihawa. Japanese patent 18418 (Dec. 1960)

[23] P.T. Hsieh, T.C. Yang, T.S. Shih and C.M.Huang Sugar refining by ion exchange, J. Formosan Sci., 15, 31-34, 85-88 (1961).

[24] M.W. Brenner, U.S. Patent 2857279 (Oct. 1958).

[25] E.W. Bingham and C.A. Zittle, Removal of acid phosphate from skim milk, Federation Proc. 24 (March 1962)

[26] O. Gawron and F. Drans: Fractionation of Popain, Ag. & Food Chem 6, 615 (Aug. 1958).

[27] C.D. Logan: U.S. Patent 3197416, (July 1965)

[28] U.S. Borax and Chemical Company : British Patent 905 204 (Feb. 1962).

[29] F.S. Chance and E.G. Martin, U.S. Patent 3053733 (Sept. 1962)

[30] H.L. Segal and others, Determination of Gastric Acidity without Intubation by use of Cation Exchange Indicator Compounds: Proc. Soc. for Exper. Biology and Medicine, 74, 218-220 (June 1950)

[31] F.M. Thurman. Use of ion exchange resins in anti-perspirant-deodorants, American Perfumer, Vol. 76, No.9, 30-32

[32] Isolation of Tuberciden, J. Ferment Technol. 45, 6[illegible]-65 (1967).

[33] H.M. Doery and E.C. Mason: Estimation of Streptomycin in Fermentation Broths (Anal. chemistry, 22(8), 1038-1039 (Aug. 1950).

[34] Bioterapico Genovese S.p.A., Belgian Patent 665502 (Oct. 1965).

[35] F. Mirando and S. Lisstsky: Scorpion Venom : Nature, 190, 443 (April 1961).

[36] P. Jolles and J. Jolles. Lysozyme from Human Milk, Nature 1962, 1187-1188, (Dec. 1961).

[37] S.G. Wolf, Jr.; R. Caputto and R.E. Trucco: U.S. Patent 3026251 (March 1962).

[38] T.L. Perry and W.A. Schroeder Amines in chrome, J. of Chromatography 12, 358-373, (Nov. 1963).

[39] C.T. Jones and W.A.Schroeder Chromotography of Human Haemoglobin J of Chrom. 10, 421-431, (April 1963).

[40] W.F. White, Lombard and R.J. Schlueter U.S. Patent No. 3033753 (May 1962)

[41] R.H. Hagemen, D. Fesker, J.J. Wabol and D.H. Stork Hydroponics. Agron. J. 53, 175-180, (May-June 1961).

[42] V. Coletta and R.B. Warfield U.S. Patent 3091574 (May 1963).

[43] M. Honda, Japan Analyst, 4, 384 (1955).

[44] T. Nortia and J. Sohlman Adsorption of Copper (II) and Nickel (II) Amine ions on weakly Acidic and Chelating Cation Exchange Resins Fm. Chem. Lett. 1976, 119-122

[45] R.A. Edge, Anal. Chem. Acta, 24, 143 (1961)

[46] H. Grays and H.F. Walton Sep. Sci., 5,653 (1970)

[47] S. Ganapathy Iyer, C.V. Krishnan and Ch. Venkateswarlu Ind. J. Chem., G, 277 (1968)

[48] E.L. Kantsev and A.N. Denisov, Russ J. inorg. chem. 8, 1149 (1963) (English Transl.)

[49] D.K. Hale and D.Reichenberg, Diss Far. Soc 7, 79 (1949)

[50] R.C. Degeiso. L.C.Donaruma and E.A. Tomic, Anal. Chem. 34, 845 (1962).

[51] M.J. Hatch, U.S. Patent 3300416 (1967)

[52] Samuelson, O. Ion exchangers in Analytical chemistry. John Wiley and Sons, Inc, New York, 1953, p.22.

[53] Inczedy, J Analytical applications of Ion exchangers, Pergamont Press, Oxford. 1966, p.24.

[54] L. Stanisavlievich: The optimum range of pH for ion exchange resins. Energetica, 20, 8, 1972 (Romania) 363-368.

[55] F.C. Nachod and J.Schubert: Ion exchange technology, Academic Press Inc. New York, 1956.

[56] Yu. A. Tolmacheva, Izv. Vyss Uchebn. Zaved. Khim Tekhol, 8, 55 (1965).

[57] A. Yu Dadabaev, P I. Kotkova and S.E. Kozhirova, Tr. Inst. Met i. Obogash, Akad. Nank Kaz. SSR. 9, 51 (1964).

[58] V.S. Soldatov, L.V.Novitskaya and G.S. Marenok, Zh. Prikl. Khim. 40, 460 (1967).

[59] V.A. Saidkhmedov, Mossob. Prot. Khim. Tekhnol No.4, 126 (1969).

[60] Efendiev, A.A., Shakhtakhtinskaya, A.T., Nicolaev, N.N. Study of the sorption kinetics of copper on carboxyl ion exchangers, Azorb. Khim. Zh. 1978, (3) 86-90, 377 (4) 137-43, Dokl. Akad. Nauk SSSR 1977, 235(2) 398-401.

[61] Padmanabhan, P.K. Venkateswarly, Ch. Exchange of cations on Zeo-Karb 226 (hydrogen (+) ion) Indian J. of Chemistry 1975, 13(3)264-6.

[62] Ch. Sitaramalakshmi and Ch. Venkateswarlu, Sorption of nickel on Zeokarp 226 (NH_4^+).Indian J. of Chemistry, Vol. 15A, No.5, 1977, 450-451.

[63] S. Soldatov, L.V. Novitskaya, and G.S. Manenok, Working with weakly acidic cation exchangers Zh. Prikl Khim. 40(2) (1967) 460 - 463.

[64] S. Evans and Y.Carmeli: Utilization of weak electrolyte ion exchange resins for marginal desalination. Ben Gurion Univ. of the Negev, R.S.D. Authority, Beer-Sheva, Israel, Jan. 1974.

[65] Arden, T.V. — Water Purification by Ion Exchange Butterworths, London 1968.

[66] K.R. Gray, L. Hartzell — U.S. Patent 2656, 245, Oct. 1953

[67] K.R. Gray, L. Hartzell — U.S. Patent 2656244, Oct. 1953.

[68] R. Kunin, — Belgian Patent 609123, April 1962

[59] R. Kunin, B. Vassilion, — Carbon dioxide regeneration. Ind. Eng. Chem. Prod. Res. Develop. 2, No 1 (1963).

[70] L. Larsen, — U.S. Patent 3691109, Sept. 1972.

[71] Kadiec, V., Matejka, Z; Ocenasek, M; — Czech. Patent 146595, Dec. 1972

[72] B.C. Wittamar, H. Sontheimer: — Equilibrium in the regeneration of cation exchangers, Chem. Eng. Techn. 1975, 47(14) 613.

[73] B.C. Wittamar, H. Southeimer; — Regeneration of weak acid ion exchangers with carbon dioxide. Vom Wasser, Vol. 47, 1976, 297-329.

[74] D.E. Weiss, B.A. Bolto, R. McNeill, A.S.Macpherson, R. Suidak, E.A. Winton and D. Willis: — An ion exchange with thermal regeneration, ustralian J. of Chemistry 19, 1966, 589-608.

[75] H.H. Euman, B. Winfried, — Ger. Offen 2726665, Jan. 1979.

[76] H. Masahide, I. Todaya, K, V. Hiroyuki — Japan Kokai 77/68, 068, June 1977.

[77] R. Kunin, — U.S. Patent, 407/446, Jan. 1978.

[78] R. Kunin, — U.S. Patent, 4116860 Sept. 1978.

[79] R. Kunin and R.E. Barry: — Carboxylic, weak acid type, cation exchange resin, Ind. and Eng. Chem. Vol. 41, No 6, (June 1949), 1269-1272.

[80] R. Kunin — Ion exchange, J. Analytical Chemistry, Vol. 21, No.1, Jan.1949.

[81] A. Chatteridge and J.A. Marinsky: — The dissociation of carboxylic cation Exchange resins: Anal. Chem. Acta 28, 205-216 (March 1963)

[82] F. Helffinch: Ion exchange kinetics, V. Ion exchange Accompanied by Reactions. J of Physical Chemistry, Vol.69, No.4, (April 1965).

[83] M.B. Hanley, S.C. Churms, E.C. Leisegang: Kinetics of exchange involving Ion Association on weak Acid Resin Chemical Communications No.2, 1967, 78-79

[84] Wolfgang Höll and Günter Geiselhar, Kinetics of the neutralization of weak acid ion exchange resins with different solutions. Desalination 25 (1978) 217-226.

[85] W. Höll and H. Southeimer: Ion exchange kinetics of the protonation of weak acid ion exchange resins, Chem. Eng. Science, 32, (1977), 755-762.

[86] Gordon, R, Youngquist and S.K. Garg: Sorption of Sulphur Dioxide by Microreticular Ion Exchange Resins. Ind Eng. Chem. Process Des. Develop. Vol.11, No.2, 1972, 259-261.

[87] Tsobanopoulos, Vasilios: Elimination of dilute sulphur dioxide by macroreticular ion exchange resins using a cyclic operation in a packed bed. Ph.D. Thesis, Carnegie-Mellon University, Chem. Engineering, 1973.

[88] Argul, N.N., Belyakova, L.D, Dadugina, N.G: Use of macroporous anion exchangers for acid gas absorption. Rasshir. Tezisy Dokl - Uses Sump Thermodin. Ionnogo Obmena, 2nd, 1975, 112-13.

[89] N.N. Argul, T.V. Barmakova, L.D. Byakova. Heats of adsorption of sulphur dioxide by macroporous weakly basic anion exchangers and determination of their pore structure. Kolloidnyi Zhurnal, Vol. 39, No.2, 339-343, March, April 1977.

[90] Lowrence Layton and G.R. Youngquist: Sorption of sulphur dioxide by ion exchange resins: I. & S.C. Progress design and development Vol.8, No.3, July 1969, 317-324.

[91] Thompson, R.W., Youngquist, R.G: Fixed bed sorption of sulphur dioxide by ion exchange resins. A.I.Ch.E. Symp. Ser. 1978, 74 (179) 53-7.

[92] Emil Krejcar: Anion exchange resins as sorbents of sulphur dioxide. Chem. Prumysl 15(2) 1965, 77-9.

[93] Shirane, Katsushi: Removal of acidic gas from polluted air, Japanese Patent 74, 130, 884, 14 Dec. 1974.

[94] M.A. Oostomezyk, J. Kuropka: Investigations on sorption of acid gases on anion exchangers. Environmental Protection Eng. Vol. 3, No. 1-2, 1977, 135-143.

[95] C.J. King: Separation Processes, McGraw Hill Co., USA, N.Y., 1971 pp.273.

[96] G.A. Morris and J. Jackson. Absorption Towers. Butterworths Scientific Publications and Imperial Chemical Industries 1953.

[97] S. Savencu, A. Bordea, J. Linde, A. Luca: Chimia Analitica Calitativa. Bucuresti, (ROMANIA) 1963.

[98] W.R. Horlacher, R.E.Bernard, R.K. Teague, P.L. Hayden: Four SO_2 Removal Systems, C.E.P., Vol. 68, No.8 Aug. 1972, 1-8.

[99] N. Arbiter and D.A.Milligan: Extractive metallurgy of copper. A.I.M.E. Metall. Soc., New York 1976, 974-993.

[100] N. Arbiter, D. Milligan, McClency, D.: I. Chem. E. Symp. Series, 42, 1975, 1.

[101] Esdaile, J.D., U.S. Patent 349476 (1970).

[102] A.J. Parker, D.M. Muir, S.A. Patent 77/6073 (1977).

[103] M.J. Semmens : Ion exchange I - Fundamental considerations. 19th Public water supply engineering conference campaign, ILL., U.S.A. April 1977, 115-127.

[104] P.R. Dana and T.D. Wheelock, Kinetics of a moving boundary ion exchange Process: Ind. Eng. Chem. Fundam. Vol.13, No.1, 1979, 20-26.

[105] F. Helfferich, Ion exchange, McGraw Hill Company, London 1962.

[106] L. Liberti, G. Boari. Chloride/Sulphate exchange on anion resins. Kinetic investigations : II Particle diffusion rates. Desalination 25 (1978) 123-134.

[107] W. Holl and H. Southeimer: Ion exchange Kinetics of the protonation of weak acid ion exchange resins. Chem. Eng. Science. 1977, Vol. 32, 755-762.

[108] O. Levenspiel : Chemical reaction engineering. John Wiley & Sons, inc. New York, 1972.

[109] W. Holl and G. Geiselhart: Kinetics of the neutralization of weak acid ion exchange resins with different solutions. Desalination, 25(1978) 217-226.

[110] W. Holl and K. Kirch: Regeneration of weak base ion exchange resins. Desalination 26(1978) 153-162.

[111] T. Kataoka, H. Yoshida and Y. Ozasa: Intraparticle ion exchange mass transfer accompanied by instantaneous irreversible reaction. Chem. Eng. Science, 1977, Vol.32, P 1237 - 1240.

[112] T. Coetzee, Sulphur Dioxide air pollution, A morbidity study, Medical Proceedings, A South African Journal for the Advancement in Medical Science. Vol. 23, Oct. 1977, 1-4.

[113] T.A. Ring and J.M. Fox, Fuel vs stack gas desulphurization, Air polution control and clean energy A.I.Ch.E. Symposium Series, Vol. 72, 1976, 1-11.

[114] Robert M. Timesor, Alexander Gakner, Demand for air pollution controls in the power industry. Recent advances in air pollution control, No. 137, Vol. 70, 1974, A.I.Ch.E. Symposium Series.

[115] Pedro M. Medellin, Removal of SO_2 and NO_x from Simulated Flue Gases by alkalized Alumina in a Radial Flow Fixed Bed. Ind. Eng. Chem. Process Des. Dev. Vol. 17, No.4, 1978, 528-536.

[116] Guy E. Weismantel, Limestone + magnesium : a new SO_2 control team. Chem.Eng. J., Sep 11, 1978, 111-113.

[117] S. Uchdo Absorption of SO_2 into limestone slurry in a stirred tank reactor. The Canadian J. of Chem. Eng., Vol. 56, December 1978, 691.

[118] Fly ash replaces limestone in sulphur dioxide removal. C & EN August 6, 1979, pp.26.

[119] S. Vasan. The Citrex Process for SO_2 Removal. Chem. Eng. Progress, Vol.71, No.5, May 1975. 61-

[120] W.F. Bischoff, Y. Habib, The FW-BF Dry adsorption System. Chem. Eng. Progress Vol.71, No.5, May 1975. 59-61.

[121] M. Hartman, Comparison of various carbonates as absorbents of sulphur dioxide from combustion gases. International Chemical Engineering, Vol.18, No.4, Oct. 1978, 712-717.

[122] A. Tamaki; The Thoroughbred 101 Desulphurization Process. Chem. Eng. Progress, Vol. 71, No.5, May 1975, 55-58.

[123] W.J. McMichael, L.S. Fon, C.Y. Wen: Analysis of Sulphur Dioxide Wet Limestone Scrubbing Data from Pilot Plant Spray and T.C.A. Scrubbers. Ind. Eng. Chem., Process Des. Dev. Vol.15 No.3, 1976, 459-467.

[124] Arthur L. Kohn, Fred C. Riesenfeld Sulphur Dioxide Removal by liquid Absorption. Chemical Engineering, June 15, 1959 147-151.

[125] R.L. Gall, E.J. Piasecki, The double alkali wet scrubbing system, Chem. Eng. Progress, Vol. 71, No.5, May 1975, 72 - 75.

[126] C.G. Cornell and D.A. Dahlstrom, Sulphur Dioxide Removal in a Double-Alkali Plant. Chem. Eng. Progress Vol. 69, No.12, Dec. 1973, appeared in Sulphur Dioxide Processing, published by A.I.Ch.E., New York, 1975.

[127] R.U. Rees, Present performance and scope for improvement in power station flue gas washing equipment for the removal of sulphur dioxide. Paper presented at Proceeding of the Conference on the Mechanical Engineer's Contribution to clean air, London 1957, 34-36.

[128] J.E. McCarty, Choosing a flue gas desulphurization system, Chemical Eng. J., March 13, 1978, 79-84.

[129] W. Strauss — Industrial gas cleaning Pergamon Press, London, 1966.

[130] E.E. Bailey, R.W. Heinz: — SO_2 recovery Plants-Materials of construction: Chem. Eng. Progress Vol.71, No 3, March 1975, 64-68.

[131] H.S. Rosenberg, R.B.Engdahl — The status of SO_2 control systems. Chem. Eng. Progress Vol.71, No.5, 66-71.

[132] T.H. Chilton, — Reducing SO_2 Emiston from Stationary Sources. Sulphur and SO_2 Developments - published by A.I.Ch.E. New York, 1971, 115-118.

[133] A.I. Kutepova, B.I. Lurie: — Removal of nitrogen and sulphur oxides from waste gases. International Chem. Eng. Vol.18, No.1, Jan. 1978, 118-120.

[134] Furusho, Saburo, Fukunda Takashi, — Treatment of waste solutions from waste gas SO_x removal process. Japanese Patent 7815262, 29 July, 1976.

[135] Yamashita, Kasane — Regeneration of waste water from waste gas desulphurization processes. Japanese Patent 7566481, 18 Oct. 1973.

[136] F.H. Yorston — Studies on Sulphite waste Liquor I : The action of Anion Exchangers. Pulp and Paper Mag. of Canada, 50, 12, (Nov.1949) 108-113.

[137] J.F. Pritchard and Company: — Treatment of waste sulphite Liquors U.S. Patent 3095265, June 1963.

[138] William J. Wilson — Ion exchange recovery of monovalent cations from spent sulphite liquor: U.S. Patent 3248278, April 26, 1966.

[139] L.J. Minnick. — Progress in the conversion of Sulphur Dioxide Scrubber sludges into environmentally acceptable products. From the proceedings of the fifth Mineral Waste Utilization Symposium, April 13-14, 1976. Chicago, Illinois, U.S.A.

[140] W.R. Effer, H.B Marshall and E.W. Hopper. — Ion exchange process for recovery of Monovalent ions from waste sulphite pulping liquor. U.S. Patent 3095265, June 25, 1963.

[141] Burns William C, Robinson, Donald H.S. Newberry. — Treatment of cation-and anion-exchange resins with sodium sulphite. U.S. Patent. 3692670, 19 Sept. 1972.

[142] K.R. Gray, H.L. Crosby. Sodium bisulphite solution. U.S. Patent 2656244, Oct. 1953

[143] L.W. Cochran. Acid regeneration process. S.A. Patent 685290, 15 Aug. 1968

[144] L. Lefevre. Spent pickling liquor. French Patent 2087504, 14 Feb. 1972.

[145] Erhard Albrecht. Device for introducing gas into liquids. S.A. Patent 78i211 30 Jan. 1978.

[146] W.L. McCabe, J.C. Smith. Unit Operations of Chemical Engineering. McGraw-Hill Book Company. New York.

[147] Max Leva Variables in fixed Bed Systems. Chemical Engineering, Aug. 1957, 263-266.

[148] Max Leva. Flow Through Packings and Beds, Chem. Eng. J., March 1957, 261-265.

[149] Maxy Brooke, Flow Packings, Beds. Chem.Eng. J., Aug. 1957, 280.

[150] Max Leva. Correlations in Fixed Bed Systems, Chem. Eng. J., Sept. 1957, 245-248.

[151] F.A. Zenz. What Every Engineer Should Know about Packed Tower Operations. Chem. Eng. J. Aug. 1953.

[152] T.K. Sherwood, R.L. Pigford. Adsorption and Extraction, McGraw Hill Book Company, 1952.

[153] E.W. Hauf, J.W. MacDonald Economic Evaluation of Wet Scrubbers. Chem. Eng., Progress, Vol. 71, No.3, March 1975 48-52.

[154] Hung Xuan Nguyen. Computer Programme expedites Packed-Tower Design. Chem. Eng. J. Nov. 30, 1978, 181-184.

[155] M.S. Peters. Plant Design and Economists for Chemical Engineers. McGraw-Hill Book Company. New York, 1958.

[156] W.S. Norman. Absorption. Distillation and Cooling Towers. Longmans, Green and Co. London.

[157] R.F. Vircles, T.L. Carter — Watch Those Hidden Packaging Costs. Chem. Eng. Aug. 1953, 185-187.

[158] T.G. Gleason. — How to Avoid Scrubber Corrosion. Chem. Eng. Progress, Vol.71, No.3, March 1975, 43-46.

[159] E.E. Bailey, R.W. Heiwg, — SO_2 Recovery Plants - Materials of Construction. Chem. Eng. Progress, Vol. 71, No.3, March 1975, 64-68.

[160] Frank X. McGarvey, — Ion exchange as a Unit Operation. Chemical Engineering, Dec. 1957, 255-260.

[161] Robert E. Anderson — Estimation of ion exchange process limits by selectivity calculations. Adsorption and Ion Exchange : A.I.Ch.E. Symposium Series, No. 152, Vol. 71. 236-242.

[162] Neven K. Hiester and R.C. Phillips. — Ion exchange, Chemical Engineering, Oct. 1954, 161-180.

[163] F.H. Kahler and A C. Reents. — Water Demineralization Costs, Chemical Engineering, Jan. 1957, 206 - 210.

[164] Max S. Peters. — Plant Design and Economics for Chemical Engineers, McGraw-Hill Book Company, New York, 1958.

[165] F.C. Nachod and J. Schubert — Ion exchange technology, Academic Press Inc., New York, 1956.

[166] T.V. Arden, — Water Purification by Ion exchange, Butterworth & Co., London, 1968.

[167] Robert Kunin and R.J. Meyers. — Ion exchange resins, John Wiley & Sons, New York, 1950.

[168] Konrad Dorfner. — Ion Exchangers, Properties and Applications, Ann Arbor Science, Michigan, U.S.A. 1972.